Fundamental Properties of Thermo-Responsive Entirely Ionic PIC (Polyion Complex) Micelles

Dongwook Kim

2021

Table of contents

Part 1

Part 2

Chapter 1.

General Introduction

1.1 Background and Objective

The betaine polymer, which is a type of zwitterionic polymer having both negative and positive charges in one repeating unit,[1-3] is an interesting polymer, unlike ordinary ionic polymers (anionic or cationic polymer), because of unique characteristics such as chain extension by salt addition.[4-6] The zwitterionic moieties of the betaine polymer have a structure similar to that of the lipids that make up cells,[7,8] high biocompatibility is observed,[9,10] it is being developed into biomedical materials.[11-13] Research on the zwitterionic polymer can be found in the 1950s as a new synthetic report by Morawetz et al.,[14] but the study of their basic physical properties began around 1970~1980.[6,15,16] The viscosity of the polymer aqueous solution increased by the addition of salt, and its extent depends on the ion species.[1,17] Different behavior from conventional ionic polymers is named the "anti-polyelectrolyte effect",[6] but the details were not clear, and the charge of the target polymer was limited to imidazolium-based cations.[17,18] Research on polybetaine has been started since 2000, but most of them are sporadic, and the examination of differences in molecular structure is limited to the case of the paper by Gauthier et al.[19] The current situation is that it has not been systematized yet. Besides, among them, sulfobetaine is known to exhibit the temperature responsivity of the upper critical solution temperature (UCST) type[6,20] and is expected to be applied to a novel temperature-responsive material, but the mechanism of responsivity has not yet been clarified. For now, it is thought that the cause is the formation and elimination of intra- or intermolecular salt (ion-pair) around the critical temperature, but it is a mystery that other betaine polymers do not exhibit temperature responsiveness.[21,22]

Zwitterionic polyion complex (PIC) micelles, which are a novel self-assembled polymeric micelle, have a polyion complex of polyanions and polycations as a core, and a zwitterionic polybetaine as a corona (shell) (Figure 1).[23] In ordinary amphiphilic block copolymers, the core is formed by the association of hydrophobic chains to form polymeric micelles,[24] but in PIC micelles, the driving force is the electrostatic attraction between polyanions and polycations and the increased entropy according to counterions released by the association.[25] Therefore, it is expected that the stability as micelles and the response to added salt will be significantly different between the two. In most cases, the shell of normal PIC micelles is water-soluble and nonionic polyethylene glycol (PEG).[25,26] In addition, it has been reported that poly(N, N-dimethylacrylamide) (PDMA),[27] poly(N-isopropylacrylamide) (PNIPAM),[28] poly(ethylene oxide) (PEO),[29] and poly(acryl amide) (PAAm),[30] etc. used as shells for PIC micelles.
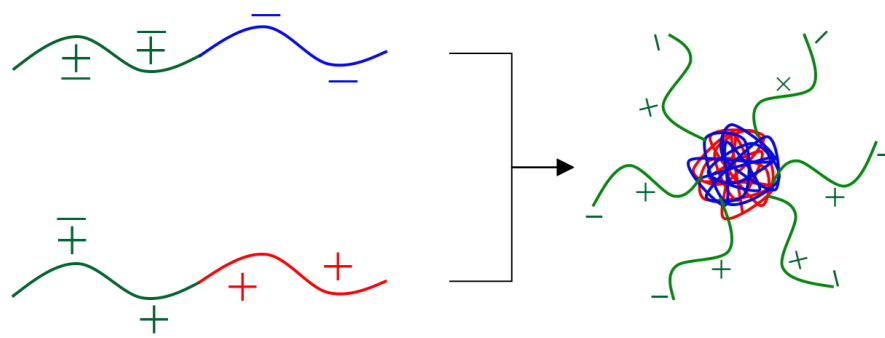
Figure 1. Schematic illustration of zwitterionic polyion complex (PIC) micelles.

Synthesize a novel polymer of block copolymers consisting of zwitterionic betaine chains and ionic chains, and clarify the formation behavior and stimuli responsivity of the aggregate. The objective of this study is to construct PIC micelles in the shell of sulfobetaine that have temperature responsivity. It is expected that micelles whose corona expands and contracts in response to temperature changes can be constructed (Figure 2).[21,22] Furthermore, clarify the correlation between the molecular structure and stimulus responsiveness, and

elucidate its expression mechanism. Establish a mechanism to freely control the nanostructure of self-assembled aggregates and the properties and functions of betaine polymers, which will lead to the development of new stimuli-responsive materials and biomaterials.

Below the critical
temperature
(Low Temp.)

Critical
Temperature

Above the critical
temperature
(High Temp.)
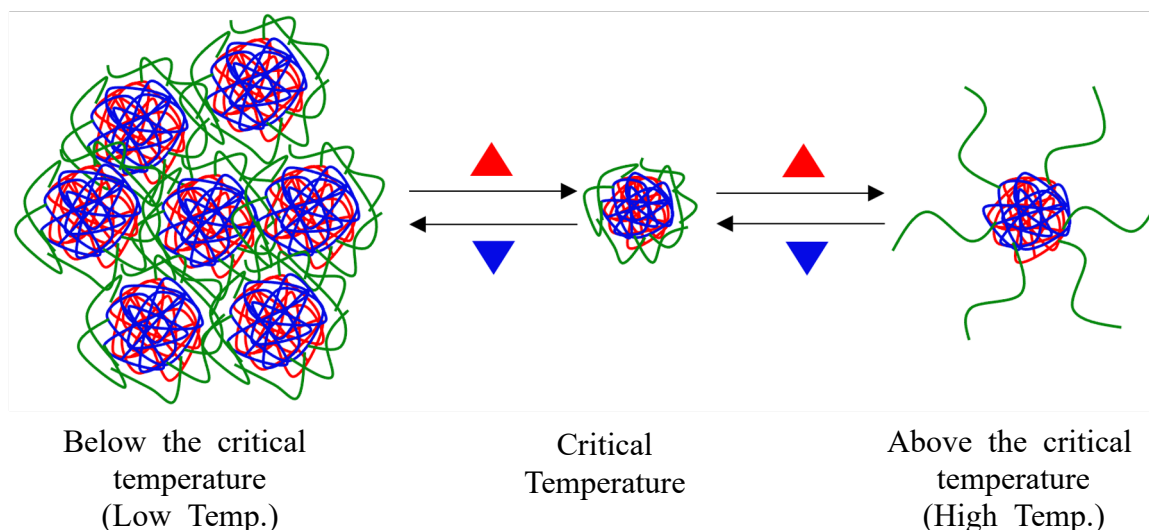
Figure 2. Schematic illustration of the shape changes of PIC micelles according to temperature change.

1.2 Polybetaines

Polybetaines has the same number of anions and cations in the one repeating unit and has an overall charge of zero under general conditions (Figure 3a).[1,2] Polybetaines are a subclass of polyampholytes.[1,31] Polyampholytes have both anionic and cationic moieties, but there is no specific mutual correlation between them.[31,32] Therefore, in polyampholytes, anions and cations are present randomly along the polymer chain, one of the charged species may be present more than the other (Figure 3b). Accordingly, polyampholytes usually take on the overall net charge (except for a particular narrow pH range, where the number of anionic and cationic moieties may be equal, thus behaving like polybetaines). The net charge can be negative or positive, which varies sensitively with pH and ionic strength.[31] On the other hand, polybetaines commonly exhibit high hydrophilicity due to strong Coulomb interaction.[33,34]

Polybetaines do not exhibit the typical "polyelectrolyte effects", but there is much similar to polar nonionic polymers.[34]
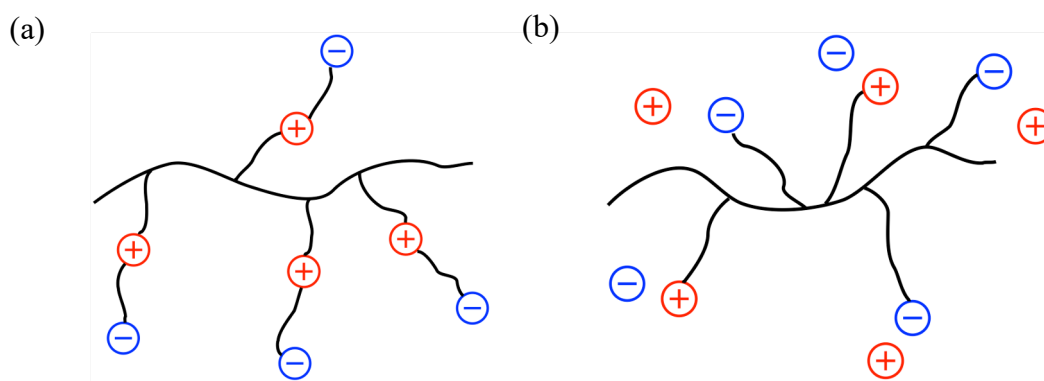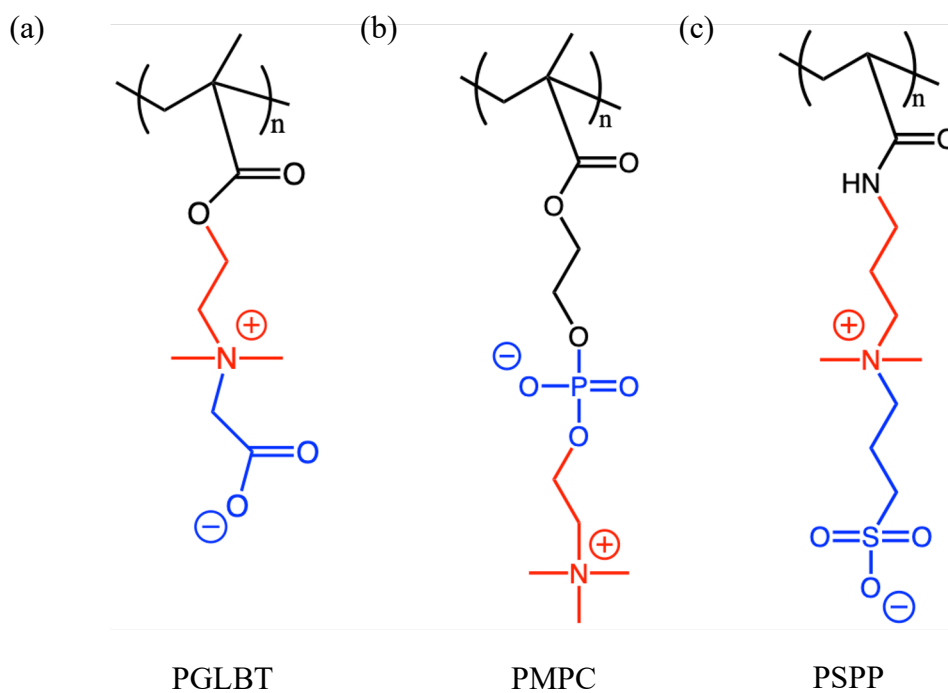

Figure 3. Simplistic model of polyzwitterions (a) and polyampholytes (b).


Figure 4. Chemical structure of polybetaines: (a) Polycarboxybetaine (CB), (b) polyphosphobetaine (PB), (c) Polysulfobetaine (SB).

Polybetaines are divided into carboxybetaine (CB), phosphobetaine (PB), and sulfobetaine (SB) according to functional groups (Figure 4).[1,2] Among them, the only

sulfobetaine polymer exhibits upper critical solution temperature (UCST) behavior in which the solubility increases rapidly when a certain temperature is exceeded.[6,20-22] The expression mechanism predicts that anions and cations form an intra- or intermolecular pair (salt) below the critical temperature, and that the intra- or intermolecular pair is relaxed and dissolved by an increase in the kinetic energy of the molecular chain above the critical temperature.[21,22] The carboxybetaine polymer by a functional group having a pH responsivity,[35,36] phosphobetaine polymer has high solubility[1,2] and biocompatibility.[9,10] The solubility of polybetaines changes depending on the concentration of the added salt, and it depends on the ionic species of the added salt.[6,17,22] In normal ionic polymers (anionic or cationic), the polymer chain shrinks according to the addition of salt,[4,5] whereas the polybetaines chain expands,[17,22] which is the opposite behavior (Figure 5). Then, its behavior strongly depends on the anionic species of the added salt.[17,22] Accordingly, polybetaines have been studied in various fields such as brushes,[37,38] micelles,[23,39] organic-inorganic hybrid solar cells,[40,41] surfactants,[42,43] and gels,[44,45] etc.
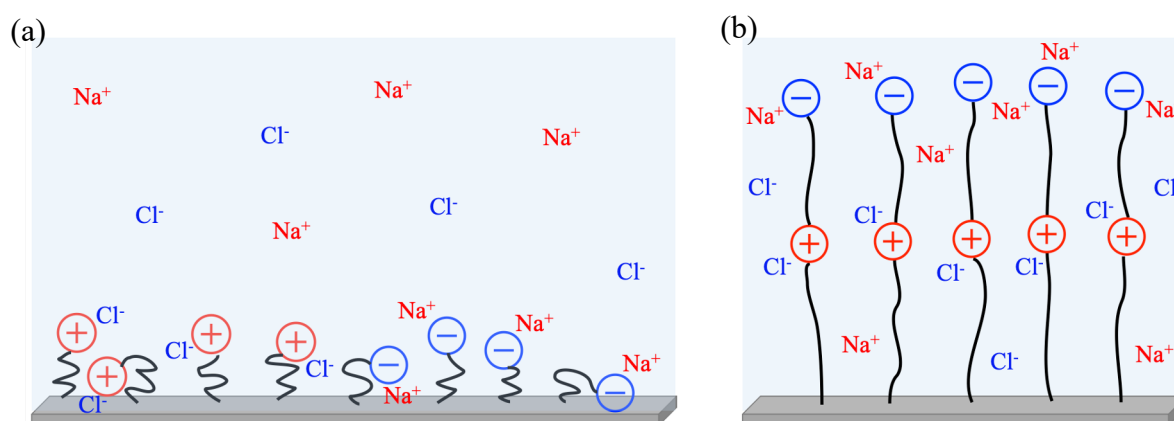

Figure 5. The effect of salt addition on (a) ionic polymer and (b) polybetaines.

1.3 Self-Assembly of Block Copolymers

Amphiphilic block copolymers that have both hydrophobic and hydrophilic moieties within a single molecule build various forms by self-assembly in a solvent (Figure 6).[46] In the

case of a diblock copolymer, it forms micelles above the critical micelle concentration (CMC), the morphology is changed in the order of spherical micelle→cylindrical micelle→lamellar formation with an increase in the ratio of hydrophobic moieties.[47] The shape of the micelles is determined by the ratio of the molecular volume of the hydrophobic chain to the actual volume occupied by the copolymer in the assembly. As a general rule, spherical micelles are formed when hydrophobic chains are much shorter than hydrophilic chains, lamellar formation (polymeric membranes) is formed when the length of the two domains are similar.[47] From a theoretical point of view, the most stable condition will be an infinitely long cylinder and infinitely large lamellar forms.[48] However, thermal fluctuations and the intrinsic fluid nature of these aggregates force finite dimensions. Thus, to avoid contact between the solvent and the hydrophobic moieties, the lamellar formation bends to form a spherical structure of vesicles.[48] In addition, the micelle-to-vesicle morphological transition occurs depending on temperature,[49] concentration,[50] solvent,[51] pH,[52] and mixing ratio,[53] etc.
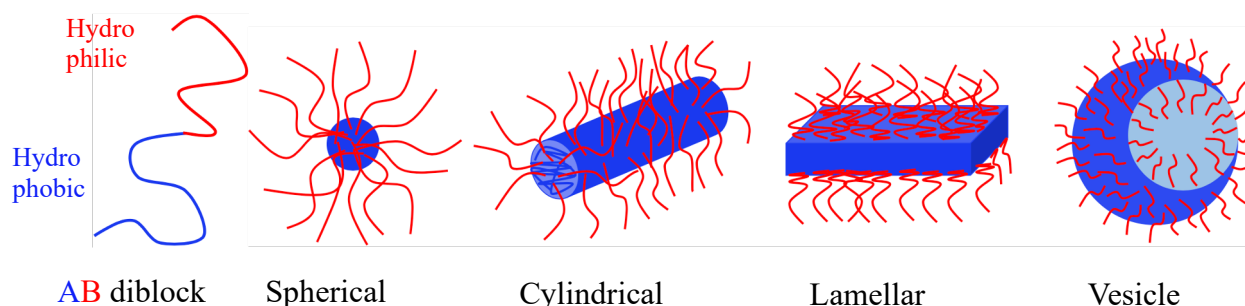
Figure 6. The morphological transition of amphiphilic diblock copolymer micelles depending on the ratio of hydrophobic moieties.

Triblock copolymers can be assembled into various types of aggregates such as flower-like micelle, spherical micelle, and vesicle depending on how the blocks are designed like ABA, BAB, and ABC (Figure 7).[54] Also, the shape is changed by changing the conditions.[55,56] Triblock copolymer systems have several advantages compared with diblock copolymer systems, because the presence of three distinct domains can provide more functional features.

| ABA triblock | Flower-like micelles | BAB triblock | Spherical micelles |
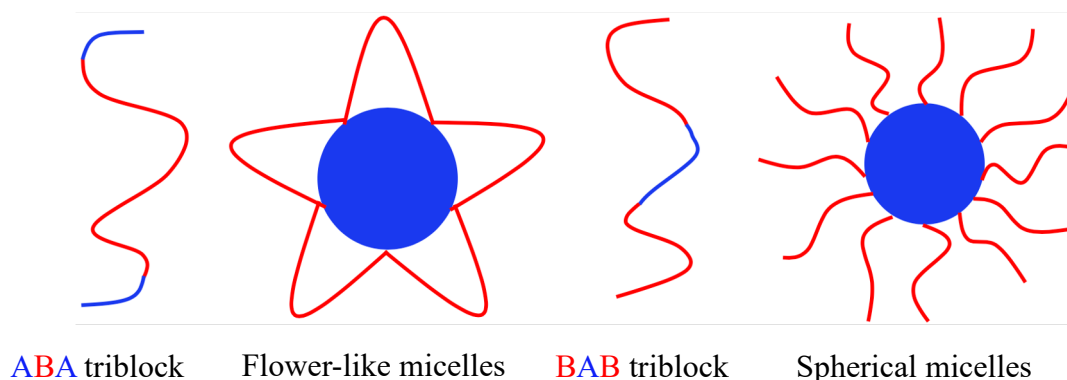
Figure 7. The morphological change of triblock copolymer micelles according to block design.

1.4 PIC (Polyion Complex) Micelles

Supramolecular assemblies formed by associations of the polymer have been studied in various fields.[57,58] Among them, research on polymeric micelles having a core-shell structure composed of block copolymers is being actively conducted.[47] The core part of the polymeric micelles is used as a carrier for various substances.[59,60] These features have been applied to drug delivery systems (DDS),[60,61] separation techniques,[62] and the like to provide significant advantages when using amphiphilic block copolymer micelles in an aqueous environment. Ordinary amphiphilic block copolymers have hydrophilic and hydrophobic moieties. In an aqueous environment, the hydrophobic moieties are self-assembled by the hydrophobic interaction to form a core-shell (hydrophobic-hydrophilic) structure.[24,46,47] The hydrophilic shell (corona) is involved in preventing progressive assembly of the core and stabilization of micelles. In addition, the stability of micelles is determined by the proportion of hydrophilic chains, low critical association concentration, solvent, pH, etc.[63] On the other hand, amphiphilic block copolymer micelles whose core is hydrophobic have the limit of being able to contain only hydrophobic compounds.[60,61]

The Polyion Complex (PIC) micelles were established by Kataoka et al.,[25,26] and are

novel polymeric micelles formed by self-assembly with a polyion complex of polyanionic chain and polycationic chain as the core and hydrophilic chain as the shell (corona). PIC micelles are prepared by dissolving two diblock copolymers or block copolymers and ionic homopolymers in a solvent, and mixing an aqueous solution so that the numbers of charges of anions and cations are equal.[25-30] At that time, the block copolymer contains an ionic block. The driving force is the electrostatic interaction between polyanions and polycations, and the increase of entropy according to the release of counterions.[25] In most cases, the shell of normal PIC micelles is polyethylene glycol (PEG), which is a nonionic hydrophilic polymer.[25-30] The reason is that if an ionic chain or amphoteric chain are used as the shell, the shell and core interact to form unstable micelles, making it difficult to control the size and stability. In addition, these new polymeric micelles (PIC micelles) can contain specific chemical compounds (hydrophilic or charged compounds) because the core is a polyion complex, and it is expected to be applied to various fields such as a drug delivery system (DDS).

1.5 Outline of This Thesis

The main objective of this thesis is to synthesize a novel entirely ionic block copolymer consisting of zwitterionic sulfobetaine chains and ionic chains, and to elucidate the formation behavior and function expression mechanism of their complex. Furthermore, create a PIC micelle with sulfobetaine as a shell, and not only to control its transition temperature and morphological changes but also to clarify the correlation between molecular structure and stimulus responsiveness. Thereby, establish a mechanism to freely control the nanostructure of self-assembled complex and the properties and functions of betaine polymers. The thesis composes of six chapters. The first chapter describes the background and objective of this thesis. The other chapters are divided into two parts.

In Part I (chapters 2-4), the author deals with the synthesis of diblock copolymers composed of sulfobetaine and ionic blocks and the influence of the block ratio on their

temperature responsivity. Furthermore, investigating the formation of temperature-responsive PIC micelles and the control of their transition temperature, size, and uniformity.

Chapter 2 describes the precision synthesis of sulfobetaine-containing entirely ionic diblock copolymers and the influence of the block ratio on their temperature responsivity. Temperature responsiveness disappeared by introducing an ionic chain into polysulfobetaines having the upper critical solution temperature (UCST) type temperature responsivity. This is probably due to the electrostatic interaction between the betaine chain and the ionic chain (anionic or cationic) formed some complex. Therefore, investigating the effect of the addition of an ionic homopolymer to sulfobetaine homopolymer and the change in responsiveness according to a change in the block ratio. The responsiveness disappeared due to the interaction between the betaine chain and the ionic chain, and the responsiveness could be exhibited by shortening the ionic block with respect to the length of the sulfobetaine block. In particular, it was revealed that the influence of the anionic block is greater than that of the cationic block.

Chapter 3 describes how to form temperature-responsive PIC micelles. The fundamental properties of the sulfobetaine-containing polymer exhibiting temperature responsivity were investigated, and it was found that the transition temperature strongly depends on the degree of polymerization (DP) and the concentration of polymer solution. On the other hand, PIC micelles prepared by block copolymer (polyanion-*b*-polysulfobetaines or polycation-*b*-polysulfobetaines) that did not exhibit temperature responsiveness due to the block ratio of 1:1 exhibited temperature responsivity, and the transition temperature depended on the concentration. In the case of block copolymers, the temperature responsivity disappears due to the influence of the block ratio by the introduction of ionic chains, but when PIC micelles are formed, the ionic chains become the core and do not behave as ionic chains. Furthermore, the transition temperature can be controlled by fixing the core and adjusting the length of the shell. That is, the transition temperature of PIC micelles can be controlled by adjusting the DP

of sulfobetaine which becomes a shell, and the concentration of the polymer aqueous solution.

Chapter 4 describes the changes in transition temperature and shape depending on the method of preparing PIC micelles. As a method for preparing micelles, comparing a simple mixing method and a reforming method by dialysis. The collapse of PIC micelles due to salt addition depends on the anionic species of the added salt and is consistent with the tendency of structural destruction in the Hofmeister series. The most important factor was how much SO_3^- on the outside of the sulfobetaine chain could be hydrated, and the anionic species play the role. Heterogeneous and large PIC micelles formed by the simple mixing method collapsed after salt addition and reformed by dialysis to form a uniform and smaller micelle. Thus, uniform and smaller micelles can be reformed in an equilibrium state by dialysis. Then, the temperature response of PIC micelles formed by the simple mixing method and PIC micelles reformed by dialysis showed similar temperature-transmittance curves. This result suggested that the responsiveness was more influenced by the concentration than the size.

In Part II (Chapter 5 and Chapter 6), the author deals with the PIC micelles of the diblock copolymer/ionic homopolymer system and the complex of zwitterionic betaine surfactant micelles and ionic polymers.

Chapter 5 describes the formation behavior of PIC micelles composed of sulfobetaine-containing diblock copolymers and ionic polymers, the influence of the degree of polymerization of ionic polymers, and changes in the transition temperature. The PIC micelles of the block/cationic polymer system exhibit temperature responsivity, and it turned out to be concentration dependent. On the other hand, the PIC micelles of the block/anionic polymer system with a core-shell structure at very low concentrations (0.05 wt%), but at higher concentration (0.1 wt%), the anionic polymer interacts with both the sulfobetaine and the cationic moieties of the block copolymer to form an unstable aggregate. Precipitation occurred when the concentration was further increased (0.3 wt% or more). Then, if the DP of the ionic

polymer was higher than that of the ionic moiety of the block copolymer, PIC micelles could not be formed.

Chapter 6 describes the complex formation of sulfobetaine surfactant micelles and ionic polymers and their stimuli responsivity. Sulfobetaine surfactant (LAPHS) micelles do not exhibit temperature responsivity. However, temperature responsivity could be exhibited by forming a complex with the cationic polymer. The unprecedented phenomenon of "clear→opaque→clear" was observed with increasing concentration in the concentration range above critical micelle concentration (CMC). This is considered to be due to the change in transition temperature accompanying the change in concentration. On the other hand, LAPHS micelles and the anionic polymer formed a large aggregate but did not exhibit temperature responsiveness. Aggregates were not formed when monomers were added or when salt concentration was high. These results revealed that 1) the LAPHS micelles and the ionic polymer form an aggregate, 2) the temperature responsivity can be expressed by the interaction with the cationic polymer, and 3) the transition temperature can be controlled by adjusting the concentration of polymer aqueous solution and the degree of polymerization of the cationic polymer.

1.6 Reference

[1] A. B. Lowe, C. L. McCormick, *Chem. Rev.* **2002**, 102, 4177-4189.

[2] A. Laschewsky, *Polymers* **2014**, 6, 1544-1601.

[3] L. D. Blackman, P. A. Gunatillake, P. Cass, K. E. S. Locock, *Chem. Soc. Rev.* **2019**, 48, 757-770.

[4] H. Matsuoka, Y. Kido, M. Hachisuka, *Chem. Lett.* **2015**, 44, 1622-1624.

[5] S. Alharthi, N. Grishkewich, R. M. Berry, K. C. Tam, *Carbohydr. Polym.* **2020**, 246, 11651-11659.

[6] D. N. Schulz, D. G. Peiffer, P. K. Agarwal, J. Larabee, J. J. Kaladas, L. Soni, B. Handwerker, R. T. Garner, *Polymer* **1986**, 27, 1734-1742.

[7] T. Umeda, T. Nakaya, M. Imoto, *Makromol. Chem. Rapid Commun.* **1982**, 3, 457-459.

[8] J. A. Hayward, D. Chapman, *Biomaterials* **1984**, 5, 135-142.

[9] K. Ishihara, T. Ueda, N. Nakabayashi, *Polym. J.* **1990**, 22, 355-360.

[10] I. Y. Ma, E. J. Lobb, N. C. Billingham, S. P. Armes, A. L. Lewis, A. W. Lloyd, J. Salvage, *Macromolecules* **2002**, 35, 9306-9314.

[11] H. Kitano, S. Tada, T. Mori, K. Takaha, M. G. Ide, M. Tanaka, M. Fukuda, Y. Yokoyama, *Langmuir* **2005**, 21, 11932-11940.

[12] G. Cheng, H. Xue, Z. Zhang, S. Chen, S. Jiang, *Angew. Chem.* **2008**, 120, 8963-8966.

[13] S. Jiang, Z. Cao, *Adv. Mater.* **2010**, 22, 920-932.

[14] H. Ladenheim, H. Marawets, *J. Polym. Sci.* **1957**, 26, 251-254.

[15] D. L. Schmidt, H. B. Smith, M. Yoshimine, M. J. Hatch, J. *Polym. Sci., Part A-1: Polym. Chem.* **1972**, 10, 2951-2966.

[16] M. Litt, T. Matsuda, *J. Appl. Polym. Sci.* **1975**, 19, 1221-1225.

[17] T. A. Wielema, J. B. F. N. Engberts, *Eur. Polym. J.* **1990**, 26, 639-642.

[18] J. C. Salamone, W. Volksen, A. P. Olson, S. C. Israel, *Polymer* **1978**, 19, 1157-1162.

[19] M. Gauthier, T. Carrozzella, A. Penlidis, *J. Polym. Sci., Part A: Polym. Chem.* **2002**, 40, 511-523.

[20] D. J. Liaw, C. C. Huang, H. C. Sang, E. T. Kang, *Langmuir* **1998**, 14, 3195-3201.

[21] L. Chen, Y. Honma, T. Mizutani, D. J. Liaw, J. P. Gong, Y. Osada, *Polymer* **2000**, 41, 141-147.

[22] V. M. M. Soto, J. C. Galin, *Polymer* **1984**, 25, 254-262.

[23] K. Nakai, M. Nishiuchi, M. Inoue, K. Ishihara, Y. Sanada, K. Sakurai, S. Yusa, *Langmuir* **2013**, 29, 9651-9661.

[24] C. Tanford, *Wiley: New York.* **1973**, 208.

[25] A. Harada, K. Kataoka, *Macromolecules* **1995**, 28, 5294-5299.

[26] A. Harada, K. Kataoka, *Science* **1999**, 283, 65-67.

[27] M. Sotiropoulou, C. Cincu, G. Bokias, G. Staikos, *Polymer* **2004**, 45, 1563-1568.

[28] J. Zhang, Y. Zhou, Z. Zhu, Z. Ge, S. Liu, *Macromolecules* **2008**, 41, 1444-1454.

[29] A. Shovsky, I. Varga, R. Makuska, P. M. Claesson, *Langmuir* **2009**, 25, 6113-6121.

[30] S. Lindhoud, W. Norde, M. A. C. Stuart, *J. Phys. Chem. B* **2009**, 113, 5431-5439.

[31] J. C. Salamone, W. C. Rice, *Wiley-Interscience: New York* **1988**, 11, 514-530.

[32] S. Kudaibergenov, W. Jaeger, A. Laschewsky, *Adv. Polym. Sci.* **2006**, 201, 157-224.

[33] R. G. Laughlin, *Langmuir* **1991**, 7, 842-847.

[34] J. C. Galin, *CRC Press: Boca Raton* **1996**, 9, 7189-7201.

[35] D. B. Thomas, Y. A. Vasilieva, R. S. Armentrout, C. L. McCormick, *Macromolecules* **2003**, 36, 9710-9715.

[36] L. Mi, M. T. Bernards, G. Cheng, Q. Yu, S. Jiang, *Biomaterials* **2010**, 31, 2919-2925.

[37] M. Kobayashi, Y. Terayama, M. Kikuchi, A. Takahara, *Soft Matter* **2013**, 9, 5138-5148.

[38] Z. Zhang, S. Chen, Y. Chang, S. Jiang, *J. Phys. Chem. B* **2006**, 110, 10799-10804.

[39] A. B. Lowe, N. C. Billingham, S. P. Armes, *Macromolecules* **1999**, 32, 2141-2148.

[40] Q. Wang, X. Zheng, Y. Deng, J. Zhao, Z. Chen, J. Huang, *Joule* **2017**, 1, 371-382.

[41] V. H. Tran, S. K. Kim, S. H. Lee, *ACS Omega* **2019**, 4, 19225-19237.

[42] R. Kumar, G. C. Kalur, L. Ziserman, D. Danino, S. R. Raghavan, *Langmuir* **2007**, 23, 12849-12856.

[43] L. Qi, Y. Fang, Z. Wang, N. Ma, L. Jiang, Y. Wang, *J. Surfact. Deterg.* **2008**, 11, 55-59.

[44] M. Das, N. Sanson, E. Kumacheva, *Chem. Mater.* **2008**, 20, 7157-7163.

[45] J. Ning, G. Li, K. Haraguchi, *Macromolecules* **2013**, 46, 5317-5328.

[46] T. Smart, H. Lomas, M. Massignani, M. V. F. Merino, L. R. Perez, G. Battaglia, *Nano today* **2008**, 3, 38-46.

[47] J. N. Israelachvili, D. J. Mitchell, B. W. Ninham, *J. Chem. Soc. Faraday Trans. 2* **1976**, 72, 1525-1568.

[48] R. A. L. Jones, Soft Condensed Matter. *Oxford University Press* **2004**.

[49] H. Yin, Z. Zhou, J. Huang, R. Zheng, Y. Zhang, *Angew. Chem. Int. Ed.* **2003**, 42, 2188-2191.

[50] S. Ohno, K. Ishihara, S. Yusa, *Langmuir* **2016**, 32, 3945-3953.

[51] A. Blanazs, S. P. Armes, A. J. Ryan, *Macromol. Rapid Commun.* **2009**, 30, 267-277.

[52] Y. I. Gonzalez, H. Nakanishi, M. Stjerndahl, E. W. Kaler, *J. Phys. Chem. B* **2005**, 109, 11675-11682.

[53] R. Takahashi, T. Sato, K. Terao, S. Yusa, *Macromolecules* **2016**, 49, 3091-3099.

[54] D. J. Pochan, Z. Chen, H. Cui, K. Hales, K. Qi, K. L. Wooley, *Science* **2004**, 306, 94-97.

[55] Z. Zhu, S. P. Armes, S. Liu, *Macromolecules* **2005**, 38, 9803-9812.

[56] J. Weiss, A. Laschewsky, *Langmuir* **2011**, 27, 4465-4473.

[57] G. M. Whitesides, J. P. Mathias, C. T. Seto, *Science* **1991**, 254, 1312-1319.

[58] J. H. Fuhrhop, P. Blumtritt, C. Lehmann, P. Luger, *J. Am. Chem. Soc.* **1991**, 113, 7437-7439.

[59] R. Nagarajan, M. Barry, E. Ruckenstein, *Langmuir* **1986**. 2, 210-215.

[60] G. S. Kwon, K. Kataoka, *Adv. Drug Deliv. Rev.* **1995**, 16, 295-309.

[61] Y. Takeoka, T. Aoki, K. Sanui, N. Ogata, M. Yokoyama, T. Okano, Y. Sakurai, M. Watanabe, *J. Control. Release* **1995**, 33, 79-87.

[62] P. N. Hurter, T. A. Hatton, *Langmuir* **1992**, 8, 1291-1299.

[63] T. N. Khan, R. H. Mobbs, C. Price, J. R. Quintana, R. B. Stubbersfield, *Eur. Polym. J.* **1987**, 23, 191-194.

Part 1

Synthesis and Stimuli Responsivity of Diblock Copolymers Composed of

Sulfobetaine and Ionic Blocks: Influence of the Block Ratio

Ionic diblock copolymers having sulfobetaine, poly(sodium styrenesulfonate)-*b*-poly(sulfopropyl dimethylammonium propylacrylamide) (PSSNa-*b*-PSPP) and poly[3-(methacrylamido)propyl trimethylammonium chloride])-*b*-poly(sulfobetaine) (PMAPTAC-*b*-PSPP), were synthesized by reversible addition-fragmentation chain transfer (RAFT) polymerization. Polysulfobetaine has the temperature responsivity of the upper critical solution temperature (UCST) type. However, sulfobetaine and PSSNa, sulfobetaine and PMAPTAC with a block ratio of 1:1.8 (36-*b*-66) and 1:1.3 (50-*b*-66), respectively, did not show temperature responsivity. This is probably due to the interaction between sulfobetaine and ionic polymer (anionic or cationic) to form some complex. Therefore, the author investigated the effect of block ratio on the temperature response and interaction between sulfobetaine and ionic polymers. The UCST behavior of the block copolymer composed of a sulfobetaine chain and ionic chain was investigated by changing the block ratio by turbidimetry. PSSNa-*b*-PSPP and PMAPTAC-*b*-PSPP with a block ratio of 1:42.5 (6:255) and 1:4 (16:61), respectively, showed temperature responsivity. The expression of temperature responsivity was found to be very sensitive to the chain length of the ionic chain block. The temperature responsivity was considered to disappear because of interaction between the sulfobetaine chain and the ionic chain. The interaction was investigated by adding the ionic polymer to the sulfobetaine homopolymer. UCST behavior was confirmed by adding 0.1% PSSNa and 1% PMAPTAC, respectively. The results suggested that the sulfobetaine chain and the ionic chain interacted

with each other, and that PSSNa was more sensitive than PMAPTAC. In addition, it was confirmed that the sulfobetaine chain and ionic chain in homopolymers mixture system and a block copolymer interact with each other by ^{1}H NMR measurement.

2.1 Introduction

Betaine polymer, which is a type of zwitterionic polymer having both an anion and cation, is an interesting polymer, unlike ordinary ionic polymers, due to unique characters such as polymer chain extension by salt addition. [1-6] The viscosity of the polymer aqueous solution increased by addition of salt, and that its extent depends on the ion species. Different behavior from conventional ionic polymers is named "anti-polyelectrolyte effect". [7-12]

Since the zwitterionic part is a structure similar to the cell membrane, high biocompatibility is observed, and application to biomedical materials is expected.[13-16]

Betaine polymers are roughly categorized into three kinds, sulfobetaine, carboxybetaine and phosphobetaine.[3,17] Among them, sulfobetaine is known to exhibit the temperature responsiveness of the upper critical solution temperature (UCST) type, [12,18-23] and it is expected to be applied to a novel temperature responsive material, but the mechanism of responsivity has not yet been clarified.

In this research, the author aimed at the development of novel thermo-responsive polymeric materials, entirely ionic diblock copolymers consisting of a sulfobetaine chain and ionic chain (anionic chain or cationic chain) were synthesized by reversible addition and fragmentation chain transfer (RAFT) polymerization.[24,25] When these two block copolymer aqueous solutions are mixed so that the charge of anions and cations are equal, they become polyion complex (PIC) micelles in which the core is PIC and the shell is sulfobetaine.[26,27] This is a new type with micelles consisting entirely of ionic polymers. Furthermore, by using sulfobetaine, the temperature responsivity can be imparted. However, the author investigated the temperature responsivity of these aqueous solutions of two block copolymers with a block

ratio of about 1:1, it was confirmed that the temperature responsivity disappeared. It is likely that the betaine chain and ionic chain form complex.[28,29] So, in order to clarify the mechanism of temperature responsivity, the author conducted measurement of transmittance and ^{1}H NMR measurements for diblock copolymers with different block ratios and mixture solution of sulfobetaine homopolymer and ionic homopolymer. The influence of block ratio on temperature responsivity and the effect of addition of ionic homopolymer on sulfobetaine were investigated.

2.2 Experimental

2.2.1 Materials

4,4′-Azobis(4-cyanovaleric acid) (ACVA, 98%), p-styrenesulfonic acid sodium salt (SSNa) were purchased from Wako (Osaka, Japan). Sulfopropyl dimethylammonium propylacrylamide (SPP) and 3-(methacrylamido)propyl trimethylammonium chloride (MAPTAC) were kindly donated from Osaka Organic Chemical Industry Ltd. (Osaka, Japan). 4-cyanopentanoic acid dithiobenzoate was used as chain transfer agent (CTA), which was synthesized as reported by Mitsukami et al.[30] Deuterium oxide (D$_2$O, 99.9%) was a product of Cambridge Isotope Laboratory (CIL) (U.K.). Water used for synthesis, solution preparation and dialysis was ultrapure water obtained by Milli-Q system (18.2 MΩcm). Dialysis for PSPP, PSSNa, PMAPTAC homopolymers and PSSNa-b-PSPP, PMAPTAC-b-PSPP diblock copolymers purification was carried out with a dialysis tube of Orange Scientific (MWCO: 3500 and 12000~16000).

2.2.2 Synthesis of Homopolymers
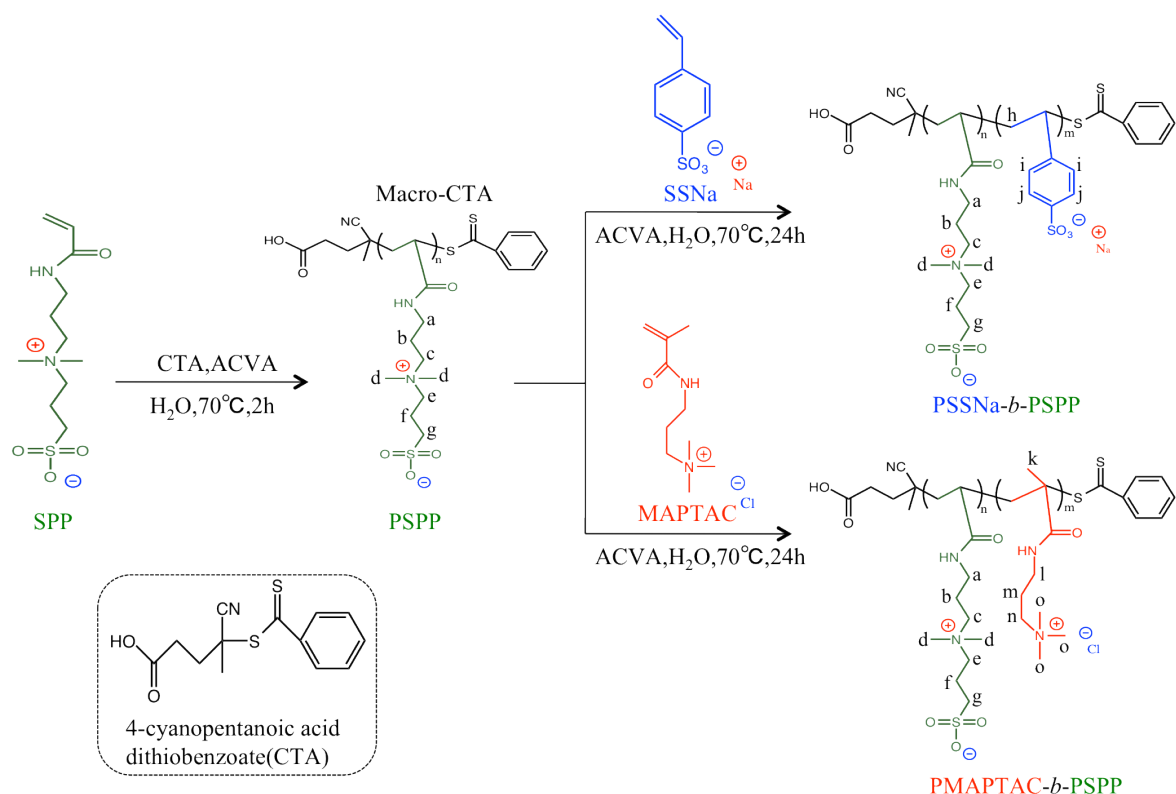
Scheme 2-1. Synthesis of Homopolymer (PSPP) and Block Copolymers (PSSNa-*b*-PSPP and PMAPTAC-*b*-PSPP)[a]

[a]Proton symbols are for ^{1}H NMR in Figure 1.

The PSPP, PSSNa and PMAPTAC homopolymers were the synthesized by Reversible Addition-Fragmentation Chain Transfer (RAFT) polymerization (Scheme 2-1). SPP, CTA and initiator (ACVA) (various molar ratio, Table 2-1) were mixed and put into a Schlenk flask. Then, the mixture was degassed with three cycles of a freeze-pump-thaw and then the flask was filled with Ar gas. Polymerization was performed at 70 °C for 2 h. The reaction was stopped by ice cooling, and the product was dialyzed using a dialysis tube (MWCO: 3500) in Milli-Q water for 5 days. The solid PSPP homopolymer was obtained by freezing-drying. In the same way, PSSNa and PMAPTAC were synthesized by RAFT technique. The degree of polymerization (DP) and polydispersity index (PDI) were evaluated by GPC (Table 2-2). Homopolymers thus obtained were confirmed by ^{1}H NMR.

Table 2-1. Polymerization Conditions for the Synthesis of Homopolymers (PSPP, PSSNa, and PMAPTAC; 70 °C)

Polymer[a]	Monomer (mmol)	RAFT agent (mmol)[b]	Initiator (mmol)[c]	Water (ml)	Polymerization Time (h)
PSPP-1	8.6	1.4×10^{-1}	7.2×10^{-2}	3	2
PSPP-2	8.6	1.4×10^{-1}	7.2×10^{-2}	3	2
PSPP-3	8.6	1.4×10^{-1}	7.2×10^{-2}	3	2
PSPP-4	9.5	1.4×10^{-1}	7.2×10^{-2}	3	2
PSPP-5	9.4	1.4×10^{-1}	7.2×10^{-2}	3	2
PSPP-6	15.1	1.4×10^{-1}	7.2×10^{-2}	3	2
PSPP-7	7.2	2.9×10^{-2}	1.4×10^{-2}	3	2
PSSNa-1	4.5	9.0×10^{-2}	9.0×10^{-2}	3	2
PSSNa-2	9.7	9.7×10^{-2}	9.7×10^{-2}	3	2
PMAPTAC-1	5.9	9.0×10^{-2}	9.0×10^{-2}	3	2
PMAPTAC-2	9.1	9.0×10^{-2}	9.0×10^{-2}	3	2

[a]SPP, sulfobetaine; SSNa, p-styrene sulfonic acid sodium salt; MAPTAC, 3-(methacrylami-do)propyl trimethylammonium chloride. [b]For the synthesis of homopolymer, the amount of macro-RAFT agent is in mmol. [c]For the synthesis of homopolymers, 4,4′-azobis(4-cyanoval-eic acid) (ACVA) was used as the initiator.

Table 2-2. Characteristics of Homopolymers (PSPP, PSSNa, and PMAPTAC).

Polymer	$M_n{}^a$ (g/mol)	PDI^a (M_w/M_n)	DP (n)
PSPP-1	15000	1.08	53
PSPP-2	16000	1.08	56
PSPP-3	17200	1.13	61
PSPP-4	17500	1.07	62
PSPP-5	18500	1.09	66
PSPP-6	29600	1.09	106
PSPP-7	71200	1.07	255
PSSNa-1	11000	1.19	52
PSSNa-2	15700	1.08	75
PMAPTAC-1	12200	1.13	54
PMAPTAC-2	19000	1.11	85

^{a}Determined by GPC with a cationic eluent (P2VP standard) or an anionic eluent (PSSNa standard). PSPP and PMAPTAC were determined with a cationic eluent (0.5 M CH_3COOH, 0.3 M Na_2SO_4), and PSSNa was used as anionic eluent (20 wt% CH_3CN(aq), 0.05 M $NaNo_3$, 0.01 M Na_2HPO_4)

2.2.3 Synthesis of Diblock Copolymers.

The macro-SPP, SSNa (or MAPTAC) monomer and ACVA (various molar ratio, Table 2-3) were dissolved in Milli-Q water and put into a Schlenk flask. The flask was degassed by

five freeze-pump-thaw cycles and filled with Ar gas. Polymerization was performed at 70 ℃ for 24 h, and the reaction was stopped by ice cooling. The product was dialyzed using a dialysis tube (MWCO: 12000~16000) in Milli-Q water for 5 days. The solid PSSNa-*b*-PSPP and PMAPTAC-*b*-PSPP were obtained by freezing-drying. The block ratio, synthesis result and PDI were determined by analyzing the ^{1}H NMR spectrum and GPC (Table 2-4).

2.2.4 [1]H Nuclear Magnetic Resonance (NMR)

^{1}H NMR spectra for PSPP, PSSNa and PMAPTAC homopolymers and block copolymers composed of PSPP and PSSNa (or PMAPTAC) were obtained with a JEOL JNM-EX 400 spectrometer. The concentration of polymer solutions was 1 wt%, and the solvent was D_2O (CIL, 99.9%).

2.2.5 Gel Permeation Chromatography (GPC)

The degree of polymerization and its polydispersity index were determined by a JASCO GPC system (Tokyo, Japan) composed of a 830-RI RI detector, UV-2075 Plus UV detector, CO-2065 Plus column oven, PU-2080 Plus HPLC pump, DG-2080-53 3-line degasser and Shodex SB-804 HQ column. The pH 3 buffer solution (0.3 M Na_2SO_4, 0.5 M CH_3COOH) was used as the cationic eluent and the mixed solution (20 wt% CH_3CN aq, 0.05 M $NaNO_3$, 0.01 M Na_2HPO_4) as the anionic eluent. Poly(2-vinylpyridine) (P2VP) (Scientific Polymer Product, Inc.) and poly(*p*-styrenesulfonic acid sodium salt) (PSSNa) (Sigma-Aldrich) samples were used as cationic and anionic standards, respectively.

2.2.6 Turbidity

The temperature responsivity and cloud point of polymer aqueous solutions composed of PSPP were determined with a UV-vis spectrometer U-3310 (Hitachi) for 10 mg/mL solution.

The author designated the cloud point as the temperature at which the transmittance of the solution is 50% or less at a wavelength of 400 nm.

Table 2-3. Polymerization Conditions for the Synthesis of Diblock Copolymers (PSSNa-*b*-PSPP, PMAPTAC-*b*-PSPP) (70 ℃).

Polymer	Monomer (mmol)	RAFT agent (mmol)	Initiator (mmol)	Water (ml)	Polymerization Time (h)
PSSNa$_m$-*b*-PSPP$_n$-3	9.8×10^{-1}	2.0×10^{-2}	2.0×10^{-2}	3	24
PSSNa$_m$-*b*-PSPP$_n$-1	4.9×10^{-1}	2.0×10^{-2}	2.0×10^{-2}	3	24
PSSNa$_m$-*b*-PSPP$_n$-2	2.5×10^{-1}	2.0×10^{-2}	2.0×10^{-2}	3	24
PSSNa$_m$-*b*-PSPP$_n$-4	2.4×10^{-1}	2.0×10^{-2}	2.0×10^{-2}	3	24
PSSNa$_m$-*b*-PSPP$_n$-5	6.4×10^{-2}	5.4×10^{-3}	5.4×10^{-3}	3	24
PMAPTAC$_m$-*b*-PSPP$_n$-3	9.8×10^{-1}	2.0×10^{-2}	2.0×10^{-2}	3	24
PMAPTAC$_m$-*b*-PSPP$_n$-1	4.5×10^{-1}	2.0×10^{-2}	2.0×10^{-2}	3	24
PMAPTAC$_m$-*b*-PSPP$_n$-1	3.9×10^{-1}	2.0×10^{-2}	2.0×10^{-2}	3	24
PMAPTAC$_m$-*b*-PSPP$_n$-1	3.3×10^{-1}	2.0×10^{-2}	2.0×10^{-2}	3	24
PMAPTAC$_m$-*b*-PSPP$_n$-5	6.3×10^{-2}	3.9×10^{-3}	3.9×10^{-3}	3	24

Table 2-4. Characteristics of Diblock Copolymers (PSSNa-*b*-PSPP and PMAPTAC-*b*-PSPP).

Polymer	Yield (%)	M_n (g/mol)	PDI (M_w/M_n)	Degree of polymerization	
				m^a	n^a
PSSNa$_m$-*b*-PSPP$_n$-3	88	25900	1.12	36	66
PSSNa$_m$-*b*-PSPP$_n$-1	88	20300	1.12	15	61
PSSNa$_m$-*b*-PSPP$_n$-2	71	18700	1.06	6	62
PSSNa$_m$-*b*-PSPP$_n$-4	93	30800	1.14	6	106
PSSNa$_m$-*b*-PSPP$_n$-5	81	72400	1.22	6	255
PMAPTAC$_m$-*b*-PSPP$_n$-3	64	29500	1.17	50	66
PMAPTAC$_m$-*b*-PSPP$_n$-1	44	22500	1.08	24	61
PMAPTAC$_m$-*b*-PSPP$_n$-1	29	21800	1.11	21	61
PMAPTAC$_m$-*b*-PSPP$_n$-1	45	20700	1.09	16	61
PMAPTAC$_m$-*b*-PSPP$_n$-5	50	83100	1.05	54	255

[a]*m*, *n*: Degrees of polymerization of ionic and sulfobetaine blocks, respectively. (*m* was determined by ^{1}H NMR)
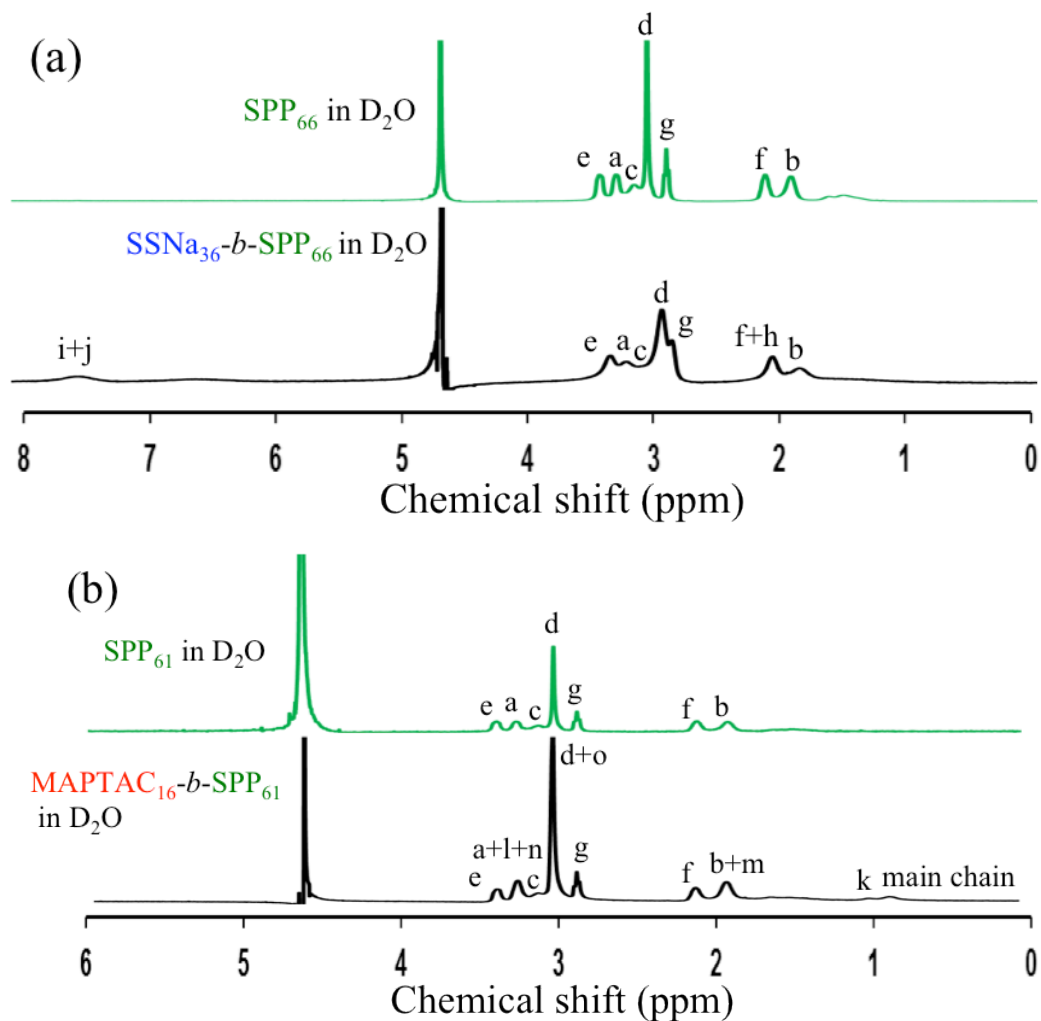
Figure 2-1. ^{1}H NMR spectra of (a) PSPP and PSSNa-*b*-PSPP and (b) PSPP and PMAPTAC-*b*-PSPP in D$_2$O. The block ratio, *m:n*, was estimated by the area of peaks (a) i + j:a + c + d + e + g and (b) b + m:f, respectively. Peak symbols are shown in Scheme 2-1.

2.3 Results and Discussion

2.3.1 Characterization of Homopolymers and Block Copolymers

PSPP, PSSNa and PMAPTAC homopolymers with various degree of polymerization (DP) could be synthesized. As shown in Table 2-3, the degree of polymerization (DP) and polydispersity index (PDI) were confirmed by GPC. Figure 2-1 shows ^{1}H NMR spectra for (a) PSPP homopolymer (macro-CTA) and PSSNa-*b*-PSPP block copolymer, (b) PSPP

homopolymer and PMAPTAC-*b*-PSPP block copolymer. These spectra indicated successful synthesis of the polymers. From the peak area ratio, the block ratio, *m:n*, was determined to be 36:66 (a) and 16:61 (b), respectively. Information on other block copolymers was summarized in Table 2-4, and GPC estimation of the PDI (M_w/M_n) of the block copolymers was successful. (see Appendix for the details).
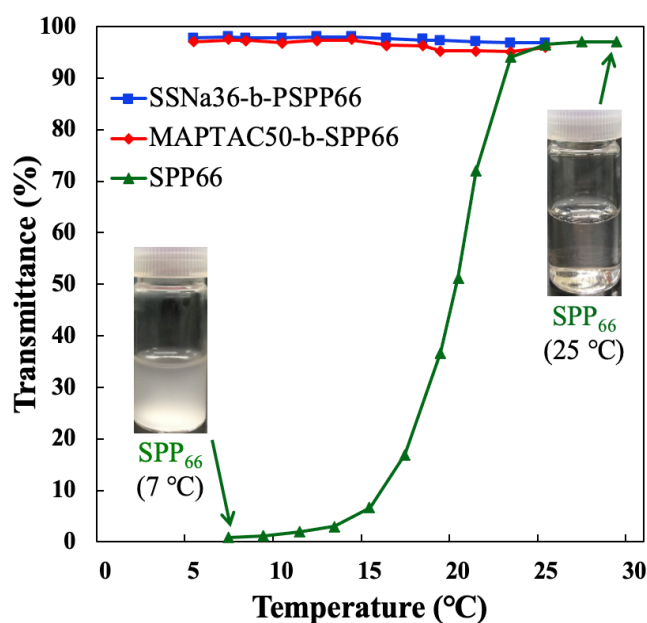

Figure 2-2. Temperature dependence of turbidity of SPP_{66}, $SSNa_{36}$-*b*-SPP_{66}, and $MAPTAC_{50}$-*b*-SPP_{66} aqueous solutions at 1 wt% concentration.

2.3.2 Disappearance of Temperature Responsivity

The temperature responsivity of homopolymer and block copolymers, SPP_{66}, $SSNa_{36}$-*b*-SPP_{66}, $MAPTAC_{50}$-*b*-SPP_{66} aqueous solution at 1 wt% concentration was investigated by UV-vis spectrometer. For the SPP_{66} homopolymer aqueous solution, a temperature-transmittance curve of a typical upper critical solution temperature (UCST) type behavior was obtained. As shown in Figure 2-2, with lowering the temperature sudden decrease of transmittance was observed. However, by transmittance measurement of the aqueous solutions of two block copolymers ($SSNa_{36}$-*b*-SPP_{66} and $MAPTAC_{50}$-*b*-SPP_{66}), it was confirmed that the

temperature responsivity disappeared. When sulfobetaine and PSSNa, sulfobetaine and PMAPTAC had a block ratio of 1:1.8 (36:66) and 1:1.3 (50:60), respectively, the temperature responsivity disappeared. This is probably due to the interaction between sulfobetaine and ionic polymer to form some complex. Therefore, the author investigated the effect of block ratio on the temperature response and interaction between sulfobetaine and ionic polymers.
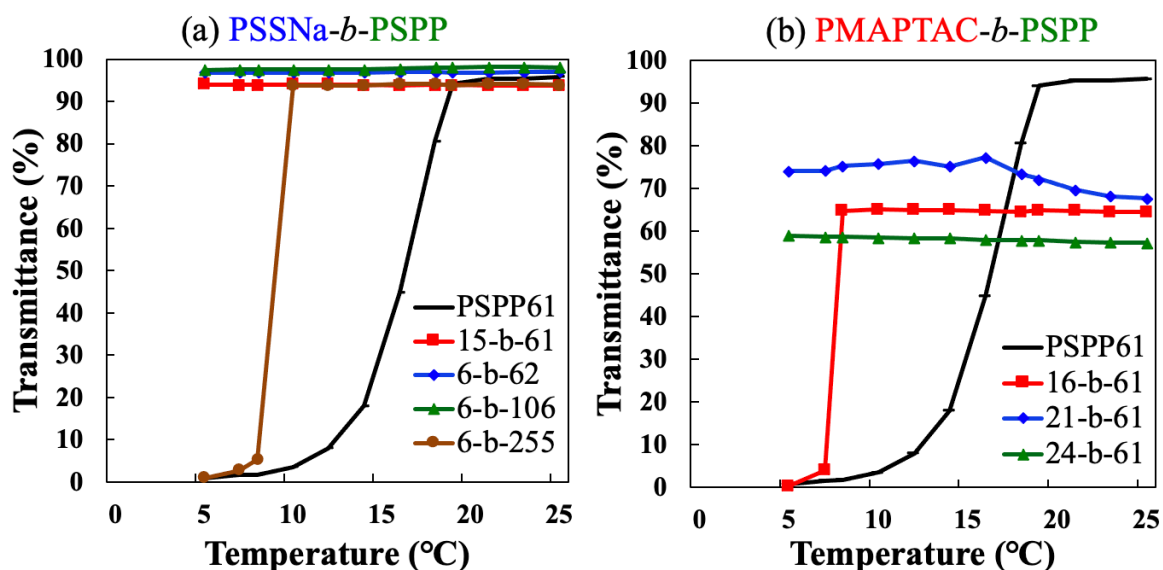

Figure 2-3. Block ratio dependence on the temperature responsivity of block copolymers having sulfobetaine: (a) PSSNa-*b*-PSPP and (b) PMAPTAC-*b*-PSPP.

2.3.3 Influence of Block Ratio on Temperature Responsivity

Since the temperature responsivity was considered to be very sensitive to the chain length of the ionic chain block, the influence of block ratio on the temperature responsivity was investigated. First, PSSNa-*b*-PSPP block copolymers with different block ratio were synthesized. The block ratios were 1:4.1 (15:61), 1:10.3 (6:62), 1:17.7 (6:106) and 1:42.5 (6:255). Transmittances of the samples were measured at a concentration of 1 wt% and a wavelength of 400 nm. As shown in Figure 2-3a, the temperature response was confirmed when the block ratio was about 1:43 (6:255). Next, the transmittance was measured in the same way

for PMAPTAC-*b*-PSPP of different block ratios (1:3.8 (16:61), 1:2.9 (21:61) and 1:2.5 (24:61)). As shown in Figure 2-3b, the temperature response was confirmed when the block ratio was about 1:4 (16:61). On the basis of these results, block copolymers with temperature responsiveness were synthesized using SPP_{255}, $SSNa_6$-*b*-SPP_{255} (A block ratio of about 1:43) and $MAPTAC_{54}$-*b*-SPP_{255} (A block ratio of about 1:5) were obtained. Aqueous solutions of these polymers were prepared, and changes of the cloud point were observed by the transmittance. As a result, the cloud point shifted to a lower temperature by connecting ionic polymers. In particular, as shown in Figure 2-4, there was a large decrease of cloud point when PSSNa was introduced. This is thought to be due to the interaction between the sulfobetaine chains and the ionic chain. These results indicated that the temperature responsiveness is very sensitive to the chain length and the sign of the charge of the ionic chain block (anionic or cationic).
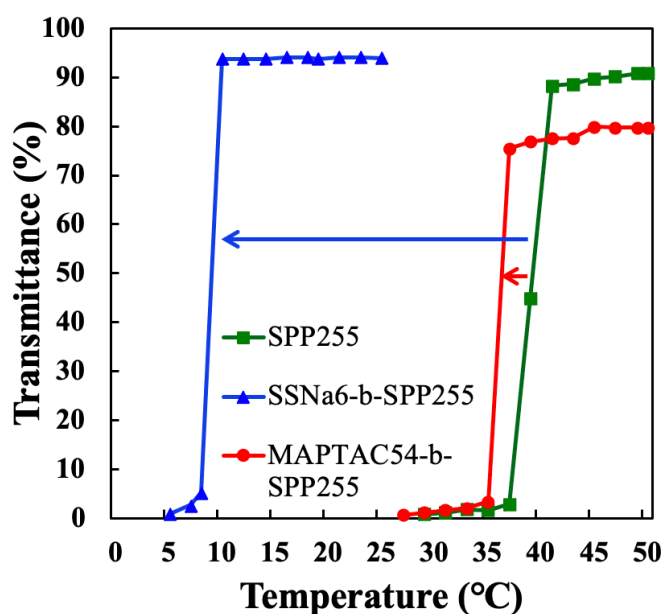

Figure 2-4. Change in cloud point by introducing an anionic chain block and a cationic chain block into SPP_{255} as evaluated by transmittance.

2.3.4 Effect of Addition of Ionic Homopolymer to Sulfobetaine

The interaction between the sulfobetaine chain and the ionic chain was investigated. PSPP, PSSNa which is an anionic polymer, and PMAPTAC which is a cationic polymer were each synthesized by RAFT polymerization. The degrees of polymerization were SPP$_{53}$, SPP$_{56}$, SPP$_{61}$, SSNa$_{52}$, SSNa$_{75}$, MAPTAC$_{54}$ and MAPTAC$_{85}$. First, the effect of anionic polymer addition on the temperature responsivity of the sulfobetaine homopolymer was investigated. Transmittance measurement was carried out by adding 1, 1/10, 1/100, 1/1000 and 0 equivalent of PSSNa homopolymers having different degrees of polymerization (DP: 52 and 75) to an aqueous solution of 1 wt% sulfobetiane homopolymer (SPP$_{53}$ and SPP$_{56}$). As a result, as shown in Figure 2-5a and 2-5b, in both cases, it was found that the addition of PSSNa homopolymers of about 1/100 equivalent eliminated the temperature response. However, it was found that the temperature response was more sensitive to PSSNa with a lower degree of polymerization (DP: 52) than the higher degree of polymerization (DP: 75). In the case of PSSNa, it interacts with quaternary ammonium cation (positive charge) in the middle of the sulfobetaine side chain. Therefore, it is considered that PSSNa with a lower DP (52) than the higher DP (75) is likely to enter inside the sulfobetaine chain to form complex. This might be the origin of sensitiveness. Next, the effect of cationic polymer addition on the temperature responsiveness of the sulfobetaine homopolymer was investigated. 1, 1/10, 1/100 and 0 equivalent of PMAPTAC homopolymer with different degree of polymerization (DP: 54 and 85) was added to the 1 wt% PSPP (DP: 56 and 61) aqueous solution, and them the transmittance was measured. As a result, disappearance of temperature responsiveness was observed with addition of about 1/10 equivalent as shown in Figure 2-6a and 2-6b. Further, it was found that they are less influenced by the degree of polymerization on the temperature responsivity. Because PMAPTAC interacts with the sulfonic acid (negative charge) located at the outside of PSPP side chain, it is considered that the influence of the degree of polymerization on the temperature

responsiveness, i.e., on complex formation, is small. From these results, it was suggested that the polysulfobetaine chain and the ionic chain interacted with each other, and that PSSNa was more sensitive than PMAPTAC.
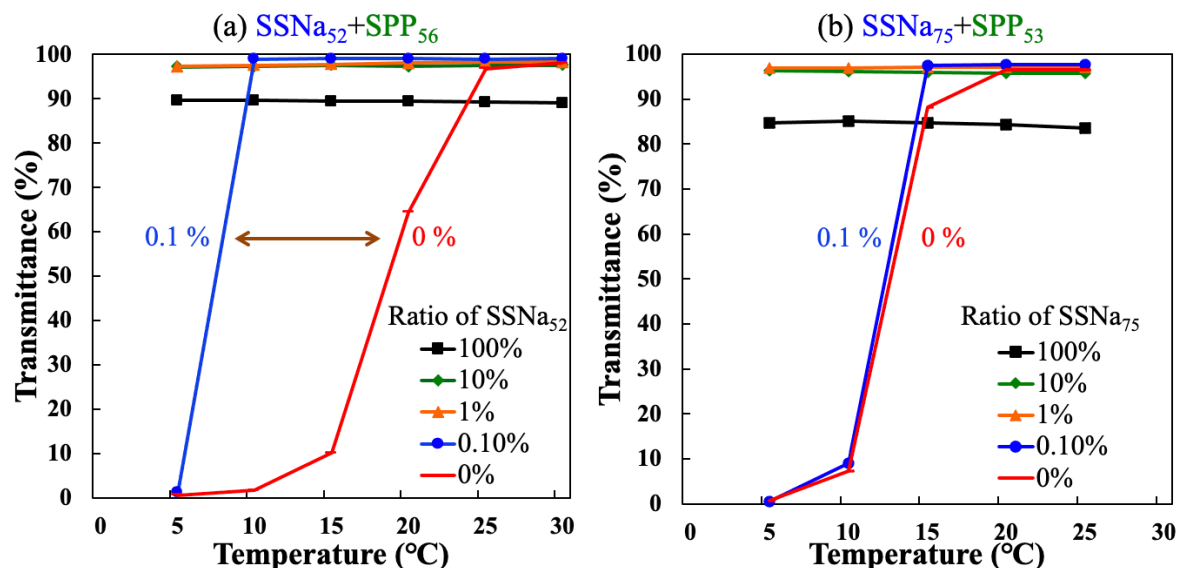
Figure 2-5. Addition effect of anionic polymers with different DPs on the temperature responsivity of sulfobetaine homopolymers in aqueous solutions: (a) SSNa$_{52}$ + SPP$_{56}$ and (b) SSNa$_{75}$ + SPP$_{53}$.
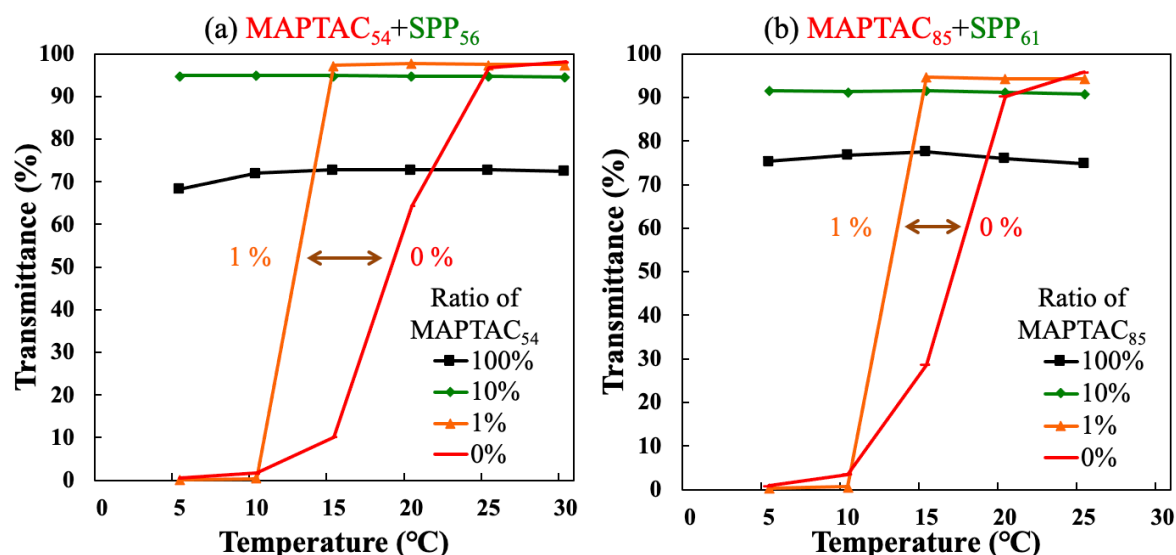

Figure 2-6. Addition effect of cationic polymers with different DPs on the temperature responsivity of sulfobetaine homopolymers in aqueous solutions: (a) MAPTAC$_{54}$ + SPP$_{56}$ and (b) MAPTAC$_{85}$ + SPP$_{61}$.

2.3.5 Interaction between Sulfobetaine Chain and Ionic Chain

Interaction between sulfobetaine chain and ionic chain was investigated by ^{1}H NMR spectra.[31-35] Using deuterium oxide (D_2O) as a solvent, all sample solutions were prepared to be 1 wt%. Firstly, the interaction between PSPP and PSSNa was investigated. The interaction between positive charge (quaternary ammonium cation) of PSPP and negative charge (sulfurous acid) of PSSNa was investigated by the change of the peak of 6 protons in the positive charge of PSPP. As shown in Figure 2-7, it was confirmed that by addition of PSSNa homopolymer (DP: 75) to PSPP homopolymer (DP: 53), the d peak of PSPP decreased. It was also confirmed that the d peak was small even in the case of the block copolymer ($SSNa_{36}$-*b*-SPP_{66}). Further, it was found that the peaks of a, c, e and g in the vicinity of the quaternary ammonium ion as well as the d peak of PSPP are totally broadened by the interaction of PSSNa and PSPP. In both the mixed system of homopolymers and the block copolymer, it was found that the positive charge of PSPP and the negative charge of PSSNa interact. Similarly, the interaction between PSPP and PMAPTAC was confirmed from ^{1}H NMR spectra. Paying attention to the change in the peak of 9 protons at the positive charge (quaternary ammonium cation) of PMAPTAC, it was observed whether the negative charge (sulfurous acid) of PSPP and the positive charge of PMAPTAC interacted or not. As shown in Figure 2-8, it was confirmed that by PMAPTAC homopolymer (DP: 85) addition to PSPP homopolymer (DP: 61), the d+o peak of the mixed solution of homopolymers decreased. It was also confirmed that the d+o peak was small even in the case of the block copolymer ($MAPTAC_{16}$-*b*-SPP_{61}). In addition, in the case of PMAPTAC and PSPP systems, unlike PSSNa and PSPP systems, the d+o peak is mainly affected. In both the mixed system of homopolymers and the block copolymer, it was confirmed that the negative charge of PSPP and the positive charge of PMAPTAC interact. These results proved that the sulfobetaine chain and the ionic chain

interact with each other.
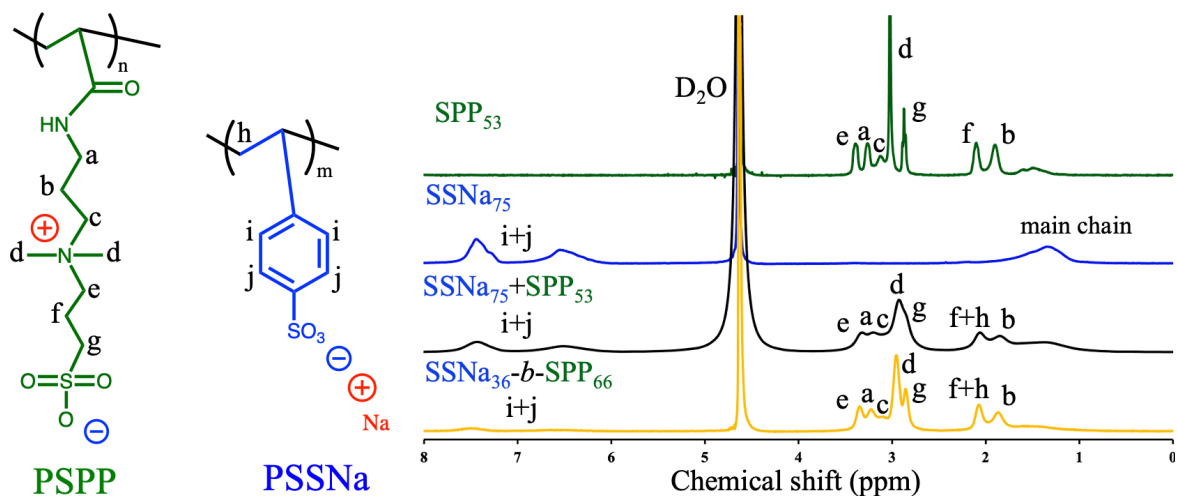
Figure 2-7. ^{1}H NMR spectra of PSPP, PSSNa, their mixture, and the block copolymer in D$_2$O.
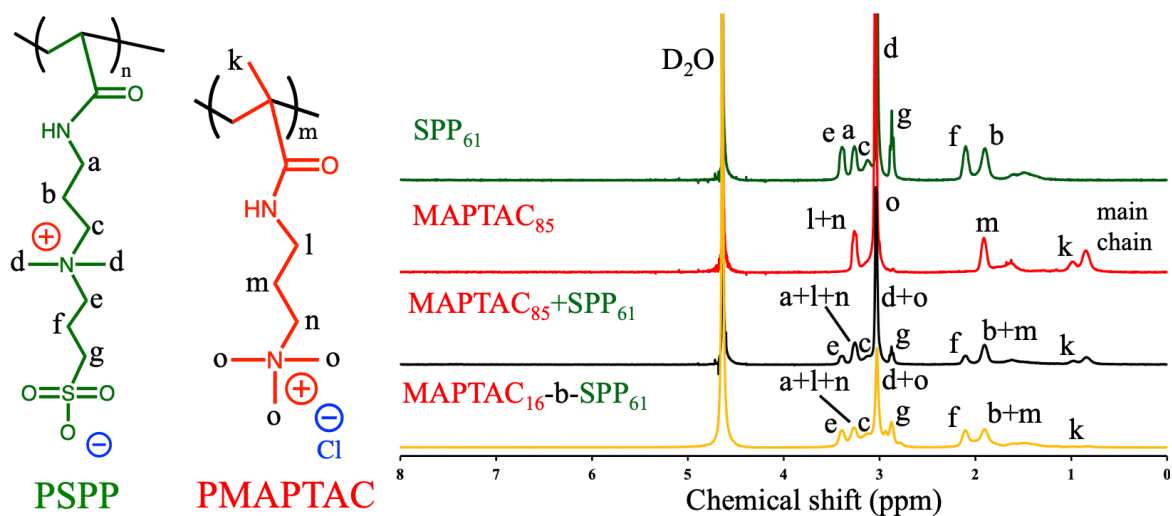
Figure 2-8. ^{1}H NMR spectra of PSPP, PMAPTAC, their mixture, and the block copolymer in D$_2$O.

2.4 Conclusions

Homopolymers of PSPP, PSSNa, PMAPTAC and block copolymers composed of polysulfobetaine (PSPP) and polyanion (PSSNa), polysulfobetaine and polycation (PMAPTAC) were synthesized by RAFT polymerization. First, the block ratio dependence of the temperature responsiveness of the block copolymer comprising a sulfobetaine chain and an ionic chain was investigated. The temperature responsivity was found to be exhibited at a block ratio of about 1:43 (2.3% or less) for PSSNa. On the other hand, in PMAPTAC, the temperature responsiveness was found at a block ratio of about 1:4 (25% or less). The temperature responsivity was confirmed to be very sensitive to the chain length of the ionic chain block.

The effect of addition of PSSNa and PMAPTAC homopolymer on the temperature responsiveness of the PSPP homopolymer was investigated by the transmittance. The temperature responsiveness was found to be exhibited by addition of 0.1% and 1%. Furthermore, ^{1}H NMR measurement revealed that the sulfobetaine chain and the ionic chain interacted with each other in a mixed system of homopolymers and a block copolymer. This might be the origin of disappearance of responsivity.

These results suggested that the polysulfobetaine chain and ionic chain interacted with each other, and PSSNa was more sensitive than PMAPTAC. This is because PSSNa is a strong acid, and it has a stronger interaction with PSPP. It may be possible to develop a novel temperature responsive polymeric material by adjusting the block ratio of sulfobetaine chain and ionic chain.

Mixing the two block copolymer aqueous solutions results in PIC micelles with sulfobetaine as the shell. This should serve as a basic for construction of temperature responsive, entirely ionic PIC micelles. It is expected that micelles with corona expansion and contraction in response to temperature changes can be formed.
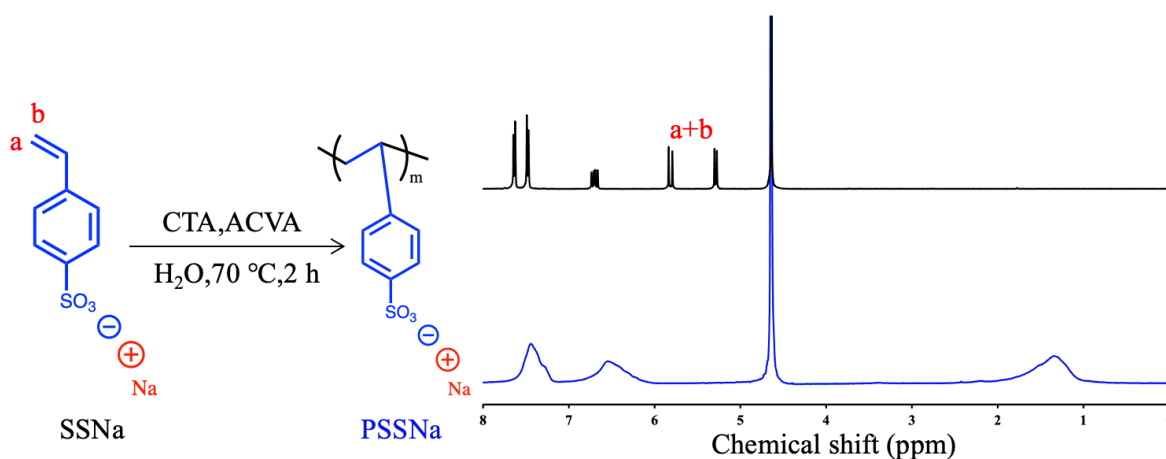
2.5 Appendix

2.5.1 Confirmation of the Synthesis of Homopolymers.

The synthesis could be confirmed by disappearance of the double bond peak of the monomer in ^{1}H NMR spectra.
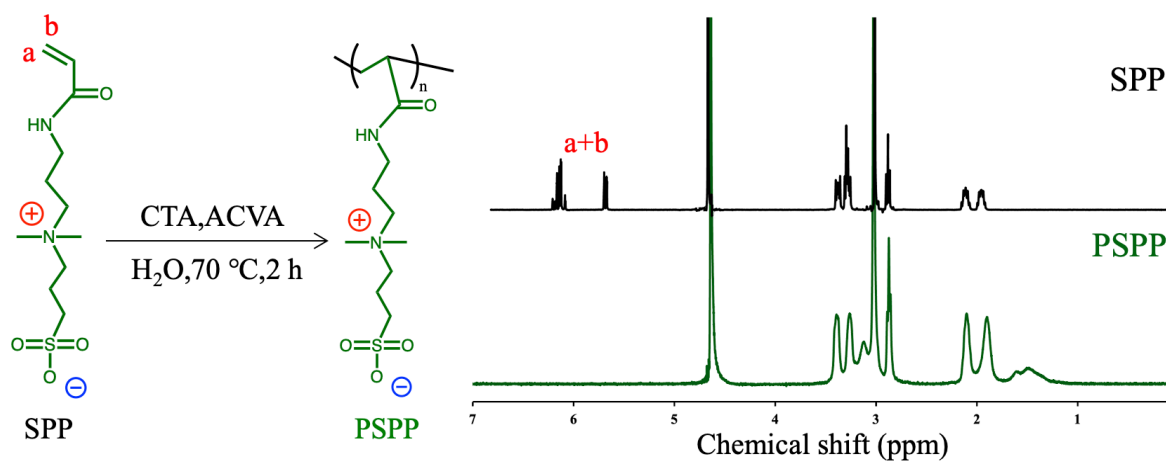
Figure 2-A1. Synthesis scheme of PSPP homopolymer (left) and ^{1}H NMR spectra of SPP monomer and PSPP homopolymer (right).

**Figure 2-A2.** Synthesis scheme of PSSNa homopolymer (left) and 1H NMR spectra of SSNa monomer and PSSNa homopolymer (right).
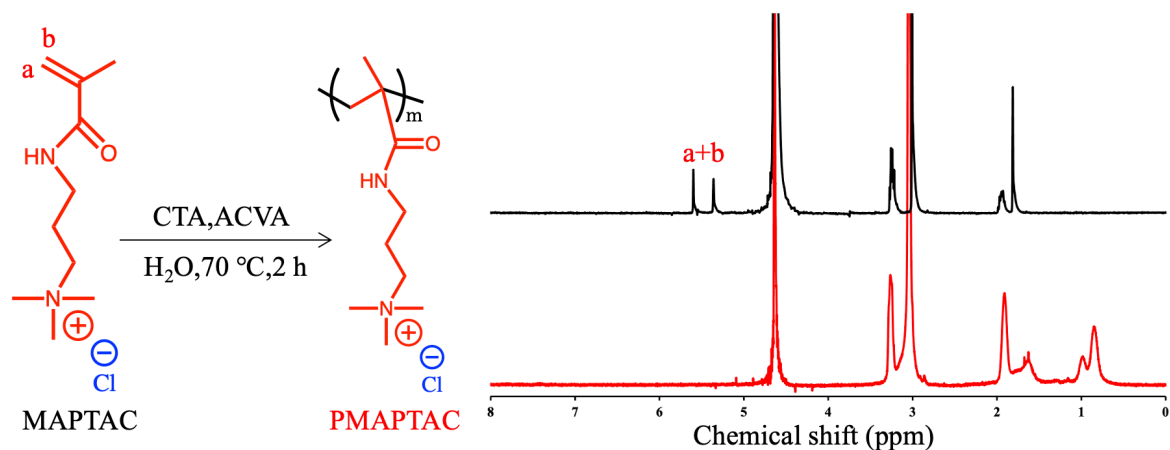
Figure 2-A3. Synthesis scheme of PMAPTAC homopolymer (left) and 1H NMR spectra of MAPTAC monomer and PMAPTAC homopolymer (right).

2.5.2 Estimation of Polydispersity Index (M_w/M_n) of PSSNa-*b*-PSPP and PMAPTAC-*b*-PSPP Block Copolymers.

The author conducted GPC measurement using two kinds of eluents. An anionic eluent (20 wt% CH$_3$CH aq, 0.05 M NaNO$_3$, 0.01 M Na$_2$HPO$_4$) was used for PSSNa-*b*-PSPP block copolymer. PSSNa was used as the standard sample. The result is shown in Figure A2-4. Then, a cationic eluent (0.5 M CH$_3$COOH, 0.3 M Na$_2$SO$_4$) was used for PMAPTAC-*b*-PSPP. P2VP was used as the standard sample. The result is shown in Figure A2-5.
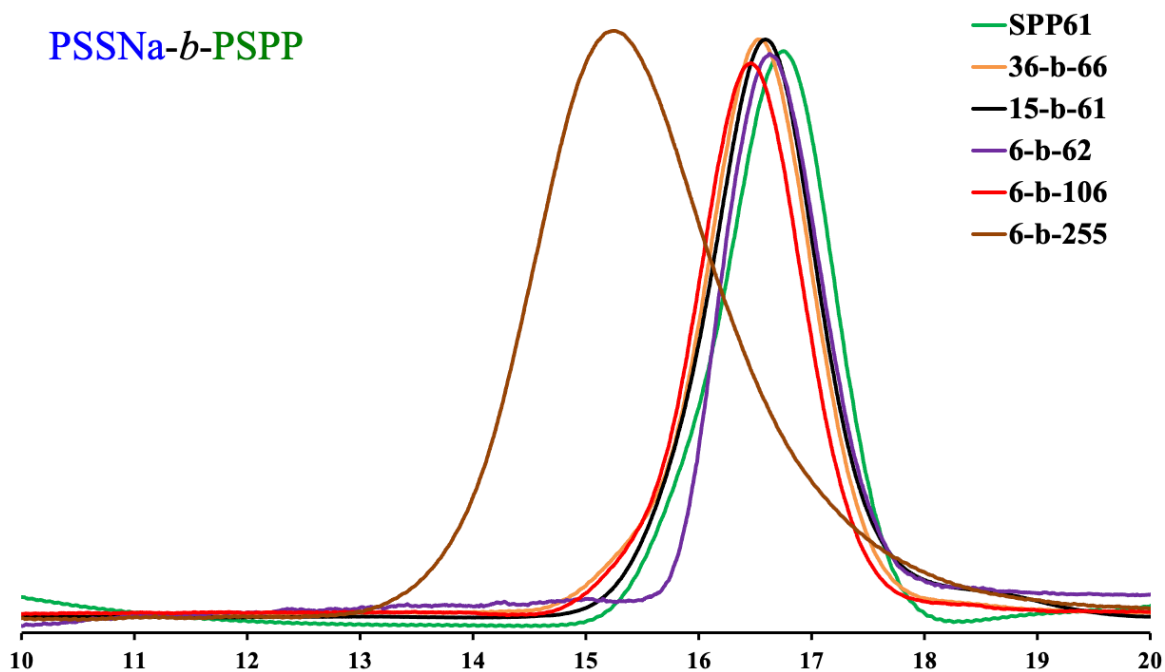
Figure 2-A4. GPC charts for PSSNa-*b*-PSPP with different block ratio.

SPP$_{61}$: M_n=17176 and M_w/M_n=1.13

SSNa$_{36}$-*b*-SPP$_{66}$: M_n =27103 and M_w/M_n =1.12

SSNa$_{15}$-*b*-SPP$_{61}$: M_n=24250 and M_w/M_n =1.12

SSNa$_{6}$-*b*-SPP$_{62}$: M_n=22638 and M_w/M_n =1.06

SSNa$_{6}$-b-SPP$_{106}$: M_n =30578 and M_w/M_n =1.14
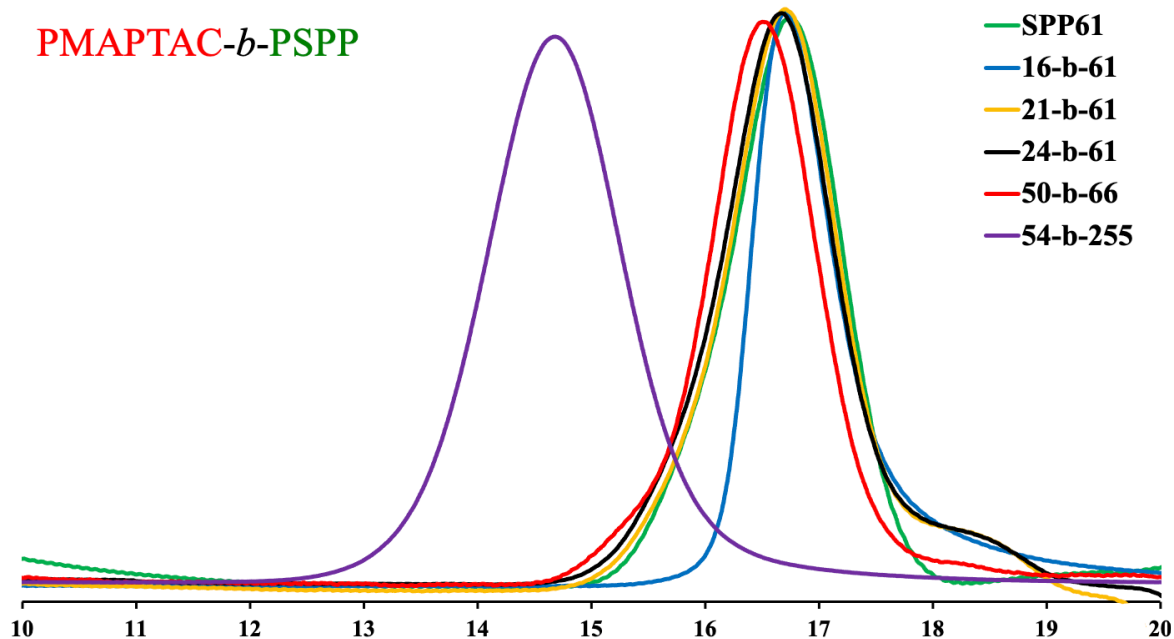
Figure 2-A5. GPC charts for PMAPTAC-*b*-PSPP with different block ratio.

SPP_{61}: M_n=17176 and M_w/M_n=1.13

$MAPTAC_{16}$-*b*-SPP_{61}: M_n =19801 and M_w/M_n =1.09

$MAPTAC_{21}$-*b*-SPP_{61}: M_n =19081 and M_w/M_n =1.11

$MAPTAC_{24}$-*b*-SPP_{61}: M_n =20245 and M_w/M_n =1.08

$MAPTAC_{50}$-*b*-SPP_{66}: M_n =30163 and M_w/M_n =1.17

$MAPTAC_{54}$-*b*-SPP_{255}: M_n =112356 and M_w/M_n =1.05

2.6 Reference

[1] H. Ladenheim, H. Morawetz, *J. Polym. Sci.* **1957**, 26, 251-254.

[2] R. Hart, M. Timmerman, *J. Polym. Sci., Part A: Polym. Chem.* **1958**, 28, 638-640.

[3] A. Laschewsky, *Polymers* **2014**, 6, 1544-1601.

[4] H. Matsuoka, Y. Yamakawa, A. Ghosh, Y. Saruwatari, *Langmuir* **2015**, 31, 4827-4836.

[5] S. Murugaboopathy, H. Matsuoka, *Colloid Polym. Sci.* **2015**, 293, 1317-1328.

[6] A. Ghosh, S. Yusa, H. Matsuoka, Y. Saruwatari, *J. Chem. Biol. Interfaces* **2013**, 1, 41-48.

[7] G.S. Georgiev, E.B. Kamenska, E.D. Vassileva, I.P. Kamenova, V.T. Georgieva, S.B. Iliev, I.A. Ivanov, *Biomolecules* **2006**, 7, 1329-1334.

[8] S. Xiao, Y. Zhang, M. Shen, F. Chen, P. Fan, M. Zhong, B. Ren, J. Yang, J. Zheng, *Langmuir.* **2018**, 34, 97-105.

[9] R. Quintana, D. Janczewski, V.A. Vasantha, S. Jana, S.S. Lee, F.J. Parravelandia, S. Guo, A. Parthiban, S.L. Teo, G.J. Vancso, *Colloids Surf., B* **2014**, 120 (8), 118-124.

[10] Z. Zhang, M. Moxey, A. Alswieleh, A.J. Morse, A.L. Lewis, M. Geoghegan, G.J. Leffett, *Langmuir* **2016**, 32 (20), 5048-5057.

[11] F. Wang, J. Yang, J. Zhao, *Polym. Int.* **2015**, 64, 999-1005.

[12] V. Hildebrand, A. Laschewsky, D. Zehm, *J. Biomater. Sci. Polym. Ed.* **2014**, 25, 1602-1618.

[13] T. Nakaya, Y.J. Li, *Prog. Polym. Sci.* **1999**, 24, 143-181.

[14] S. Jiang, Z. Cao, *Adv. Mater.* **2010**, 22, 920-932.

[15] D.W. Grainger, *Nat. Biotechnol.* **2013**, 31, 507-509.

[16] J. Du, Y. Tang, A.L. Lewis, S.P. Armes, *J. Am. Chem. Soc.* **2005**, 127, 17982-17983.

[17] A.B. Lowe, C.L. McCormick, *Chem. Rev.* **2002**, 102, 4177-4189.

[18] D.N. Schulz, D.G. Peiffer, P.K. Agarwal, J. Larabee, J.J. Kaladas, L. Soni, B. Handwerker, R.T. Garrner, *Polymer* **1986**, 27, 1734-1742.

[19] J.C. Salamone, W. Volksen, A.P. Olson, S.C. Israel, *Polymer* **1978**, 19, 1157-1162.

[20] P. Mary, D.D. Bendejacp, M.P. Labeau, P. Dupuis, *J. Phys. Chem. B* **2007**, 111, 7767-7777.

[21] M.V.M. Soto, J.C. Galin, *Polymer* **1984**, 25, 254-262.

[22] V. Hildebrand, A. Laschewsky, E. Wischerhoff, *Polym. Chem.* **2016**, 7, 731-740.

[23] B.J. Niebuur, J. Puchmayr, C. Herold, L.P. Kreuzer, V. Hildebrand, P.M. Buschbaum, A. Laschewsky, C.M. Paradakis, *Materials* **2018**, 11, 850.

[24] J. Chiefari, Y.K. Chong, F. Ercole, J. Krstina, J. Jeffery, T.P.T. Le, R.T.A. Mayadunne, G.F. Meijs, C.L. Moad, G. Moad, E. Rizzardo, S.H. Thang, *Macromolecules* **1998**, 31, 5559-5562.

[25] S. Perrier, *Macromolecules* **2017**, 50, 7433-7447.

[26] A. Harada, K. Kataoka, *Macromolecules* **1995**, 28, 5294-5299.

[27] K. Nakai, K. Ishihara, M. Kappl, S. Fujii, Y. Nakamura, S. Yusa, *Polymers* **2017**, 9, 49

[28] J. Seuring, S. Agarwal, *Macromol. Rapid Commun.* **2012**, 33, 1898-1920.

[29] S. Kudaibergenov, W. Jaeger, A. Laschewsky, *Adv. Polym. Sci.* **2006**, 201, 157-224.

[30] Y. Mitsukami, M.S. Donovan, A.B. Lowe, C.L. McCormick, *Macromolecules* **2001**, 34, 2248-2256.

[31] M. Bieri, A.H. Kwan, M. Mobli, G.F. King, J.P. Mackay, P.R. Gooley, *FEBS Journal* **2011**, 278, 704-715.

[32] Z. Fei, D. Zhao, T.J. Geldbach, R. Scopelliti, P.J. Dyson, S. Antonijevic, G. Bodenhausen, *Angew. Chem. Int. Ed.* **2005**, 44, 5720-5725.

[33] B. Sellergren, M. Lepisto, K. Mosbach, *J. Am. Chem. Soc.* **1988**, 110, 5853-5860.

[34] V. McBrierty, D.C. Douglass, *J. Polym. Sci. Macromol. Rev.* **1981**, 16, 295-366.

[35] W.F. Lee, C.C. Tsai, *Polymer* **1994**, 35, 2210-2217.

Chapter 3

Formation of Sulfobetaine-Containing Entirely Ionic PIC (Polyion Complex) Micelles and Their Temperature Responsivity

Sulfobetaine, a type of zwitterionic polymer, is a highly biocompatible polymer with temperature responsiveness of the upper critical solution temperature (UCST) type. The objective of this research was to construct polyion complex (PIC) micelles in the shell of sulfobetaine that had these properties. The author used poly(sulfopropyl dimethylammonium propylacrylamide) (PSPP) as sulfobetaine, poly(sodium styrenesulfonate) (PSSNa) as the anionic polymer and poly[3-(methacrylamido)propyl trimethylammonium chloride] (PMAPTAC) as the cationic polymer. The fundamental properties of the sulfobetaine-containing polymer and the complex were investigated in order to construct micelles in which corona expands and contracts in response to temperature change. Changes in cloud point were observed from transmittance for sulfobetaine homopolymers with different degrees of polymerization and concentration and aqueous solution of temperature- responsive diblock copolymers with different concentrations. The concentration and degree of polymerization dependencies on temperature responsivity were determined. Then the author mixed two diblock copolymer aqueous solutions which did not have temperature responsivity so that the charge numbers of anions and cations became equal, and the temperature responsivity and the formation of micelles were confirmed from ^{1}H NMR, DLS and transmittance. This confirmed the formation of PIC micelles with temperature responsivity. The diblock copolymer did not have temperature responsivity due to the influence of block ratio by introduction of ionic chain.

However, it is considered to have temperature responsivity because the ionic chain becomes the core when PIC micelles are formed. Furthermore, the PIC micelles with temperature responsivity also had a degree of polymerization and concentration dependencies.

3.1 Introduction

Betaine polymers have both anions and cations in the same molecule.[1-3] The structural properties are highly biocompatible since the structure of the betaine polymer is similar to that of phosphatidylcholine (PC) that make up the cells.[4,5] There is much research on biomaterials and medical materials.[6-9]

The betaine polymer is divided into carboxybetaine, sulfobetaine and phosphobetaine,[2,3] and they have characteristics pH response,[10-13] temperature response of the upper critical solution temperature (UCST) type,[14-18] and high biocompatibility,[4,5,19] respectively.

Taking advantage of such characteristics, micelles were prepared using diblock copolymers consisting of betaine polymers (carboxybetaine or sulfobetaine) that showed a response to stimuli and a hydrophobic chain. In these micelles, the core part is a hydrophobic chain, and the shell part is a betaine polymer chain. Micelles expand and contract part of the shell in response to external stimuli,[20,21] and their responsiveness depends on the concentration of the polymer solution, the molecular weight of the polymer, and the concentration of added salt.[17,22-27] Much research has been done on betaine brushes, polyion complex (PIC) micelles and biomaterials using the phosphobetaine polymer.[28-32]

In this study, with the aim of constructing a micelle in which the corona is expanded and contracted in response to temperature change, PIC micelles were prepared using an entirely

ionic diblock copolymer consisting of a sulfobetaine with the UCST-type temperature response and an ionic chain (anionic chain or cationic chain). Unlike ordinary micelles, which have a hydrophobic core, PIC micelles have a hydrophilic core because they are polyion complex. Furthermore, since the shell is sulfobetaine having temperature responsiveness, it is expected to be applied as a temperature targeting type carrier that transfers a hydrophilic drug. In order to clarify the fundamental properties of the sulfobetaine-containing polymer, the author investigated the dependence of the polymer on the degree of polymerization (DP) and the concentration dependence of the temperature response. First, in order to confirm the degree of polymerization dependency and concentration dependency on the temperature response of sulfobetaine homopolymers and entirely ionic diblock copolymer (PSSNa-*b*-PSPP and PMAPTAC-*b*-PSPP), the change in transition temperature due to the temperature change was examined by the transmittance. Then, the formation of PIC micelles consisting of sulfobetaine-containing entirely ionic diblock copolymers and the degree of polymerization dependency and concentration dependency on their temperature response were examined by ^{1}H NMR, DLS, and transmittance.

3.2 Experimental

3.2.1 Materials

Sulfobetaine (SPP) and 3-(methacrylamido)propyl trimethylammonium chloride (MAPTAC) monomers were kindly donated by Osaka Organic Chemical Industry Ltd. (Osaka, Japan). 4,4′-Azobis(4-cyanovaleric acid) (ACVA, 98%), *p*-styrenesulfonic acid sodium salt (SSNa), sodium nitrate (NaNO$_3$), and disodium hydrogenphosphate (Na$_2$HPO$_4$), were purchased from Wako (Osaka, Japan). Sodium sulfate (Na$_2$SO$_4$) and acetonitrile (CH$_3$CN, 99.5%) were purchased from FUJIFILM Wako Pure Chemical Corporation (Osaka, Japan). Acetic acid (CH$_3$COOH) was purchased from Nacalai Tesque (Kyoto, Japan). 4-

Cyanopentanoic acid dithiobenzoate was used as a chain transfer agent (CTA), which was synthesized as reported by Mitsukami et al.[33] Deuterium oxide (D_2O, 99.9%) was a product of Cambridge Isotope Laboratory (CIL) (U.K.). The water used for synthesis, solution preparation and dialysis were ultrapure water obtained using the Milli-Q system (18.2 MΩcm). Dialysis for PSPP homopolymers and PSSNa-*b*-PSPP, PMAPTAC-*b*-PSPP diblock copolymers purification was carried out with a dialysis tube from Orange Scientific (MWCO: 3500 and 12000~16000).

3.2.2 Synthesis of Homopolymers and Diblock Copolymers.

The PSPP (poly(sulfopropyl dimethylammonium propylacrylamide)) homopolymers were the synthesized by the reversible addition-fragmentation chain transfer (RAFT) technique. The synthesis was carried out by mixing SPP monomer, CTA and initiator (ACVA) in various molar ratios as reported previously.[34] The degree of polymerization (DP) and dispersity (Đ) of the obtained solid PSPP homopolymers were evaluated by GPC (Table 3-1). Homopolymers thus obtained were confirmed by ^{1}H NMR.

The PSPP homopolymer was used as macro-CTA, and diblock copolymers were synthesized by adding SSNa (sodium styrenesulfonate) as the anionic monomer or MAPTAC [3-(methacrylamido)propyl trimethylammonium chloride] as the cationic monomer and ACVA in various molar ratios. The solid PSSNa-*b*-PSPP and PMAPTAC-*b*-PSPP were obtained in the same way. The block ratio, synthesis result and PDI were determined by analyzing the ^{1}H NMR spectrum and GPC (Table 3-2).

3.2.3 ^{1}H Nuclear Magnetic Resonance (NMR)

^{1}H NMR spectra for PSPP homopolymers and diblock copolymers composed of PSPP and PSSNa (or PMAPTAC) were obtained with a JEOL JNM-EX 400 spectrometer using as a

solvent D_2O (CIL, 99.99%). The concentration of polymer solutions was 10 mg/mL.

Table 3-1. Polymerization Conditions for the Synthesis and Characteristics of PSPP Homopolymers (Polymerization Temperature and Time: 70 °C, 2 h).

Polymer	Monomer (mmol)	RAFT agent (mmol)[a]	Initiator (mmol)[b]	Water (mL)	Yield (%)	M_n (g/mol)[c]	PDI (M_w/M_n)[c]	DP (n)
PSPP-1	9.5	7.2×10^{-2}	7.2×10^{-2}	3	52	11200	1.15	39
PSPP-2	8.6	1.4×10^{-1}	7.2×10^{-2}	3	75	15000	1.08	53
PSPP-3	8.6	1.4×10^{-1}	7.2×10^{-2}	3	69	15600	1.09	55
PSPP-4	8.6	1.4×10^{-1}	7.2×10^{-2}	3	73	17200	1.13	61
PSPP-5	9.4	1.4×10^{-1}	7.2×10^{-2}	3	82	18500	1.09	66
PSPP-6	18.0	4.0×10^{-1}	2.0×10^{-1}	9	88	19100	1.06	68
PSPP-7	11.8	1.4×10^{-1}	7.2×10^{-2}	4	89	26600	1.12	95
PSPP-8	15.1	1.4×10^{-1}	7.2×10^{-2}	5	87	29600	1.09	106
PSPP-9	25.0	2.9×10^{-2}	1.4×10^{-2}	10	90	150300	1.08	540

[a]SPP, sulfobetaine. For the synthesis of homopolymers, the amount of the macro-RAFT agent is in mmol. [b]For the synthesis of homopolymers, 4,4′-azobis(4-cyanovaleic acid) (ACVA) was used as the initiator. [c]Determined by GPC with a cationic eluent (P2VP standard). PSPP was determined with a cationic eluent.

Table 3-2. Polymerization Conditions for the Synthesis and Characteristics of Diblock Copolymers (PSSNa-*b*-PSPP and PMAPTAC-*b*-PSPP; Polymerization Temperature and Time: 70 °C, 24 h).

Polymer[a]	monomer (mmol)	RAFT agent (mmol)	Initiator (mmol)	Yield (%)	M_n (g/mol)	PDI (M_w/M_n)	degree of polymerization m^b	n^b
SSNa_m-*b*-PSPP_n-9	1.2×10^{-1}	5.4×10^{-3}	5.4×10^{-3}	64	153200	1.16	14	540
SSNa_m-*b*-PSPP_n-6	3.9	7.9×10^{-2}	7.9×10^{-2}	81	26700	1.12	37	68
SSNa_m-*b*-PSPP_n-7	1.4	3.8×10^{-2}	3.8×10^{-2}	92	33800	1.08	35	95
MAPTAC_m-*b*-PSPP_n-3	4.3×10^{-1}	3.9×10^{-2}	3.9×10^{-2}	41	18400	1.09	13	55
MAPTAC_m-*b*-PSPP_n-6	3.9	7.9×10^{-2}	7.9×10^{-2}	79	30300	1.17	51	68
MAPTAC_m-*b*-PSPP_n-7	1.4	3.8×10^{-2}	3.8×10^{-2}	75	37900	1.17	51	95

[a]SPP, sulfobetaine; SSNa, *p*-styrenesulfonic acid sodium salt; and MAPTAC, 3-(methacryl-amido)propyl trimethylammonium chloride. [b]*m* and *n*: degree of polymerization of ionic and sulfobetaine blocks, respectively (*m* was determined by ^{1}H NMR).

3.2.4 Gel Permeation Chromatography (GPC)

The degree of polymerization and its dispersity were determined by a JASCO GPC system (Tokyo, Japan) composed of a 830-RI RI detector, UV-2075 Plus UV detector, CO-2065 Plus column oven, PU-2080 Plus HPLC pump, DG-2080-53 3-line degasser and Shodex SB-804 HQ column. The pH 3 buffer solution (0.3 M Na_2SO_4, 0.5 M CH_3COOH) was used as the cationic eluent and the mixed solution (20 wt% CH_3CN aq, 0.05 M $NaNO_3$, 0.01 M Na_2HPO_4) as the anionic eluent. Poly(2-vinylpyridine) (P2VP) (Scientific Polymer Product, Inc.) and poly(*p*-styrenesulfonic acid sodium salt) (PSSNa) (Sigma-Aldrich) samples were used as cationic and anionic standards, respectively.

3.2.5 UV-Vis Measurement

The temperature responsiveness and cloud point of polymer aqueous solutions composed of PSPP were determined with a UV-vis spectrometer U-3310 (Hitachi) for various concentrations of solution. The turbidity of the sulfobetaine-containing polymers and PIC micelles was measured for 5-10 minutes after the temperature change. The author designated the cloud point as the temperature at which the transmittance of the solution is 50% or less of the maximum value at a wavelength of 400 nm.

3.2.6 Dynamic Light Scattering (DLS)

The hydrodynamic radius (R_h) of PIC micelles in water was estimated using a Photal SLS-7000DL (Otsuka electronics Co., LTD, Osaka, Japan) equipped with a GC-1000 photon correlator and a 15-mW He-Ne laser (wavelength 632.8 nm). DLS measurements were made at various concentrations and temperatures. The measurement was carried out for about 10 minutes after the temperature change. The time correlation function of the scattered field was measured at four scattering angles (60°, 75°, 90°, and 105°) with an accumulation time of 30

min. The double exponential method was used to analyze the time correlation function to estimate the decay rate Γ. The translational diffusion coefficient (D) was calculated from the plot of relaxation rate, Γ, against value of scattering wave vector, q^2. Then, from the obtained D value, the hydrodynamic radius (R_h) was calculated using the Stoke-Einstein equation, where η, k_B, and T are the solvent viscosity, Boltzmann constant, and absolute temperature, respectively.

$$\Gamma = Dq^2 \tag{1}$$

$$R_h = \frac{k_B T}{6\pi\eta D} \tag{2}$$
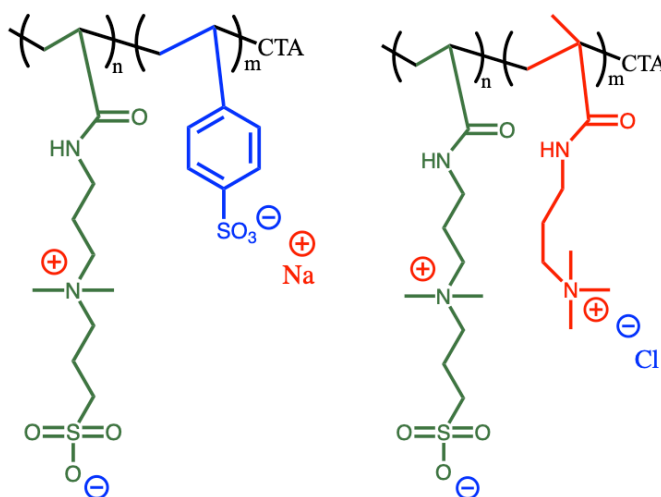
Figure 3-1. Chemical structures of (left) PSSNa-*b*-PSPP and (right) PMAPTAC-*b*-PSPP.

3.3 Results and Discussion

3.3.1 Characterization of Homopolymers and Block Copolymers

PSPP homopolymers with various degrees of polymerization (DP) could be synthesized. The degrees of polymerization and narrow dispersity (1.15 or less) confirmed from GPC are listed in Table 3-1. Using the obtained PSPP homopolymers as macro-CTA, PSSNa-*b*-PSPP and PMAPTAC-*b*-PSPP were synthesized under the conditions shown in Table

2. The block ratio of the diblock copolymers was calculated as reported previously.[34] Information on diblock copolymers is summarized in Table 3-2, and the dispersity (*Đ*) of the diblock copolymers was estimated by GPC (See the Supporting Information for details). The chemical structures of PSSNa-*b*-PSPP and PMAPTAC-*b*-PSPP are shown in Figure 3-1.
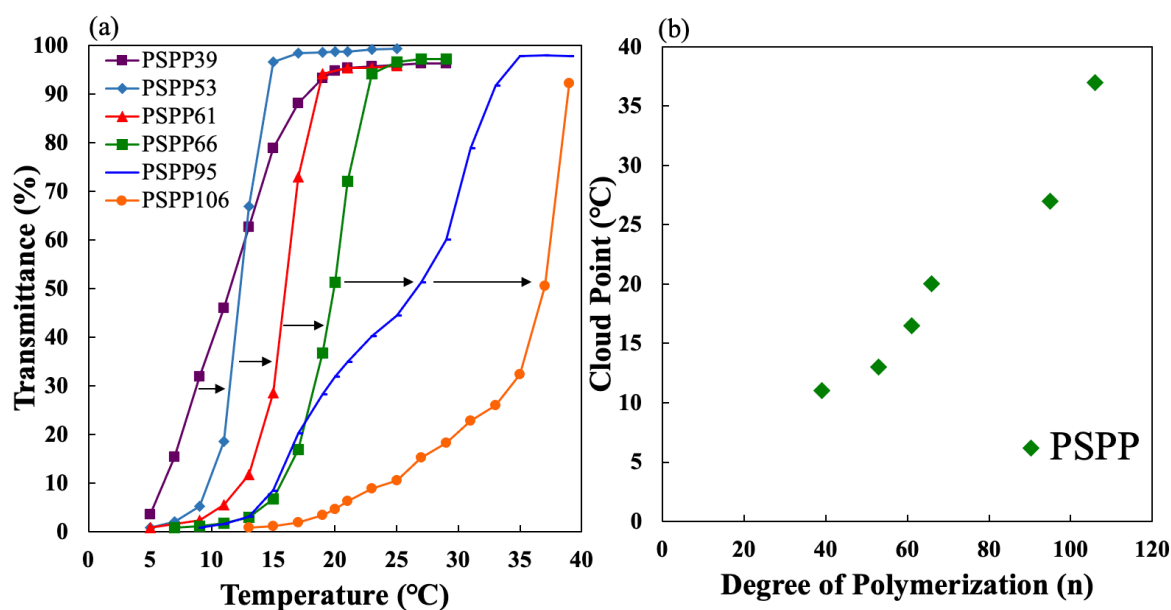
Figure 3-2. DP dependence on the temperature responsivity of PSPP homopolymers in aqueous solutions: (a) change of temperature-transmittance curve and (b) cloud point change due to DP change.

3.3.2 DP and Concentration Dependence on Temperature Responsivity of the Sulfobetaine Homopolymers

In order to investigate the degree of polymerization (DP) and the concentration dependencies of temperature responsiveness of the PSPP homopolymer, transmittance was measured. First, when the transmittance was measured for PSPP aqueous solution (10 mg/mL) with different degrees of polymerization (DP: 39~106), as shown in Figure 3-2a, the temperature-transmittance curve shifted to the higher temperature side and the cloud point increased with the increase in DP. In the case of low DP (39-66) of PSPP, electrostatic

interaction of the zwitterionic sulfobetaine group forms an intra- and intermolecular pair, and a drastic phase transition occurs. On the other hand, high DP (95 and 106) of PSPP, solubility declines with an increase in the overall hydrophobicity due to an increase in DP. So, it exhibits a slow phase transition.[2,35,36] As shown in Figure 3-2b, the degree of polymerization increased by about 2 times (DP: from 53 to 106), and the transition temperature also increased by about 24 °C (from 13 to 37 °C). The temperature responsivity of PSPP homopolymer depended on the degree of polymerization of the polymer. This is considered to be due to the increased overall hydrophobicity of the PSPP as the degree of polymerization increases.[16,17,22] Then, an aqueous solution of SPP$_{53}$ different concentration (2.5~40 mg/mL) were prepared and the change of these cloud point was observed by the transmittance. As shown in Figure 3-3, the cloud point increased with increasing concentration, and the transition temperature became constant above a certain concentration. The transition temperature increased by 10 °C (from 5 to 15 °C) at the concentration from 2.5 to 15 mg/mL, and it became constant at the concentration of 15 mg/mL or more. Detailed information on shift of temperature-transmittance curve due to concentration change can be confirmed from Figure 3-A2. This showed that the transition temperature can be controlled by adjusting the degree of polymerization of the sulfobetaine homopolymer and the concentration of the polymer aqueous solution.

3.3.3 Concentration Dependence on Temperature Responsivity of Diblock Copolymers

From the influence of the block ratio of sulfobetaine chain and ionic chain which was clarified by our previous study,[34] diblock copolymers SSNa$_{14}$-*b*-SPP$_{540}$ and MAPTAC$_{13}$-*b*-SPP$_{55}$ having temperature responsivity were synthesized by RAFT polymerization. First, an aqueous solution of SSNa$_{14}$-*b*-SPP$_{540}$ was prepared at different concentrations (2.5~40 mg/mL), and changes in cloud point were observed by transmittance. As a result, as shown in

Figure 3-4a, the cloud point increased with increasing concentration, and it turned out that it became constant above a certain concentration. The transition temperature increased by 12 °C (from 21 to 33 °C) at the concentration from 2.5 to 10 mg/mL, and it became constant at the concentration of 10 mg/mL or more. This behavior was the same as the concentration dependence on temperature responsiveness of PSPP homopolymer. Likewise, in MAPTAC$_{13}$-b-SPP$_{55}$ (Concentration: 15~40 mg/mL), as a result of observing the concentration dependence on the temperature responsiveness, as shown in Figure 3-4b, the cloud point increased with increasing concentration. In this concentration range, the transition temperature rose by 16 °C (from 5 to 21 °C), but it did not become constant. Detailed information on shift of temperature-transmittance curve of diblock copolymers due to concentration change is shown in Figure 3-A3a and 3-A3b.
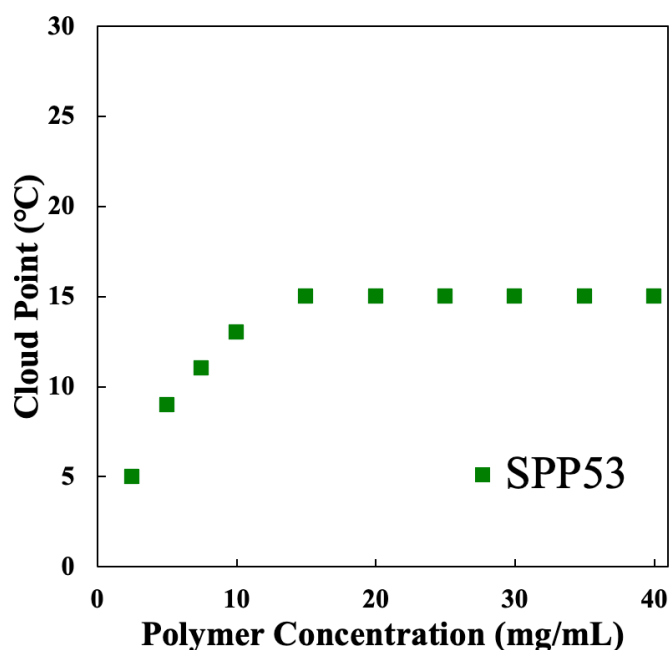
**Figure 3-3.** Change in the cloud point by concentration change of SPP$_{53}$ aqueous solution.
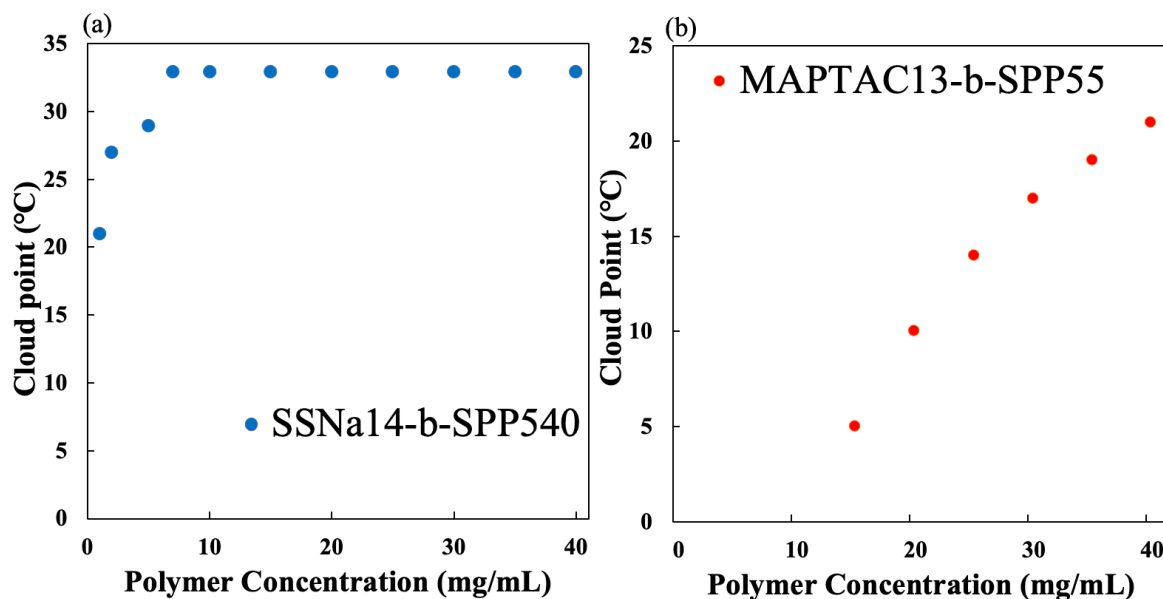
Figure 3-4. Concentration dependence of temperature-responsive diblock copolymers: (a) SSNa$_{14}$-*b*-SPP$_{540}$ and (b) MAPTAC$_{13}$-*b*-SPP$_{55}$.

3.3.4 Formation of Temperature-Responsive PIC Micelles

PIC (polyion complex) micelles were prepared using SSNa$_{37}$-*b*-SPP$_{68}$ and MAPTAC$_{51}$-*b*-SPP$_{68}$ with a block ratio of sulfobetaine chain to ionic chain of 50:50. These two block copolymers did not have temperature responsivity or concentration dependence due to the block ratio effect.[34] Detailed information is shown in Figure 3-A4a and 3-A4b. In the case of block copolymers, the temperature responsiveness disappears due to the influence of the block ratio by introduction of ionic chains, but when PIC micelles are formed, the ionic chains become the core and do not behave as ionic chains. This demonstrates the presence of temperature responsiveness PIC micelles were prepared by mixing two diblock copolymer aqueous solution so that the charge of the anion and cation are equal. Unless the mixing ratio is 1:1, the ionic chains and the sulfobetaine chains interact, and proper micelles cannot be formed. Then, it becomes difficult to express temperature responsivity. The concentration of

the overall PIC micelles in aqueous solution was adjusted to be 10 mg/mL. The formation of temperature-responsive PIC micelles was confirmed by ^{1}H NMR, DLS (dynamic light scattering) and transmittance. As shown in Figure 3-5, when the PIC micelles can be formed, the peak of the PSSNa (i + j) of SSNa$_{37}$-b-SPP$_{68}$ and the peak of PMAPTAC (m) of MAPTAC$_{51}$-b-SPP$_{68}$ disappear. Furthermore, the l, n, o peaks of the PMAPTAC had disappeared. This showed that micelles with the ionic chain as a core and sulfobetaine chain as the shell was formed.
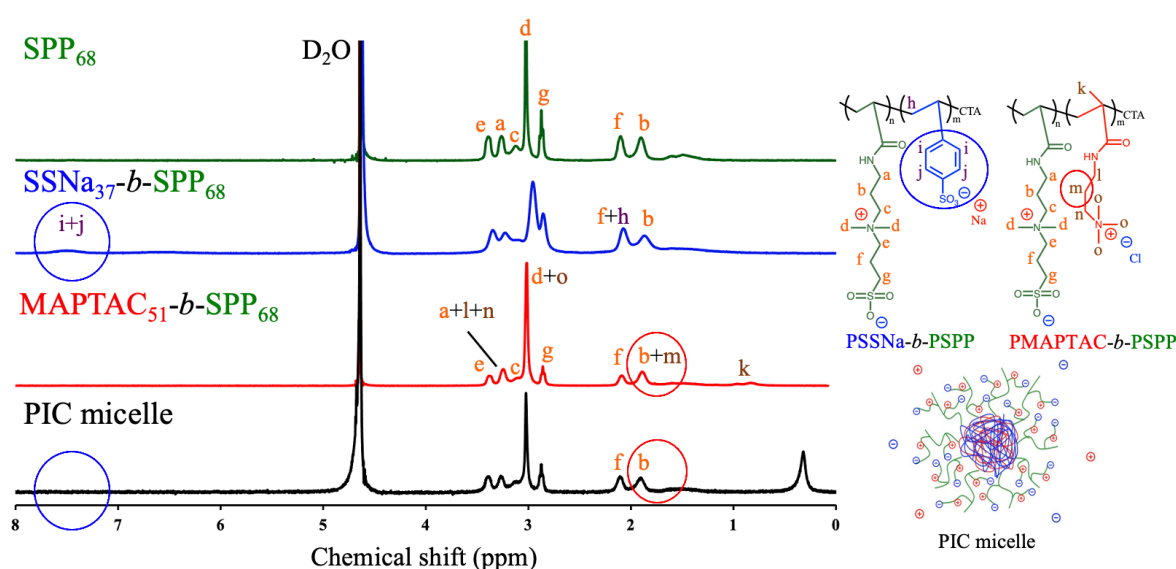
Figure 3-5. Confirmation of formation of PIC micelles by ^{1}H NMR spectra.

The DLS measurement confirmed that the micelles had a hydrodynamic radius (R_h) of 72 nm at 60 °C. PIC micelles were considered to have formed since they formed a large aggregate as compared with the extended chain length of each block copolymers being 26.7 nm (SSNa$_{37}$-b-SPP$_{68}$) and 30.2 nm (MAPTAC$_{51}$-b-SPP$_{68}$). Detailed DLS information is shown in Figure 3-A5. Furthermore, the temperature responsivity confirmed from the transmittance, as shown in Figure 3-6, revealed that the diblock copolymer that did not have temperature responsivity formed PIC micelles and thereby exhibited temperature responsivity. Since

micelles were formed in the PIC micelle aqueous solution at 10 mg/mL, it was blue at a temperature above the transition temperature and turned white and turbid at temperatures below the transition temperature.
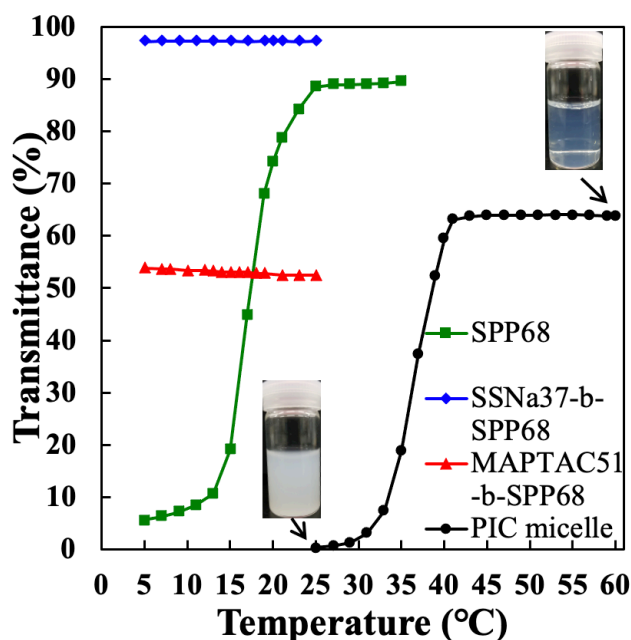

Figure 3-6. Formation of PIC micelles and confirmation of temperature responsivity.

3.3.5 Concentration Dependence on Temperature Responsiveness of PIC Micelles

Figure 3-7a shows the temperature-transmittance curve due to temperature change in PIC micelles aqueous solution at different concentrations (1~10 mg/mL). At 1 mg/mL, the PIC micelles aqueous solution did not have temperature responsivity. However, the temperature response began to appear from the concentration of 2.5 mg/mL, and the transition temperature shifted to the higher temperature side as the concentration increased (from 11 to 37 °C). Temperature responsiveness was also investigated using PIC micelles at 15 and 20 mg/mL, but it was instable and formed large aggregates of micelles and precipitated immediately even at 95 °C. The details are shown in Figure 3-A6. These results showed stable PIC micelles having temperature responsiveness are formed in aqueous solutions at concentrations from 1 to 10

mg/mL. The hysteresis (cooling-heating cycles) of the temperature response of PIC micelles due to changes in concentration can be confirmed by Figure 3-A7. The stable PIC micelles were maintained for several weeks to several months in the concentrations range (1~10 mg/mL) where precipitation did not occur.
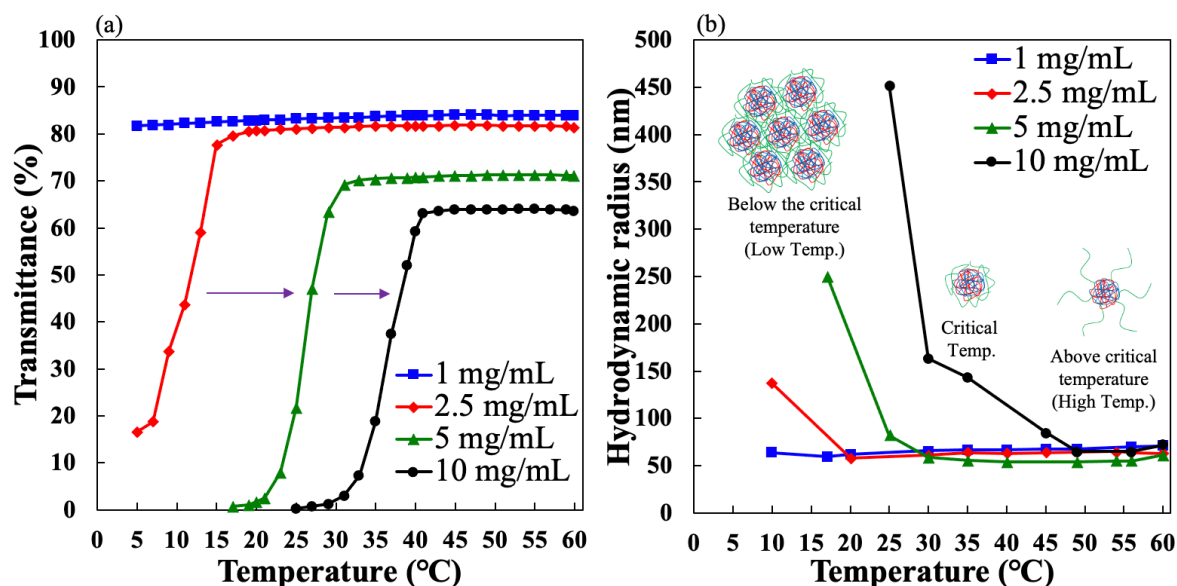
Figure 3-7. Concentration dependence of PIC micelle aqueous solutions: (a) change of the temperature-transmittance curve and (b) change of the hydrodynamic radius (R_h) with different concentrations.

Figure 3-7b is the cause of the shift in the transition temperature due to the concentration change of the PIC micelles aqueous solution. Changes in hydrodynamic radius (R_h) due to temperature changes of PIC micelles at different concentrations were observed by DLS. The micelle radius decreased with temperature increase in temperature-responsive PIC micelles. This is because the shell part is a sulfobetaine having the UCST-type temperature responsivity. Therefore, it is considered to exist in single micelles at high temperatures, the sulfobetaine chain begins to shrink near the transition temperature, and aggregates of micelles are formed below the transition temperature. Furthermore, PIC micelles at all concentrations

exhibiting temperature responsiveness began to form aggregates of micelles near the transition temperature, and at the higher concentrations they formed larger aggregates. At high concentrations, the sulfobetaine chains tend to aggregate and form large aggregates.[15,23] Therefore, it is considered that the transition temperature of PIC micelles shifts to the higher temperature side as the concentration increases.
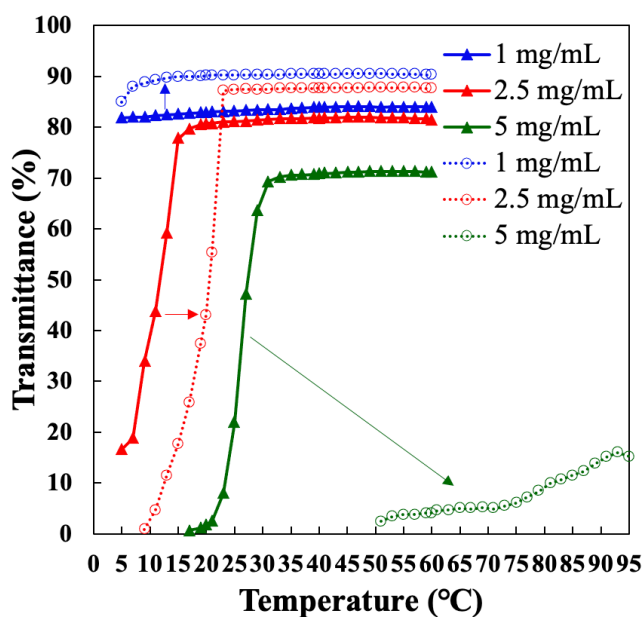
Figure 3-8. DP and concentration dependence on temperature responsivity of PIC micelles: PIC micelles ($SSNa_{37}$-b-SPP_{68} + $MAPTAC_{51}$-b-SPP_{68}, solid lines) and ($SSNa_{35}$-b-SPP_{95} + $MAPTAC_{51}$-b-SPP_{95}, broken lines).

3.3.6 Degree of Polymerization Dependence on Temperature Responsivity of PIC Micelles

By fixing the ionic chain as the core, the change in the transition temperature was investigated by adjusting the length of only the sulfobetaine chains as the shell (from SPP_{68} to SPP_{95}). The author obtained the $SSNa_{35}$-b-SPP_{95} and $MAPTAC_{51}$-b-SPP_{95} on this basis. Figure 3-8 compares the temperature responsiveness of PIC micelles prepared using these findings and the temperature responsiveness of PIC micelles with the SPP_{68} shell. The solid line has a

shell of sulfobetaine with a DP of 68 and the broken line is 95. At the concentration from 1 to 5 mg/mL, the cloud point where the sulfobetaine chain was longer shifted to the higher temperature side. Especially at 5 mg/mL, the cloud point shifted around 50 °C (from 27 to 77 °C). In addition, the PIC micelle with the SPP_{95} shell precipitated immediately because it is unstable at a concentration of 10 mg/mL at 95 °C. Compared to the micelle with the SPP_{68} shell, it formed unstable micelles at a low concentration. The temperature responsiveness of PIC micelles revealed the degree of polymerization and concentration dependencies. Large aggregates were easily formed as the concentration and degree of polymerization is increased.

3.4 Conclusions

PSPP homopolymers of various degrees of polymerization and sulfobetaine-containing diblock copolymers (PSSNa-*b*-PSPP and PMAPTAC-*b*-PSPP) were synthesized by the RAFT technique. The degree of polymerization and the concentration dependencies on the temperature responsiveness of the sulfobetaine homopolymer aqueous solution were investigated. The transition temperature shifted to the higher temperature side due to the increase in the degree of polymerization (DP: 39 to 106). The degree of polymerization increased by about 2 times (DP: from 53 to 106), and the transition temperature also increased by about 24 °C (from 13 to 37 °C). Then, in the aqueous solution of SPP_{53}, the cloud point increased by 10 °C (from 5 to 15 °C) as the concentration increased from 2.5 to 15 mg/mL, and became constant at concentrations above 15 mg/mL. Also, the sulfobetaine-containing diblock copolymers having temperature responsivity exhibited the same tendency depending on the concentration change. The transition temperature of an aqueous solution of $SSNa_{14}$-*b*-SPP_{540} increased by 12 °C (from 21 to 33 °C) as the concentration increased from 2.5 to 10 mg/mL, and it became constant at a concentration above 10 mg/mL. Whereas, in an aqueous solution of $MAPTAC_{13}$-*b*-SPP_{55}, the cloud point increased by 16 °C (from 5 to 21 °C) as the concentration increased from 15 to 40 mg/mL, but it did not become constant.

PIC micelles were prepared using two diblock copolymers (block ratio is roughly 50:50) that did not have temperature responsiveness. To form a proper PIC micelle, the length of the ionic chains forming the core must be 10 or more. The block copolymers which did not exhibit temperature responsiveness due to the effect of block ratio by introduction of an ionic chain (anionic chain or cationic chain) showed temperature responsiveness by forming PIC micelles. Then, if the mixing ratio is not 1:1, the ionic chain and the sulfobetaine chain interact, and it becomes difficult to form PIC micelles and exhibit temperature responsiveness. The temperature responsiveness was observed with PIC micelles in which the core is an ionic chain and the shell is a sulfobetaine chain. Formation of micelles in which corona expands and contracts in response to temperature change was confirmed by DLS. The sulfobetaine chain began to shrink near the transition temperature, and aggregates of micelles were formed below the transition temperature. Furthermore, the temperature responsiveness in PIC micelles revealed the degree of polymerization and concentration dependencies. When the concentration of the PIC micelles aqueous solution was 5 mg/mL, the cloud point was shifted by about 50 °C (from 27 to 77 °C) by changing the DP of PSPP from 68 to 95. Then, PIC micelles consisting of $PSSNa_{37}$-b-SPP_{68} and $MAPTAC_{51}$-b-SPP_{68} exhibited a critical temperature of 11 to 37 °C in the concentration range of 2.5~10 mg/mL.

These results suggested that the transition temperature can be controlled by adjusting the concentration of PIC micelle aqueous solution and degree of polymerization of sulfobetaine chain which serves as a shell. These PIC micelles are expected to be applicable to drug delivery systems carrying hydrophilic medicine because the core is the polyion complex.

3.5 Appendix

3.5.1 Estimation of Polydispersity Index (M_w/M_n) of PSSNa-*b*-PSPP and PMAPTAC-*b*-PSPP Block Copolymers.

The author conducted GPC measurements using two kinds of eluents. An anionic eluent (20 wt% CH_3CH aq, 0.05 M $NaNO_3$, 0.01 M Na_2HPO_4) was used for the PSSNa-*b*-PSPP block copolymer. PSSNa was used as the standard sample. Then, a cationic eluent (0.5 M CH_3COOH, 0.3 M Na_2SO_4) was used for PMAPTAC-*b*-PSPP. P2VP was used as the standard sample. The result is shown in Figure 3-A1.
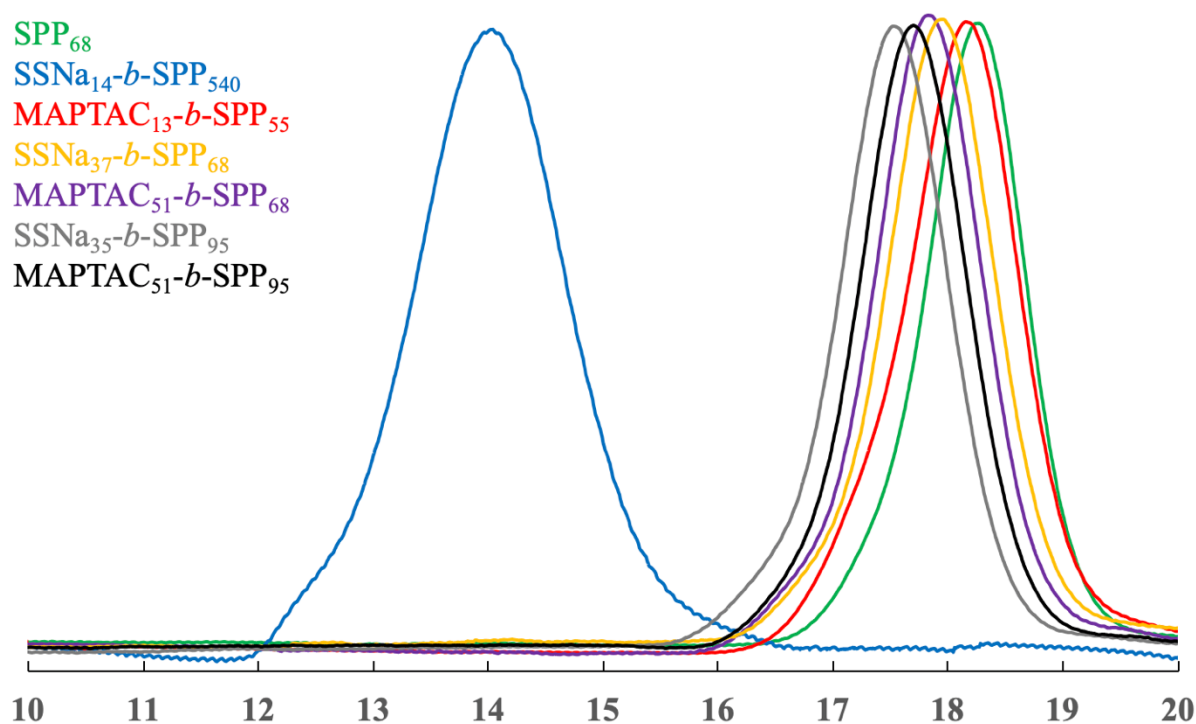
Figure 3-A1. GPC charts for PSSNa-*b*-PSPP and PMAPTAC-*b*-PSPP block copolymers.

SPP$_{68}$: M_n=19076 and M_w/M_n=1.06

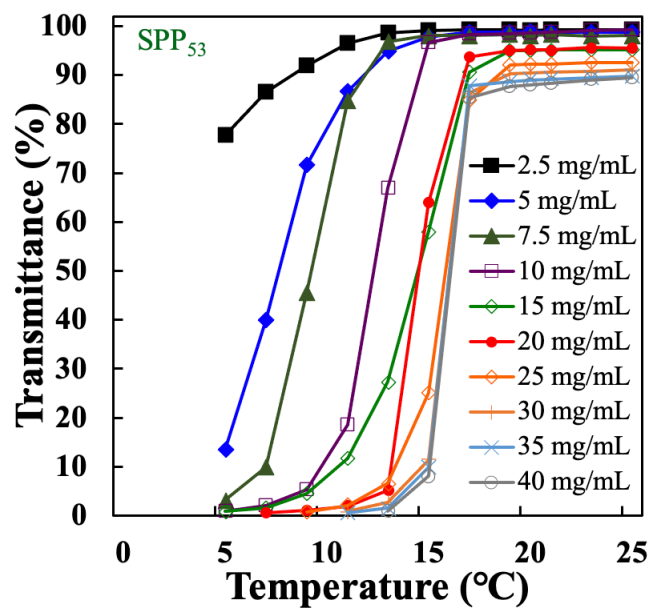SSNa$_{14}$-*b*-SPP$_{540}$: M_n=139636 and M_w/M_n=1.16

MAPTAC$_{13}$-*b*-SPP$_{55}$: M_n=21709 and M_w/M_n=1.09

SSNa$_{37}$-*b*-SPP$_{68}$: M_n=27107 and M_w/M_n=1.12

MAPTAC$_{51}$-b-SPP$_{68}$: M_n=30163 and M_w/M_n=1.17

SSNa$_{35}$-b-SPP$_{95}$: M_n=37997 and M_w/M_n=1.08

MAPTAC$_{51}$-b-SPP$_{95}$: M_n=33645 and M_w/M_n=1.17

Figure 3-A2. Shift of temperature-transmittance curve by concentration change of SPP$_{53}$ aqueous solution.
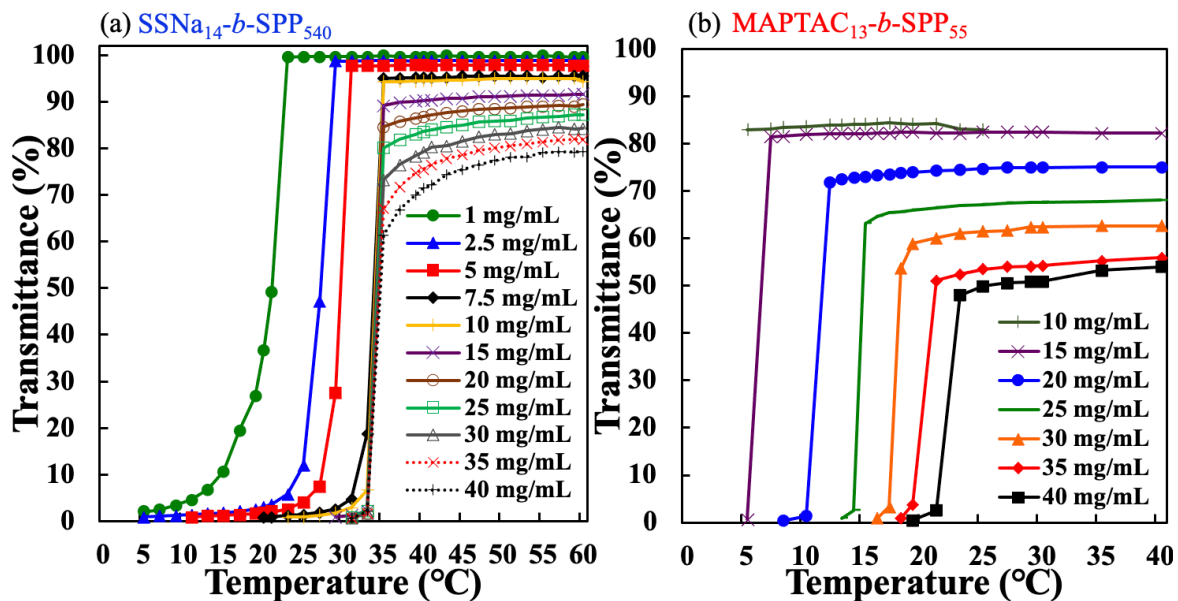
Figure 3-A3. Shift of temperature-transmittance curve by concentration change of block copolymer aqueous solutions: (a)SSNa$_{14}$-*b*-SPP$_{540}$, (b)MAPTAC$_{13}$-*b*-SPP55.
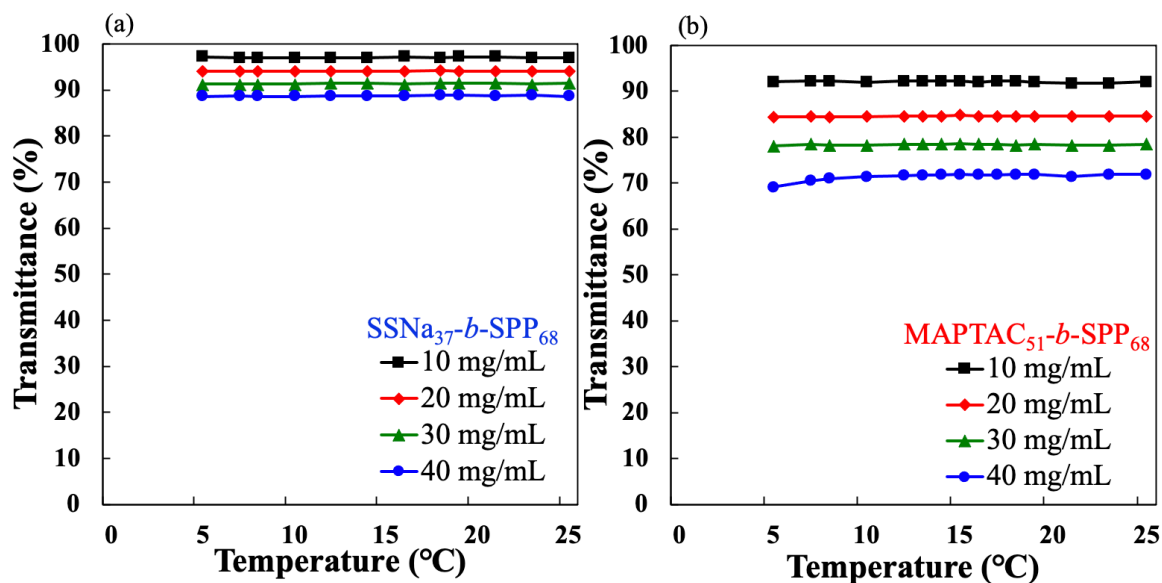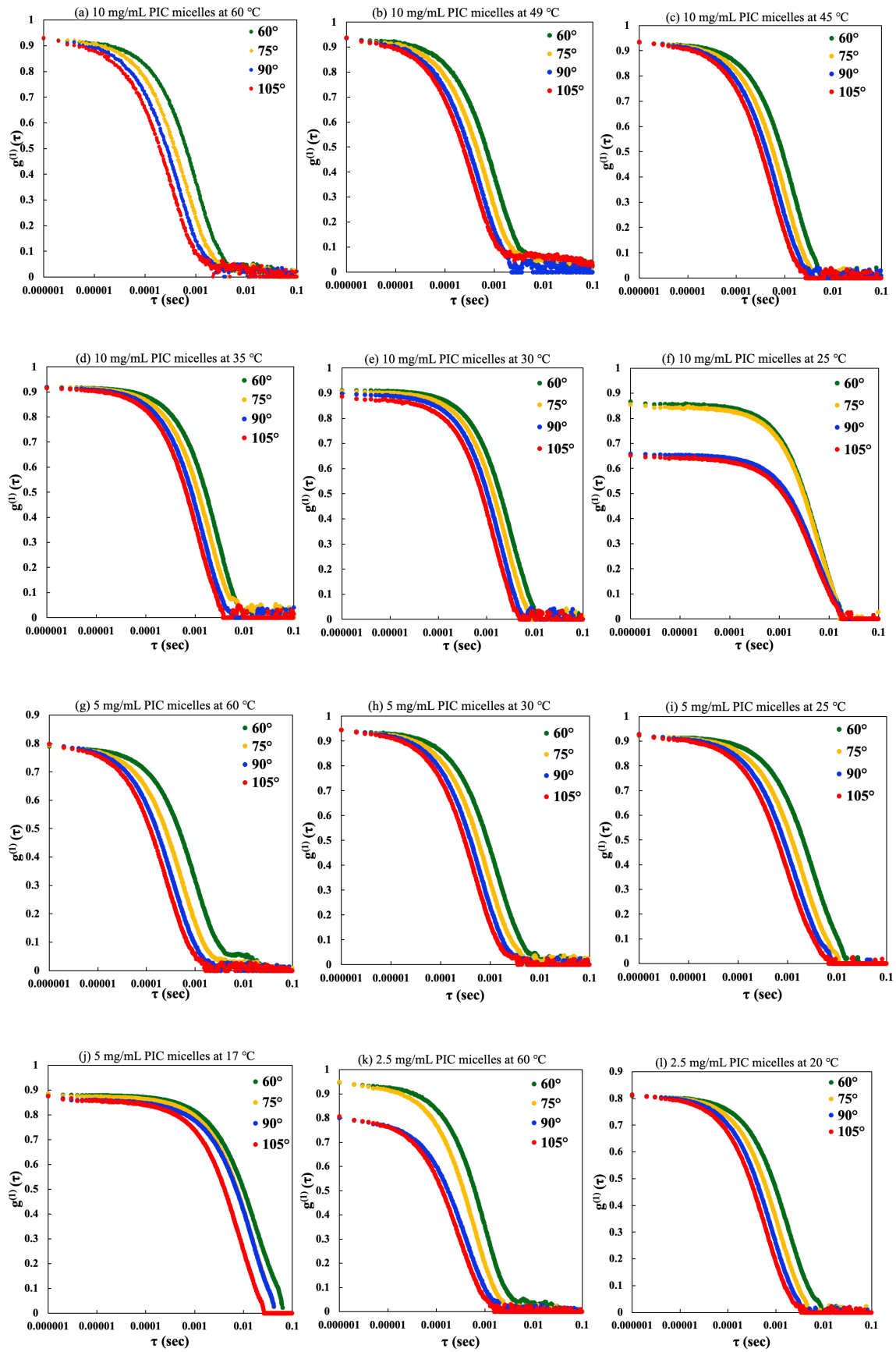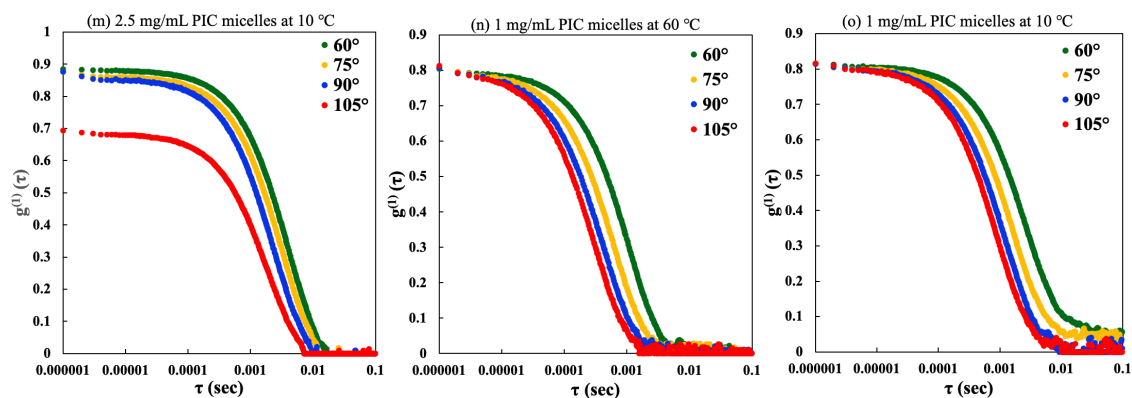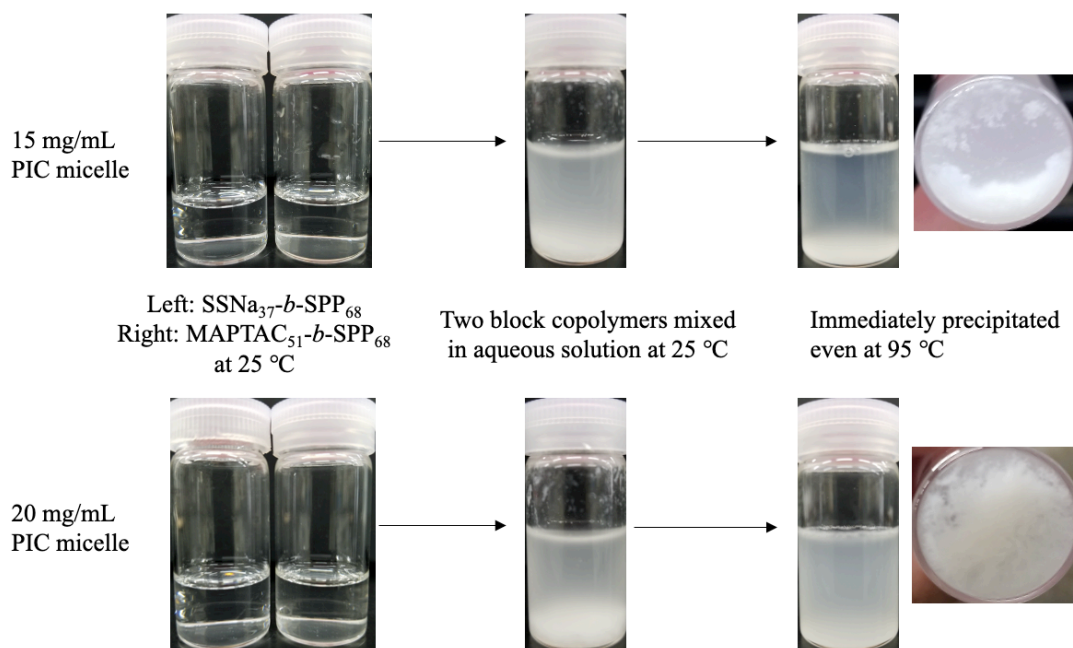

Figure 3-A4. Confirmation of concentration dependency of block copolymers without temperature responsivity: (a)SSNa$_{37}$-*b*-SPP$_{68}$ and (b)MAPTAC$_{51}$-*b*-SPP$_{68}$.

(a) 10 mg/mL PIC micelles at 60 ℃
(b) 10 mg/mL PIC micelles at 49 ℃
(c) 10 mg/mL PIC micelles at 45 ℃
(d) 10 mg/mL PIC micelles at 35 ℃
(e) 10 mg/mL PIC micelles at 30 ℃
(f) 10 mg/mL PIC micelles at 25 ℃
(g) 5 mg/mL PIC micelles at 60 ℃
(h) 5 mg/mL PIC micelles at 30 ℃
(i) 5 mg/mL PIC micelles at 25 ℃
(j) 5 mg/mL PIC micelles at 17 ℃
(k) 2.5 mg/mL PIC micelles at 60 ℃
(l) 2.5 mg/mL PIC micelles at 20 ℃

(m) 2.5 mg/mL PIC micelles at 10 ℃
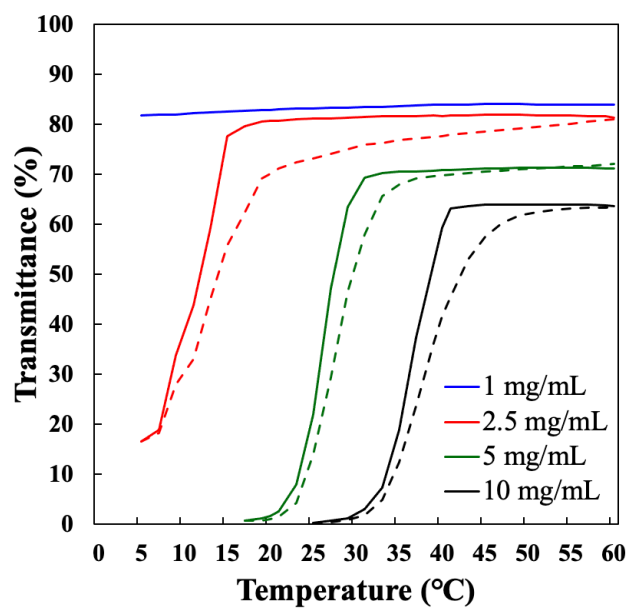
(n) 1 mg/mL PIC micelles at 60 ℃

(o) 1 mg/mL PIC micelles at 10 ℃

Figure 3-A5. DLS autocorrelation functions for different concentrations of PIC micelles obtained at four angles (60°, 75°, 90°, and 105°): 10 mg/mL PIC micelles at (a)60, (b) 49, (c) 45, (d)35, (e)30, (f)25 ℃, 5 mg/mL PIC micelles at (g)60, (h)30, (i)25, (j)17 ℃, 2.5 mg/mL PIC micelles at (k)60, (l)20, (m)10 ℃ and 1 mg/mL PIC micelles at (n) 60, (o) 10 ℃.

15 mg/mL PIC micelle

Left: SSNa$_{37}$-b-SPP$_{68}$
Right: MAPTAC$_{51}$-b-SPP$_{68}$
at 25 ℃

Two block copolymers mixed in aqueous solution at 25 ℃

Immediately precipitated even at 95 ℃

20 mg/mL PIC micelle

Figure 3-A6. PIC micelles were prepared at concentration of 15 and 20 mg/mL.

Figure 3-A7. Hysteresis of temperature response due to the concentration change of PIC micelles prepared by SSNa$_{37}$-*b*-SPP$_{68}$ and MAPTAC$_{51}$-*b*-SPP$_{68}$. Solid lines are cooling curves, broken lines are heating curves.

3.6 Reference

[1] H. Ladenheim, H. Morawetz, *J. Polym. Sci.* **1957**, 26, 251-254.

[2] A. B. Lowe, C. L. McCormick, *Chem. Rev.* **2002**, 102, 4177-4189.

[3] A. Laschewsky, *Polymers* **2014**, 6, 1544-1601.

[4] T. Nakaya, Y. J. Li, *Prog. Polym. Sci.* **1999**, 24, 143-181.

[5] K. Ishihara, R. Aragaki, T. Ueda, A. Watenabe, N. Nakabayashi, *J. Biomed. Mater. Res.* **1990**, 24, 1069-1077.

[6] J. Du, Y. Tang, A. L. Lewis, S. P. Armes, *J. Am. Chem. Soc.* **2005**, 127, 17982-17983.

[7] J. T. Sun, Z. Q. Yu, C. Y. Hong, C. Y. Pan, *Macromol. Rapid Commun.* **2012**, 33, 811-818.

[8] L. Mi, S. Jiang, *Angew. Chem. Int. Ed.* **2014**, 53, 1746-1754.

[9] W. W. Yue, H. J. Li, T. Xiang, H. Qin, S. D. Sun, *J. Membrane Sci.* **2013**, 446, 79-91.

[10] D. B. Thomas, Y. A. Vasilieva, R. S. Armentrout, C. L. McCormick, *Macromolecules.* **2003**, 36, 9710-9715.

[11] M. J. Fevola, J. K. Bridges, M. G. Kellum, R. D. Hester, C. L. McCormick, *J. Appl. Polym. Sci.* **2004**, 94, 24-39.

[12] L. Mi, M. T. Bernards, G. Cheng, Q. Yu, S. Jiang, *Biomaterials* **2010**, 31, 2919-2925.

[13] J. Ma, K. Kang, Q. Yi, Z. Zhang, Z. Gu, *RSC Adv.* **2016**, 6, 64778-64790.

[14] J. C. Salamone, W. Volksen, A. P. Olson, S. C. Israel, *Polymer* **1978**, 19, 1157-1162.

[15] J. Virtanen, M. Arotcarena, B. Heise, S. Ishya, A. Laschewsky, H. Tenhu, *Langmuir* **2002**,18, 5360-5365.

[16] D. N. Schulz, D. G. Peiffer, P. K. Agarwal, J. Larabee, J. J. Kaladas, L. Soni, B. Handwerker, R. T. Garrner, *Polymer* **1986**, 27, 1734-1742.

[17] V. Hildebrand, A. Laschewsky, E. Wischerhoff, *Polym. Chem.* **2016**, 7, 731-740.

[18] V. M. M. Soto, J. C. Galin, *Polymer* **1984**, 25, 254-262.

[19] M. C. Sin, S. H. Chen, Y. Chang, *Polym. J.* **2014**, 46, 436-443.

[20] H. Matusoka, Y. Yamakawa, A. Ghosh, Y. Saruwatari, *Langmuir* **2015**, 31, 4827-4836.

[21] S. Murugaboopathy, H. Matsuoka, *Colloid Polym. Sci.* **2015**, 293, 1317-1328.

[22] V. Hildebrand, A. Laschewsky, D. Zehm, *J. Biomater. Sci. Polym. Ed.* **2014**, 25, 1602-1618.

[23] Y. J. Shin, Y. Chang, *Langmuir* **2010**, 26, 17286-17294.

[24] H. Willcock, A. Lu, C. F. Hansell, E. Chapman, I. R. Collins, R. K. O'Reilly, *Polym. Chem.* **2014**, 5, 1023-1030.

[25] R. Lalani, L. Liu, *Polymer* **2011**, 52, 5344-5354.

[26] A. V. Lezov, P. S. Vlasov, A. A. Lezov, N. S. Domnina, G. E. Polushina, *Polym. Sci. Ser. A* **2011**, 53, 1012-1018.

[27] E. K. Perttu, F. C. Szoka, *Chem. Commun.* **2011**, 47, 12613-12615.

[28] K. Nakai, M. Nishiuchi, M. Inoue, K. Ishihara, Y. Sanada, K. Sakurai, S. Yusa, *Langmuir.* **2013**, 29, 9651-9661.

[29] S. Sakamoto, Y. Sanada, M. Sakashita, K. Nishina, K. Nakai, S. Yusa, K. Sakurai, *Polym. J.* **2014**, 46, 617-622.

[30] Y. Ohara, K. Nakai, S. Ahmed, K. Matsumura, K. Ishihara, S. Yusa, *Langmuir* **2019**, 35, 1249-1256.

[31] M. Kobayashi, Y. Terayama, H. Yamaguchi, M. Terada, D. Murakami, K. Ishihara, A. Takahara, *Langmuir* **2012**, 28, 7212-7222.

[32] Y. Higaki, J. Nishida, A. Takenaka, R. Yoshimatsu, M. Kobayashi, A. Takahara, *Polym. J.* **2015**, 47, 811-818.

[33] Y. Mitsukami, M. S. Donovan, A. B. Lowe, C. L. McCormick, *Macromolecules* **2001**, 34, 2248-2256.

[34] D. Kim, H. Matsuoka, Y. Saruwatari, *Langmuir* **2019**, 35, 1590-1597.

[35] B. Yang, C. Wang, Y. Zhang, L. Ye, Y. Qian, Y. Shu, J. Wang, J. Li, F. Yao, *Polym. Chem.*

2015, 6, 3431-3442.

[36] Y. Chang, W. Chen, W. Yandi, Y. Shih, W. Chu, Y. Liu, C. Chu, R. Ruaan, A. Higuchi, *Biomacromolecules* **2009**, 10, 2092-2100.

Chapter 4

Collapse Behavior of Polyion Complex (PIC) Micelles upon Salt Addition and Reforming Behavior by Dialysis and Its Temperature Responsivity

Temperature responsive polyion complex (PIC) micelles were prepared using two diblock copolymers composed of a sulfobetaine chain (poly(sulfopropyl dimethylammonium propylacrylamide) ; PSPP) and ionic chains (poly(sodium styrenesulfonate) ; PSSNa or poly[3-(methacrylamido)propyl trimethylammonium chloride] ; PMAPTAC). Because the core is PIC and the shell is sulfobetaine with UCST-type temperature response, the corona expands and contracts in response to temperature. To control the size and uniformity of the PIC micelles, the collapse of PIC micelles by salt addition and the reforming behavior by dialysis were investigated by transmittance, DLS, TEM, AFM, and ^{1}H NMR measurements. Investigation of the ionic species dependence of the added salt in the collapse behavior of PIC micelles revealed that it was dependent on the anionic species, although no dependence on the cationic species was observed. Its effectiveness was in the order of I$^-$>Br$^-$>Cl$^-$>F$^-$, which is in agreement with the order of ionic species with strong structural destruction in the Hofmeister series. Heterogeneous and large PIC micelles were formed by the simple mixing method. They collapsed by salt addition and were reformed by the dialysis method to form uniform and smaller PIC micelles. This is considered to be because a uniform and smaller micelle is formed to reform in equilibrium state by dialysis. The temperature response of PIC micelles formed by the simple mixing method and PIC micelles reformed by dialysis, showed nearly the same temperature-transmittance curves. These results indicate that the temperature response of PIC micelles is affected by the concentration rather than the hydrodynamic radius. Furthermore, the

stability of PIC micelles was found to be affected by the concentration temperature (the temperature at the time of concentration).

4.1 Introduction

A zwitterionic polymer having both a negative charge and a positive charge in one repeating unit is similar in structure to lipids that constitute the cell and has high biocompatibility,[1-3] so that it is applied to various biomedical materials.[1-7] Furthermore, it is well known that this zwitterionic polymer has temperature responsivity,[8-12] pH-responsivity,[13-15] ionic species dependence of added salt,[16-18] and dependence of salt concentration.[14-16,19] Therefore, it has been studied in various fields such as brushes,[4-7,13,19] gels,[18,20,21] micelles,[2,9,17] vesicles,[3,22] and surfactants[23-25] based on their properties.

For application to a drug delivery system (DDS), research on micelles and vesicles with stimuli responsivity has been actively conducted.[4,26-30] In the case of core-shell-type stimuli-responsive micelles and vesicles formed by diblock copolymers consisting of hydrophilic and hydrophobic blocks, the corona expands and contracts or shape transitions occur in response to external stimuli.[23,26-30] Therefore, they may be applicable as carriers that can carry hydrophilic or hydrophobic drugs.[26-30] Furthermore, polyion complex (PIC) micelles and PIC vesicles, which are prepared in aqueous media by electrostatic self-assembly of the oppositely charged block- and ionic homopolymer or two diblock copolymers composed of hydrophilic or hydrophobic and ionic (anionic or cationic) blocks.[9,31-34] PIC micelles are expected to transport hydrophilic drugs because the core is a polyion complex.[9,31,32]

Typically, the size and uniformity of micelles and vesicles can be controlled by adjusting the block ratio,[2,35-37] mixing ratio,[38,39] and concentration[33,35] of the polymer or surfactant, solvent mixture,[37,40] and temperature[9,41,42] and so on. However, the PIC micelles systems tend to form inter- or intramolecular pairs, making it difficult to regulate morphology.

In addition, the concentration of polymer solution and the degree of polymerization of the block including thermoresponsiveness have a significant effect on the stability of the aggregate, causing precipitation and heterogeneous association.[8,9] Thus, the system is worth studying because our knowledge of the micellization of block copolymers with thermo-responsive blocks by polyionic interaction is quite limited.

In this study, to control the size and uniformity of temperature responsive PIC micelles, the author investigated the collapse behavior of PIC micelles by salt addition and the reforming behavior by dialysis. PIC micelles were prepared by mixing two diblock copolymers consisting of sulfobetaine chain (PSPP) and ionic chains (PSSNa or PMAPTAC) in water so that the anion and cation charge numbers would be equal.[9,31-34] PIC micelles with a core of PIC and a shell of sulfobetaine are formed.[9] Sulfobetaine is a kind of zwitterionic polymer and exhibits upper critical solution temperature (UCST)-type temperature response.[8-12] The ionic species dependence on the added salt in the collapse behavior of PIC micelles was investigated by measuring transmittance, and the shape change by a method of forming the PIC micelles was investigated by measuring transmittance, dynamic light scattering (DLS), with a transmission electron microscopy (TEM), atomic force microscopy (AFM), and ^{1}H NMR. Finally, the author compared the temperature response of PIC micelles prepared by the simple mixing method and PIC micelles reformed by the dialysis method. Furthermore, the relationship between the concentration temperature and transition temperature of PIC micelles was investigated.

4.2 Experimental

4.2.1 Materials

3-(Methacrylamido)propyltrimethylammonium chloride (MAPTAC) and sulfopropyl dimethylammonium propylacrylamide (SPP) were kindly donated by Osaka Organic Chemical Industry Ltd. (Osaka, Japan). 4,4′-Azobis(4-cyanovaleric acid) (ACVA, 98%), *p*-styrenesulfonic acid sodium salt (SSNa), potassium chloride (KCl), lithium chloride (LiCl),

calcium chloride ($CaCl_2$), sodium chloride (NaCl), sodium bromide (NaBr), and sodium iodide (NaI) were purchased from Wako (Osaka, Japan). Sodium fluoride (NaF) and guanidinium chloride (GdmCl) were purchased from Nacalai Tesque (Kyoto, Japan). Deuterium oxide (D_2O, 99.9 %) was a product of Cambridge Isotope Laboratory (CIL) (U.K.). The pure water used for solution preparation and dialysis was ultrapure water obtained by Milli-Q system (18.2 MΩcm). Dialysis for PIC micelles reforming performed with a dialysis tube from Orange Scientific (MWCO: 12000~16000).

4.2.2 ^{1}H Nuclear Magnetic Resonance (NMR)

^{1}H NMR spectra for confirmation of collapse and reformation behavior of PIC micelles were obtained with a JEOL JNM-EX 400 spectrometer using as a solvent D_2O (CIL, 99.99%). Dialysis was performed by using pure water to reform PIC micelles. The PIC micelle aqueous solution which overall concentration was diluted by dialysis was concentrated to 1 wt% by natural drying for about 2 weeks. When observing reformed PIC micelles by dialysis, 0.5 mL of 1 wt% PIC micelle aqueous solution was mixed with 0.5 mL of D_2O before ^{1}H NMR was performed. The concentration of samples was 0.5~1 wt%.

4.2.3 Electrophoretic Light Scattering (ELS)

The zeta potential of 1 wt% SPP_{68}, $SSNa_{37}$-b-SPP_{68}, $MAPTAC_{51}$-b-SPP_{68}, and PIC micelles was measured at room temperature and 50 °C by using an ELSZ-2000 (Otsuka Electronics Co., Ltd, Osaka, Japan). The average value of the values obtained by repeating three times was designated as the zeta potential. The zeta potential was calculated from the obtained electrophoretic mobility via Smoluchowski's equation[43] as follows:

$$\zeta = \frac{4\pi\eta U}{\varepsilon} \qquad (1)$$

where U, η, and ε are the electrophoretic mobility, the viscosity of solvent and the dielectric

constant of the solvent, respectively.

4.2.4 Turbidity

The collapse behavior of PIC micelles upon salt addition and the change in transition temperature by a method of forming the PIC micelles were determined using a UV-vis spectrometer U-3310 (Hitachi). The collapse behavior of PIC micelles upon salt addition was observed values at a wavelength of 400 nm and 25 °C. The change in transition temperature by a method of forming the PIC micelles was observed at a wavelength of 400 nm and various temperature ranges.

4.2.5 Dynamic Light Scattering (DLS)

The change in hydrodynamic radius (R_h) due to the method of forming PIC micelles was estimated by using a Photal SLS-7000DL (Otsuka Electronics Co., LTD) (Osaka, Japan) equipped with a 15 mW He-Ne laser (wavelength 632.8 nm) and GC-1000 photon correlator. DLS measurements were made at various temperatures and concentrations. The time correlation function of the scattered field was measured at four scattering angles (60°, 75°, 90°, and 105°) with an accumulation time of 30 min. The hydrodynamic radius (R_h) was calculated via the well-known Stokes-Einstein equation.[44,45]

4.2.6 Transmission Electron Microscopy (TEM)

The shape changes by a method of forming the PIC micelles was confirmed by using a JEOL JEM-2100 (Tokyo, Japan) with an accelerating voltage of 200 kV. Samples for TEM were prepared by placing one drop of the aqueous solution on a copper grid coated with thin films of carbon and Formvar. The excess water was blotted with filter paper. The samples were stained by sodium phosphotungstate and dried under vacuum for 1 day.

4.2.7 Atomic Force Microscopy (AFM)

Images of shape change by a method of forming the PIC micelles were confirmed by using a Seiko SPI3800 probe station and a SPA300 unit system of the SPI3900 series scanning probe microscope (Tokyo, Japan). The microcantilever with an OMCL-AC240TS-C3 (Olympus Corp.) (Tokyo, Japan) and a spring constant of 1.7 N/m and the resonant frequency of 70 kHz was used. The measurement mode was a dynamic force mode (non-contact mode). Samples for AFM were prepared by placing one drop of the aqueous solution onto a 1.0 mm glass microscope slide. The samples were dried for 5-10 min in 100 °C ovens.

Table 4-1. Characteristics of Diblock Copolymers (PSSNa-*b*-PSPP and PMAPTAC-*b*-PSPP).

Polymer	M_n (g/mol)	PDI (M_w/M_n)	*m:n*
PSSNa-*b*-PSPP1	25900	1.12	36:66
PSSNa-*b*-PSPP2	26700	1.12	37:68
PMAPTAC-*b*-PSPP1	29500	1.17	50:66
PMAPTAC-*b*-PSPP2	30300	1.17	51:68

4.3 Results and Discussion

4.3.1 Characterization of Block Copolymers

The four diblock copolymers used in this study are shown in Table 4-1. Diblock copolymers consisting of a sulfobetaine chain and an ionic chain (PSSNa or PMAPTAC) having a block ratio of about 50:50 was used. These were synthesized as reported previously.[8,9]

4.3.2 Confirmation of PIC Micelles

As previously reported,[9] the author confirmed the disappearance of the peaks of the ionic chains to become a core and the size of the PIC micelles by ^{1}H NMR and DLS, respectively. Then, the presence and responsiveness of the PIC micelles were confirmed by the turbidity, and the morphology was observed by AFM and TEM.

The zeta potential of the negative value (-30.17 mV) of SSNa$_{37}$-b-SPP$_{68}$ and the positive value (36.05 mV) of MAPTAC$_{51}$-b-SPP$_{68}$ became neutral value (0.10 mV) by forming aggregate. The zeta potential of the aggregate was almost the same value as SPP$_{68}$ (1.05 mV). This showed that micelles with the ionic chain as the core and sulfobetaine chain as the shell were formed. Detailed information is shown in Figure 4-A1.
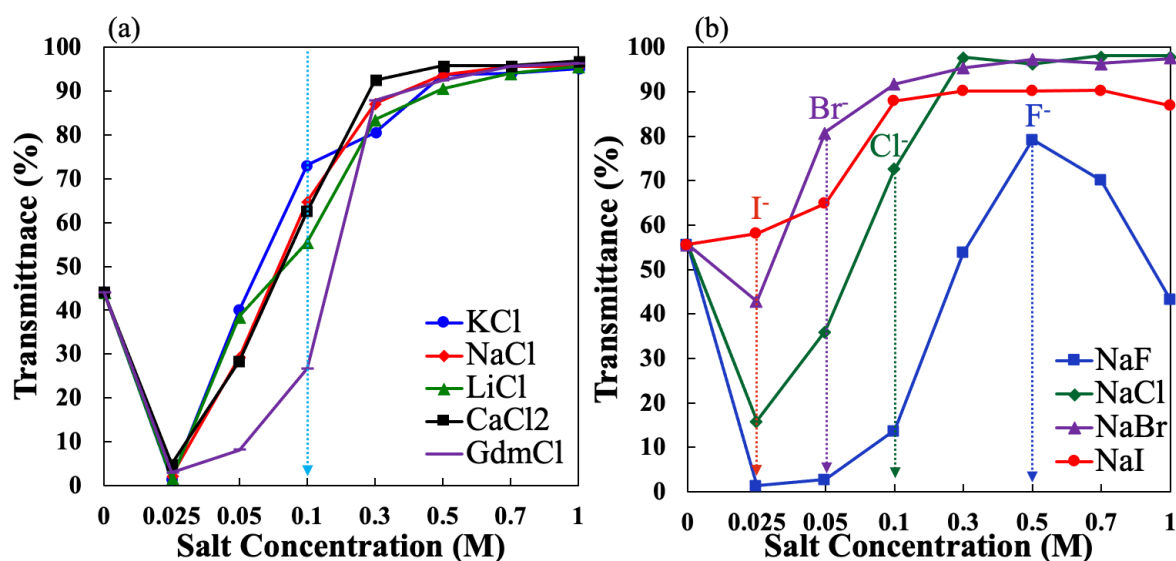
Figure 4-1. Ionic species dependence of the added salt in the collapse behavior of PIC micelles: the salt of (a) cationic species and (b) anionic species.

4.3.3 Ionic Species Dependence of the Added Salt in the Collapse Behavior of PIC Micelles

As shown in Figure 4-1a, KCl, NaCl, LiCl, CaCl$_2$, and GdmCl (salt of cationic species) were added to 0.1 wt% PIC micelles prepared from SSNa$_{36}$-b-SPP$_{66}$ and MAPTAC$_{50}$-b-SPP$_{66}$, and the micelles collapsed after addition of 0.1 M or more. However, cationic species dependence was not observed. Even, the same behavior was exhibited using guanidinium chloride (GdmCl), which is the most structurally destructive of the Hofmeister series.[46,47] On the other hand, as shown in Figure 4-1b, in order to confirm the anionic species dependence, NaI, NaBr, NaCl, and NaF (salt of anionic species) were added in the same way, the 0.1 wt% PIC micelles prepared from SSNa$_{37}$-b-SPP$_{68}$ and MAPTAC$_{51}$-b-SPP$_{68}$ collapsed by the addition of 0.025 M, 0.05 M, 0.1 M, 0.5 M, respectively. The PIC micelles collapsed in the order of I$^-$>Br$^-$>Cl$^-$>F$^-$. This is consistent with the order of ionic species with strong structural destruction in the Hofmeister series.[46,47] Herein, the reason why the transmittance decreases with the addition of 0.7 M or more NaF is that the solubility of NaF decreases. For detailed information see Figure 4-A2. These results showed that the collapse behavior of PIC micelles upon the addition of salt was more affected by anionic species than cationic species. The sulfobetaine chain is N$^+$ (quaternary ammonium cation) in the middle and SO$_3^-$ (sulfurous acid) on the outside. The fully hydrated SO$_3^-$ of the sulfobetaine chain dissolves well and is induced with a negative charge. However, it forms intra- or intermolecular salts when not fully hydrated. Therefore, the degree of hydration of SO$_3^-$ is an important factor. The author believe that the anionic species plays the role. Various studies have shown that it is the effect of anionic species to break the intra- or intermolecular salt and to increase the hydration of sulfobetaine increases from kosmotropic to chaotropic anion.[16-18] The sulfobetaine chain that is the shell is assumed to be hydrated and stretched by anionic species, so that the salt reaches the core and the PIC micelles collapsed.

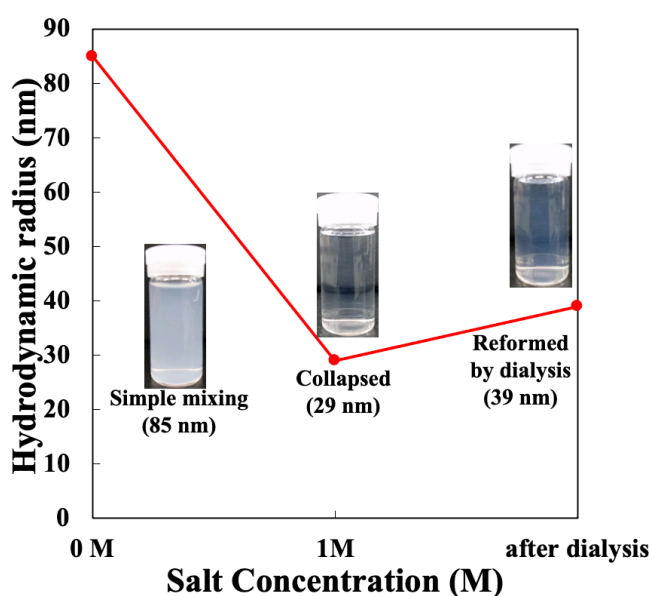## 4.3.4 Shape Change by a Method of Forming the PIC Micelles

The author confirmed from the transmittance how much salt was added to collapse 0.1 wt% PIC micelles prepared from SSNa$_{36}$-b-SPP$_{66}$ and MAPTAC$_{50}$-b-SPP$_{66}$. As shown in Figure 4-2, when a small amount of salt is initially added, it interacts only with the shell sulfobetaine, shielding the sulfobetaine charge and making it relatively hydrophobic.[48,49] Therefore, the attractive force of sulfobetaine increased to form a large aggregate, and the transmittance decreased to almost 0 %. Herein, when salt was added little by little, salt entered the core and the micelles began to collapse. At 0.5 M, the micelles were almost collapsed. The amount of salt required until collapse differs depending on the overall concentration of the PIC micelle in aqueous solution. Detailed information is shown in Figure 4-A3. Therefore, in this study, the experiment was conducted using 1 M NaCl.
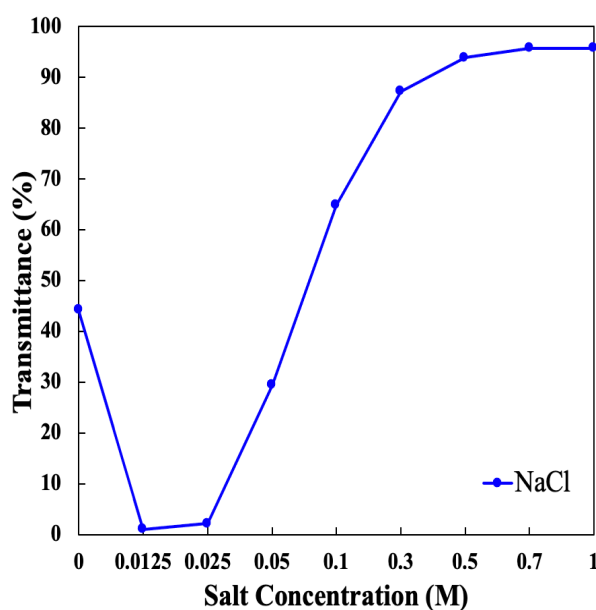
Figure 4-2. Confirmation of the collapse behavior of 0.1 wt% PIC micelles with the concentration of added salt form the transmittance.

The collapse behavior of PIC micelles upon salt addition and the reforming behavior

by dialysis were observed by DLS and TEM measurement. PIC micelles prepared by the simple mixing method were turbid as shown in Figure 4-3 with a hydrodynamic radius (R_h) of 85 nm, and as shown in Figure 4-4a, formed a large and heterogeneous aggregate. When 1 M NaCl was added, the micelles collapsed, and the PIC micelle aqueous solution became transparent. The R_h was 29 nm, and the micelles collapsed as shown in Figure 4-4b. When reformed by dialysis, the hydrodynamic radius was 39 nm, and uniform and small PIC micelles as shown in Figure 4-4c were constructed. Since a small aggregate was formed, the solution appeared blue at this time. During simple mixing, the two block copolymers rapidly interacted to form a large and heterogeneous aggregate, but the PIC micelles collapsed after salt addition. In addition, it is thought that PIC micelles were reformed in an equilibrium state by dialysis, resulting in more uniform and smaller PIC micelles.

Figure 4-3. Change in hydrodynamic radius by a method of forming the PIC micelles.

The same trend was observed with the AFM measurement. The 1 wt% PIC micelles using SSNa$_{37}$-b-SPP$_{68}$ and MAPTAC$_{51}$-b-SPP$_{68}$ prepared by simple mixing formed large and heterogeneous aggregates as shown in Figure 4-5a. On the other hand, the PIC micelles

reformed by dialysis formed more uniform and smaller aggregates. These results show that the size and uniformity can be controlled by the method of forming PIC micelles.
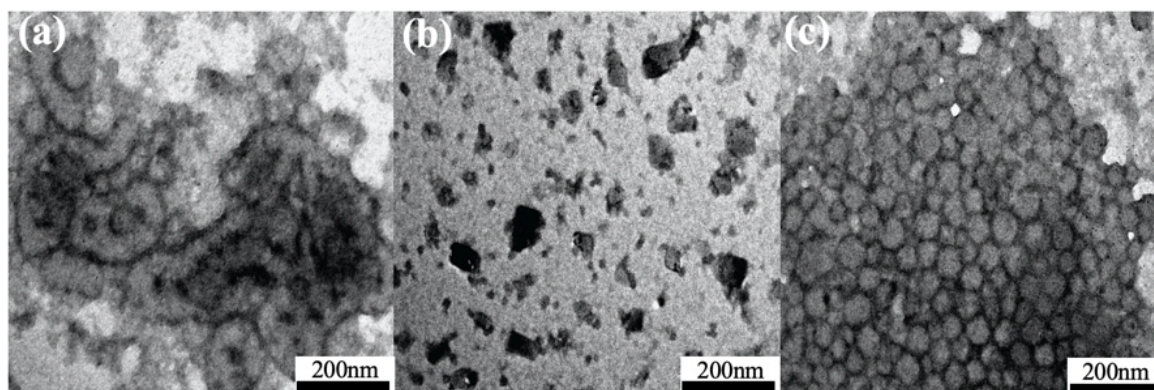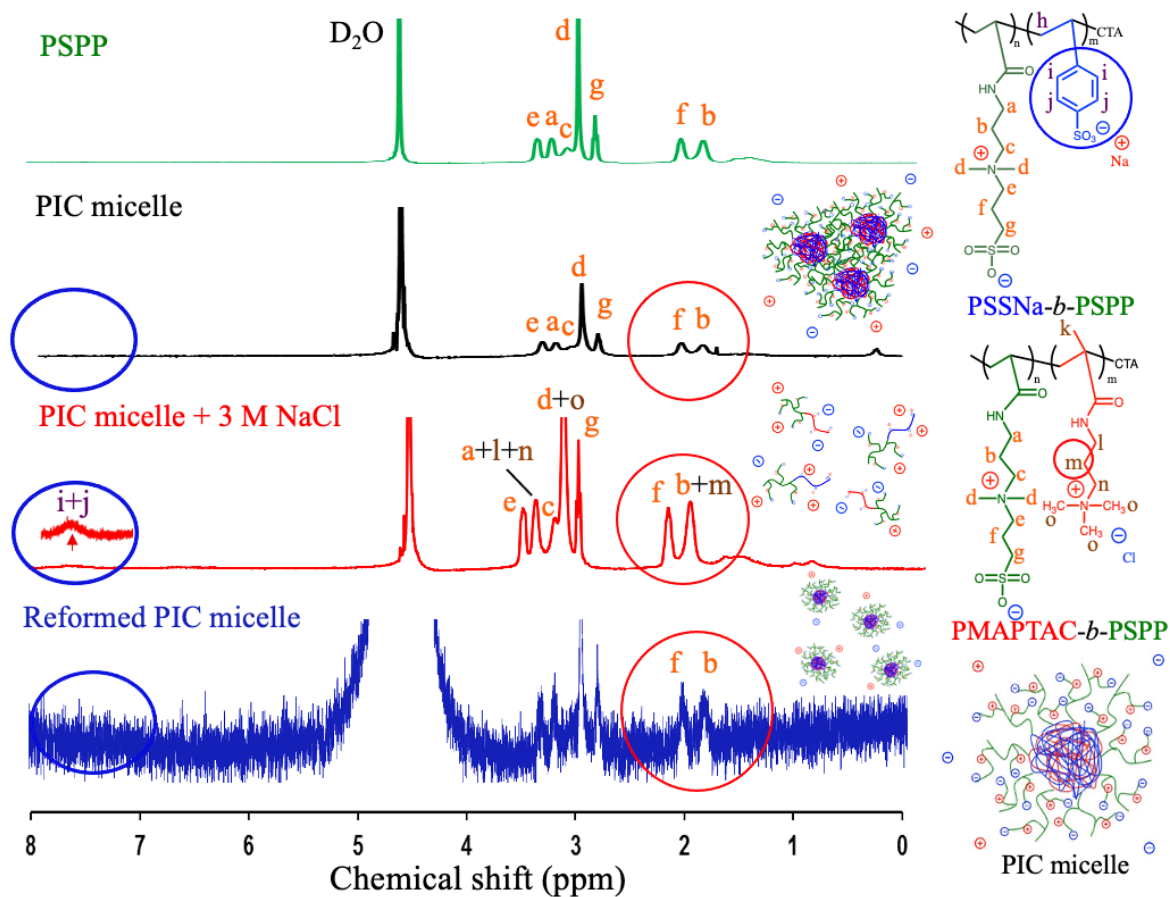

Figure 4-4. TEM image of collapse and reforming behaviors of PIC micelles: (a) PIC micelles formed by simple mixing, (b) PIC micelles add with 1 M NaCl, (c) PIC micelles reformed by dialysis.
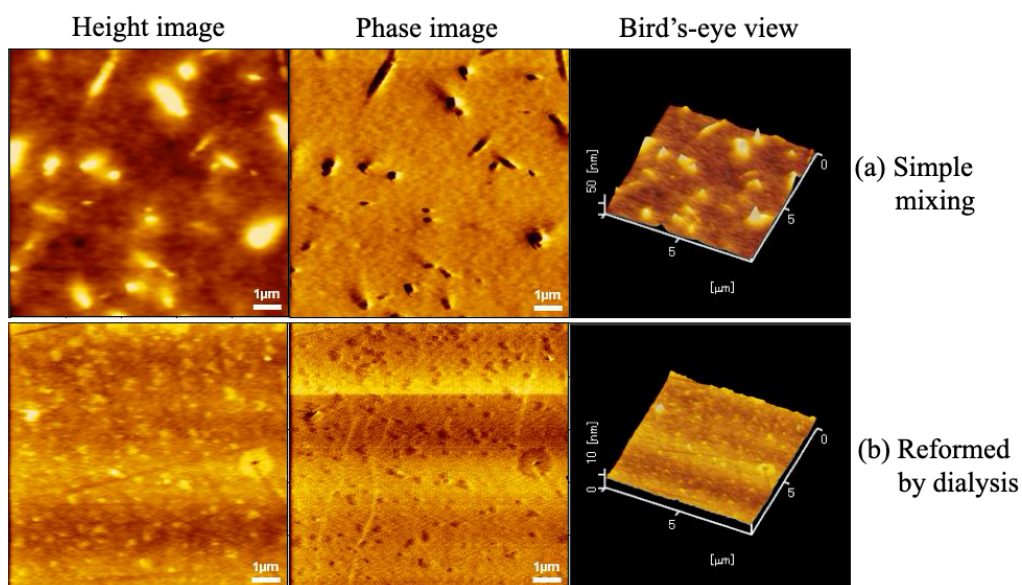
Figure 4-5. AFM image of shape change by a method of forming the PIC micelles: (a) simple mixing, (b) reforming by dialysis.

Furthermore, using ^{1}H NMR the author confirmed the collapse behavior of PIC micelles by salt addition and the reforming behavior by dialysis. As shown in Figure 4-6, the ionic chain peaks (i+j peaks of PSSNa which is an anionic chain and m peak of PMAPTAC which is a cationic chain) of each block copolymer that disappeared from the formation of PIC micelles could be observed again due to the collapse of PIC micelles caused by salt addition.[9] In addition, when PIC micelles were reformed by dialysis, the ionic chain became the core and the peaks disappeared again. Thus, PIC micelles collapsed and reformed.

Figure 4-6. Confirmation of collapse and reformation behavior of PIC micelles by ^{1}H NMR.

4.3.5 Change in Transition Temperature by a Method of Forming the PIC Micelles

The author compared the temperature response of PIC micelles formed by the simple mixing method and PIC micelles reformed by the dialysis method. A 1 wt% PIC micelle aqueous solution was prepared from $SSNa_{37}$-b-SPP_{68} and $MAPTAC_{51}$-b-SPP_{68} and showed an upper critical solution temperature (UCST)-type temperature response as shown by the black line in Figure 4-7. At room temperature, the turbid PIC micelle aqueous solution turned blue at 60 °C and the hydrodynamic radius was 72 nm. After the addition of 3 M NaCl, the PIC micelles collapsed, and as shown by the red line, the transmittance increased to 90 % or more with the disappearance of temperature response. Then the hydrodynamic radius was 12 nm at room temperature. In addition, when PIC micelles were reformed by dialysis for 4 days, the concentration of PIC micelle aqueous solution diluted due to dialysis, and the temperature-transmittance curves shifted to the lower temperature as shown by the blue line. The clear solution turned blue at room temperature and the hydrodynamic radius was 35 nm. Therefore, it was concentrated by natural drying for about 2 weeks to adjust the concentration. The temperature-transmittance curves returned to the initial state. At room temperature, the turbid PIC micelle aqueous solution became blue at 60 °C and the hydrodynamic radius was 45 nm. Furthermore, small micelles were constructed even when the PIC micelle aqueous solution reformed by dialysis was concentrated. Previously,[9] the author reported that the hydrodynamic radius of single micelles formed was roughly consistent with the concentration in the high temperature region when the PIC micelles were mixed at equal charge number of anions and cations. So, it is considered the hydrodynamic radius is the roughly consistent because the site that forms the core has been decided. However, the size of the aggregate of micelles formed in the lower temperature region depended on the concentration. It is considered that the formation behavior of micelle aggregates below the critical temperature where the temperature response can be expressed is may not be greatly influenced by the hydrodynamic radius of the single

micelle, but more affected by the concentration of the micelle aqueous solution. Therefore, it is considered that the temperature-transmittance curves are roughly consistent because the concentration is the same even if the PIC micelles formed by the simple mixing method and the PIC micelles reformed by the dialysis method have a different hydrodynamic radius. Images of PIC micelles prepared by the simple mixing method and PIC micelles reformed by thedialysis method at 60 °C can be confirmed by Figure 4-A4.
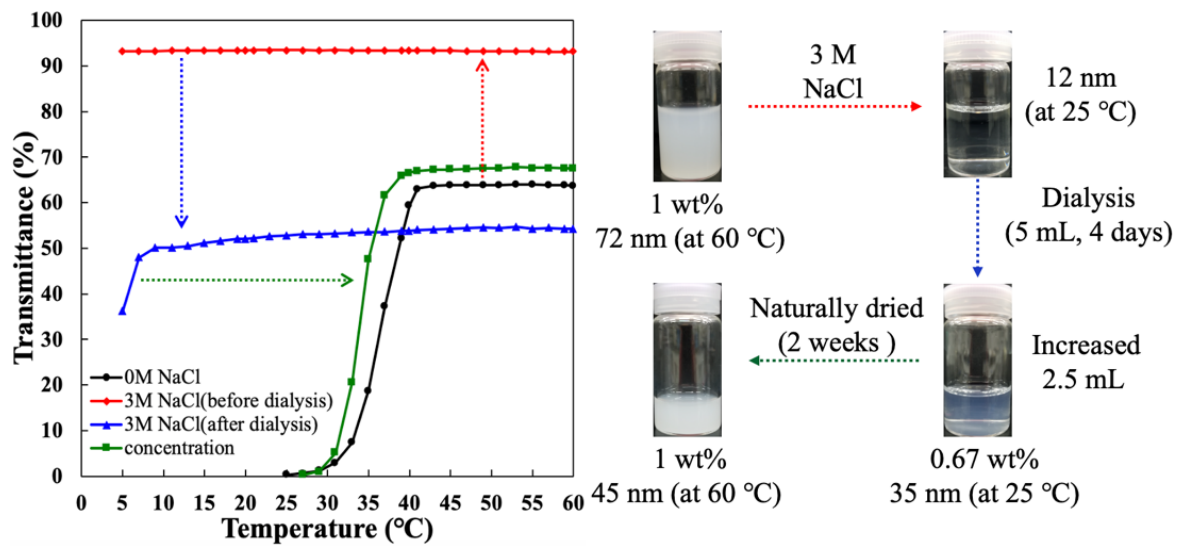
Figure 4-7. Change in transition temperature by a method of forming the PIC micelles: all sample images are at room temperature.
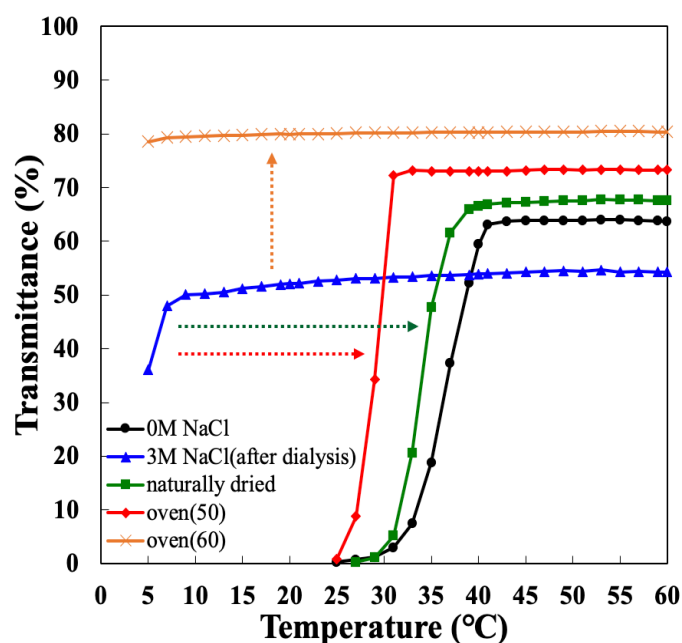
Figure 4-8. Change in transition temperature of PIC micelles with concentration temperature.

4.3.5 Relationship between Concentration Temperature and Transition Temperature of PIC Micelles

The effect of concentration temperature (the temperature at the time of concentration) on the transition temperature of PIC micelles was determined by measuring transmittance. As shown in Figure 4-8, PIC micelles concentrated by natural drying at room temperature showed UCST-type temperature responsivity which almost coincided with the temperature-transmittance curves of PIC micelles prepared by simple mixing. However, the temperature-transmittance curves of PIC micelles concentrated in an oven at 50 °C for 35 hours shifted toward the lower temperature. The transition temperature decreased by 8 °C (from 37 °C to 29 °C). Furthermore, the temperature response of PIC micelles concentrated in an oven at 60 °C for 20 hours disappeared. This is thought to be because the ionic chain, which is the core, collapsed with the increase in the kinetic energy of the molecular chain, forming an unstable

aggregate.[33,34] The hysteresis of temperature response of PIC micelles can be confirmed in Figure 4-A5.
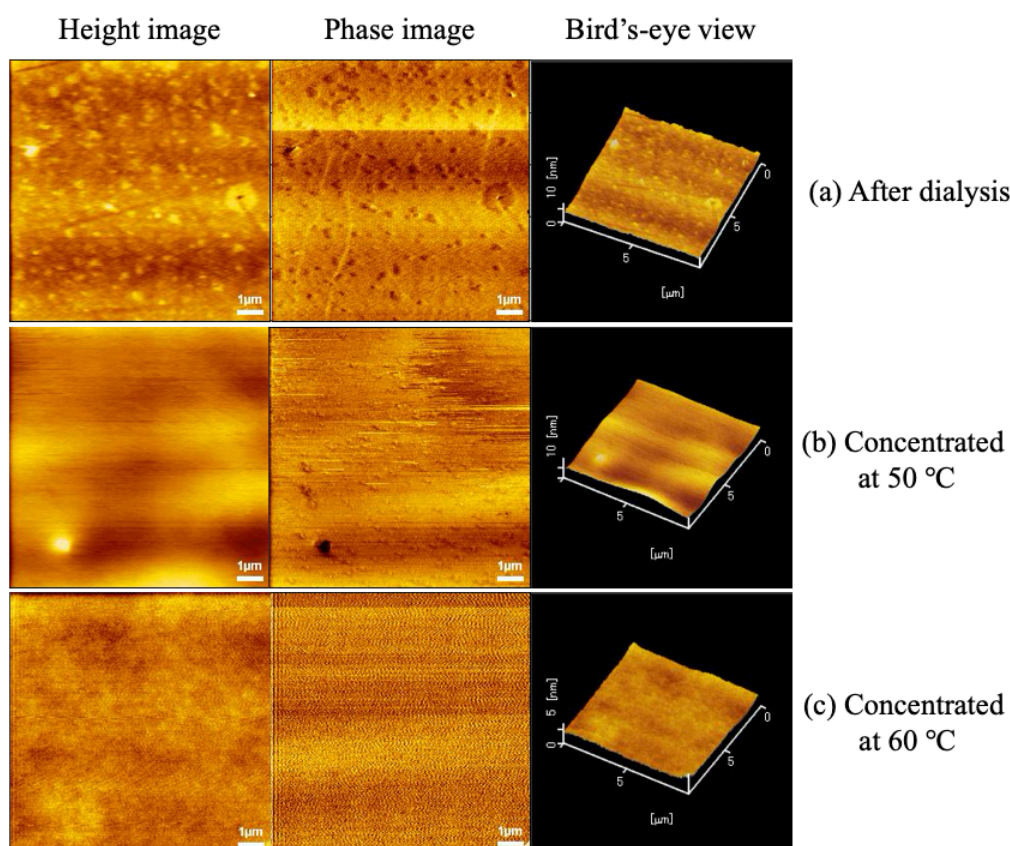

Height image	Phase image	Bird's-eye view	
			(a) After dialysis
			(b) Concentrated at 50 °C
			(c) Concentrated at 60 °C

Figure 4-9. AFM image of shape change with concentration temperature: (a) after dialysis, (b) concentrated at 50 ℃, (c) concentrated at 60 ℃.

The dependence of the shape change of PIC micelles on the concentration temperature was confirmed by AFM measurement. As shown in Figure 4-9, small and uniform spherical aggregates were observed in the PIC micelles reformed by the dialysis method. However, the number of micelles present within the same measurement scale rapidly decreased by increasing the concentration temperature. A small number of micelles could be observed in the sample concentrated at 50 ℃, but none were observed in the sample concentrated at 60 ℃. As the concentration temperature increased, the kinetic energy of the polymer chain increased, and the electrostatic attraction of the polyion complex, which is the core weakened, resulting in

unstable micelles. Finally, the PIC micelles are collapsed. This is considered to be the cause of the disappearance of temperature responsiveness due to the increase in concentration temperature. These findings showed that the stability of PIC micelles is affected by the concentration temperature.[33,34]

4.4 Conclusions

Herein, the author demonstrated that the size and uniformity of PIC micelles can be controlled by the reformation method by dialysis. There was no dependence of the added salt on the cationic species in the collapse behavior of PIC micelles. On the other hand, anionic species showed dependence, and the PIC micelles collapsed in the order of $I^- > Br^- > Cl^- > F^-$. This is consistent with the order of ionic species with strong structural destruction in the Hofmeister series. The important factor is the degree of hydration of SO_3^- on the outside of the sulfobetaine chain, and the author believe that the salt of the anionic species plays a role.

Heterogeneous and large PIC micelles formed by the simple mixing method, collapsed after salt addition and reformed by dialysis to form uniform and smaller PIC micelles. Thus, uniform and smaller micelles can be reformed in the equilibrium state by dialysis.

The temperature response of PIC micelles formed by the simple mixing method and PIC micelles reformed by dialysis, showed similar temperature-transmittance curves. The hydrodynamic radius of the PIC micelle differed with the formation method, but at the same overall concentration, the temperature-transmittance curves were roughly consistent, indicating that the effect of concentration on PIC micelles was greater than that of the hydrodynamic radius.

The stability of PIC micelles is affected by the concentration temperature. This is thought to be because the ionic chain, which is the core, collapsed with the increase in the kinetic energy of the molecular chain, forming an unstable aggregate.
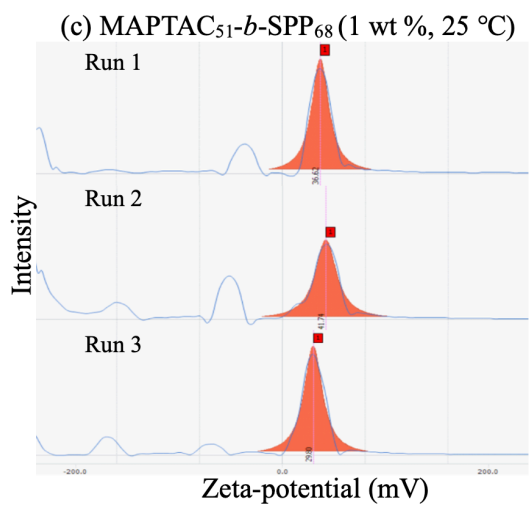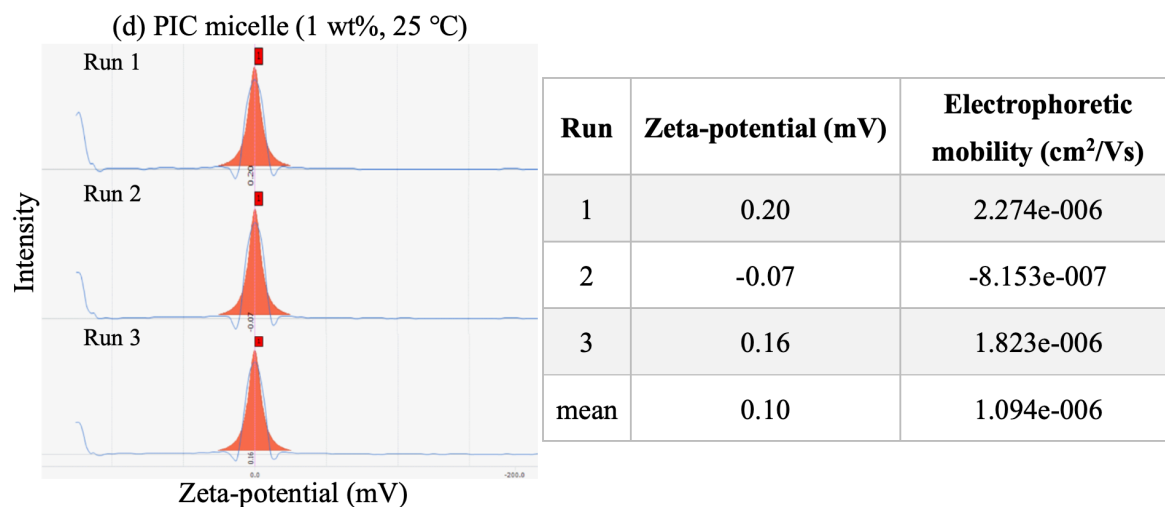
4.5 Appendix

(a) SPP$_{68}$ (1 wt%, 25 ℃)
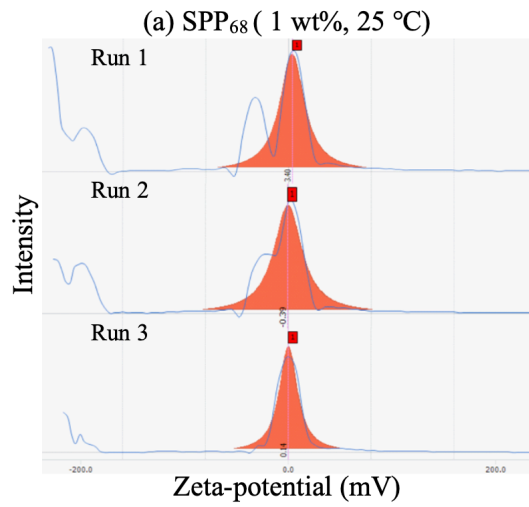
Run	Zeta-potential (mV)	Electrophoretic mobility (cm^2/Vs)
1	3.40	2.650e-005
2	-0.39	-3.077e-006
3	0.14	1.118e-006
mean	1.05	8.180e-006

(b) SSNa$_{37}$-b-SPP$_{68}$ (1 wt%, 25 ℃)
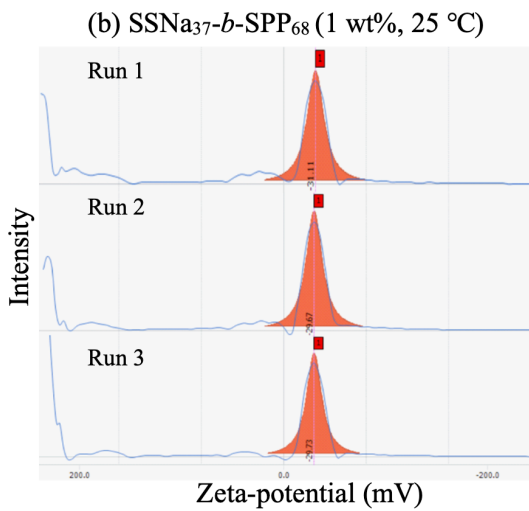
Run	Zeta-potential (mV)	Electrophoretic mobility (cm^2/Vs)
1	-31.11	-2.426e-004
2	-29.67	-2.314e-004
3	-29.73	-2.319e-004
mean	-30.17	-2.353e-004

(c) MAPTAC$_{51}$-b-SPP$_{68}$ (1 wt %, 25 ℃)

Run	Zeta-potential (mV)	Electrophoretic mobility (cm^2/Vs)
1	36.62	2.856e-004
2	41.74	3.255e-004
3	29.80	2.324e-004
mean	36.05	2.812e-004

(d) PIC micelle (1 wt%, 25 °C)

Run 1

Run 2

Run 3

Intensity

Zeta-potential (mV)

Run	Zeta-potential (mV)	Electrophoretic mobility (cm^2/Vs)
1	0.20	2.274e-006
2	-0.07	-8.153e-007
3	0.16	1.823e-006
mean	0.10	1.094e-006

Figure 4-A1. Estimation of the zeta-potential by ELS: (a) SPP$_{68}$, (b) SSNa$_{37}$-*b*-SPP$_{68}$, (c) MAPTAC$_{51}$-*b*-SPP$_{68}$, and (d) PIC micelles.
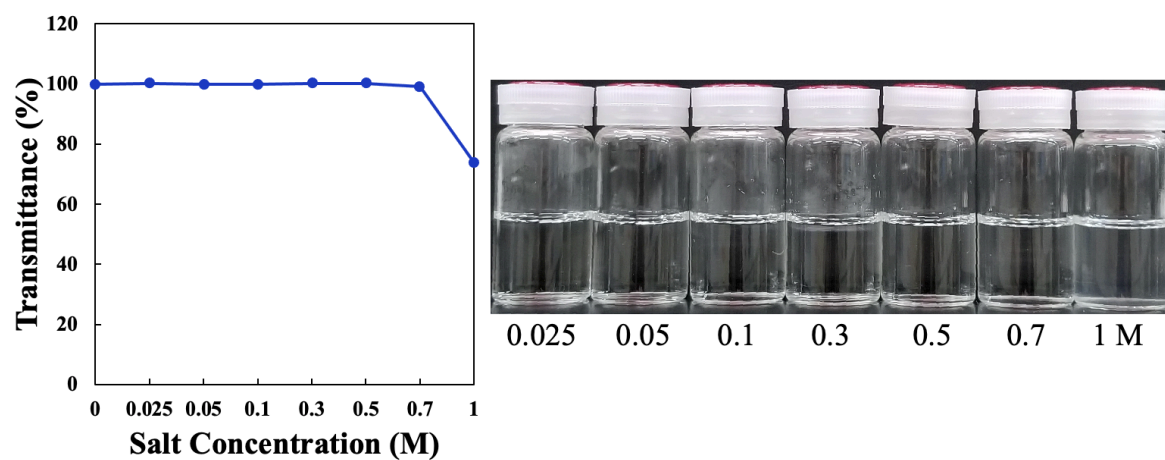
Figure 4-A2. Solubility of NaF in water.
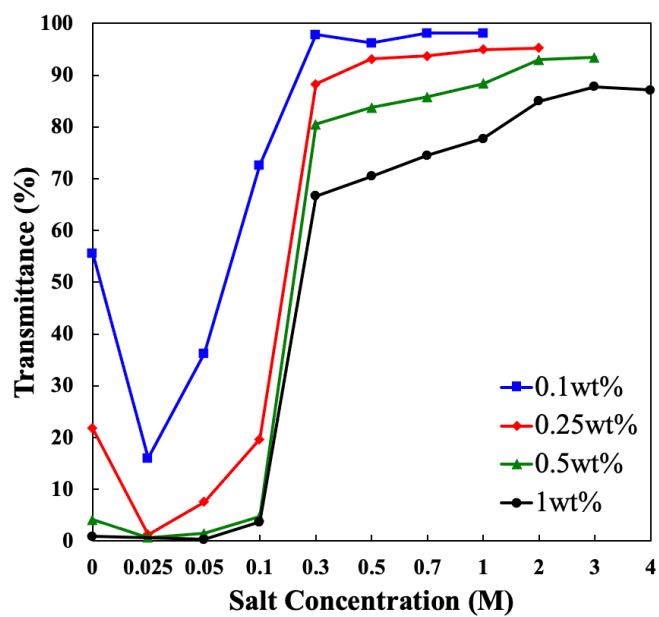
Figure 4-A3. The amount of salt required until collapse differs depending on the overall concentration of the PIC micelle aqueous solution.
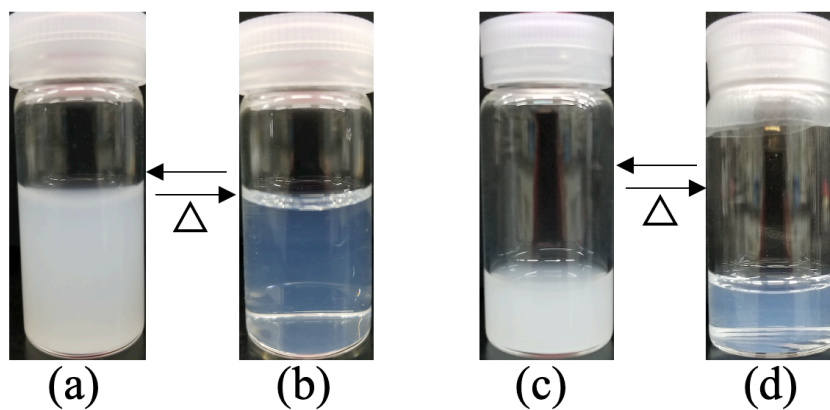
Figure 4-A4. Images of PIC micelle aqueous solution with different formation method: Images of PIC micelles were prepared by simple mixing method at (a) room temperature, (b) 60 °C, and PIC micelles reformed by dialysis at (c) room temperature, (d) 60 °C.
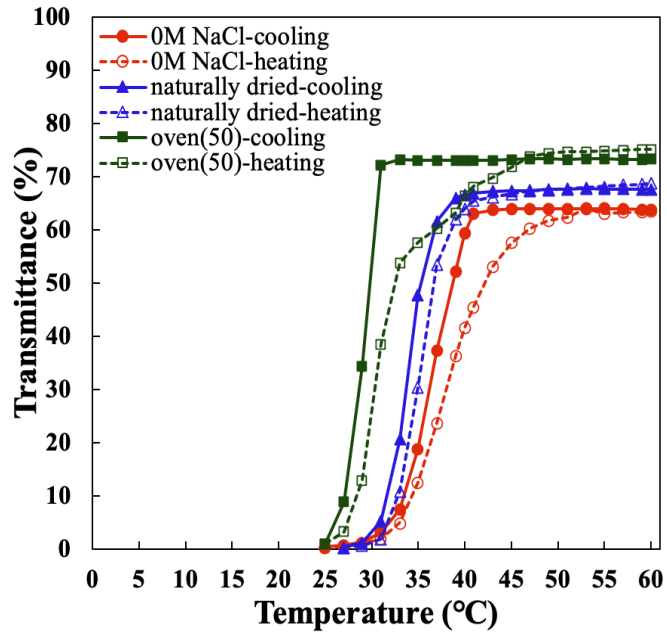
Figure 4-A5. The hysteresis of temperature response of PIC micelles: The solid line is cooling process and the broken line is heating process.
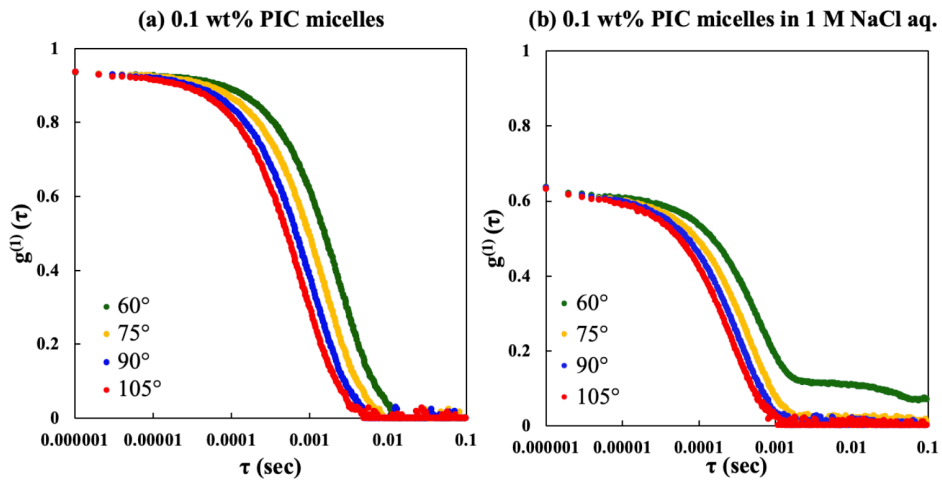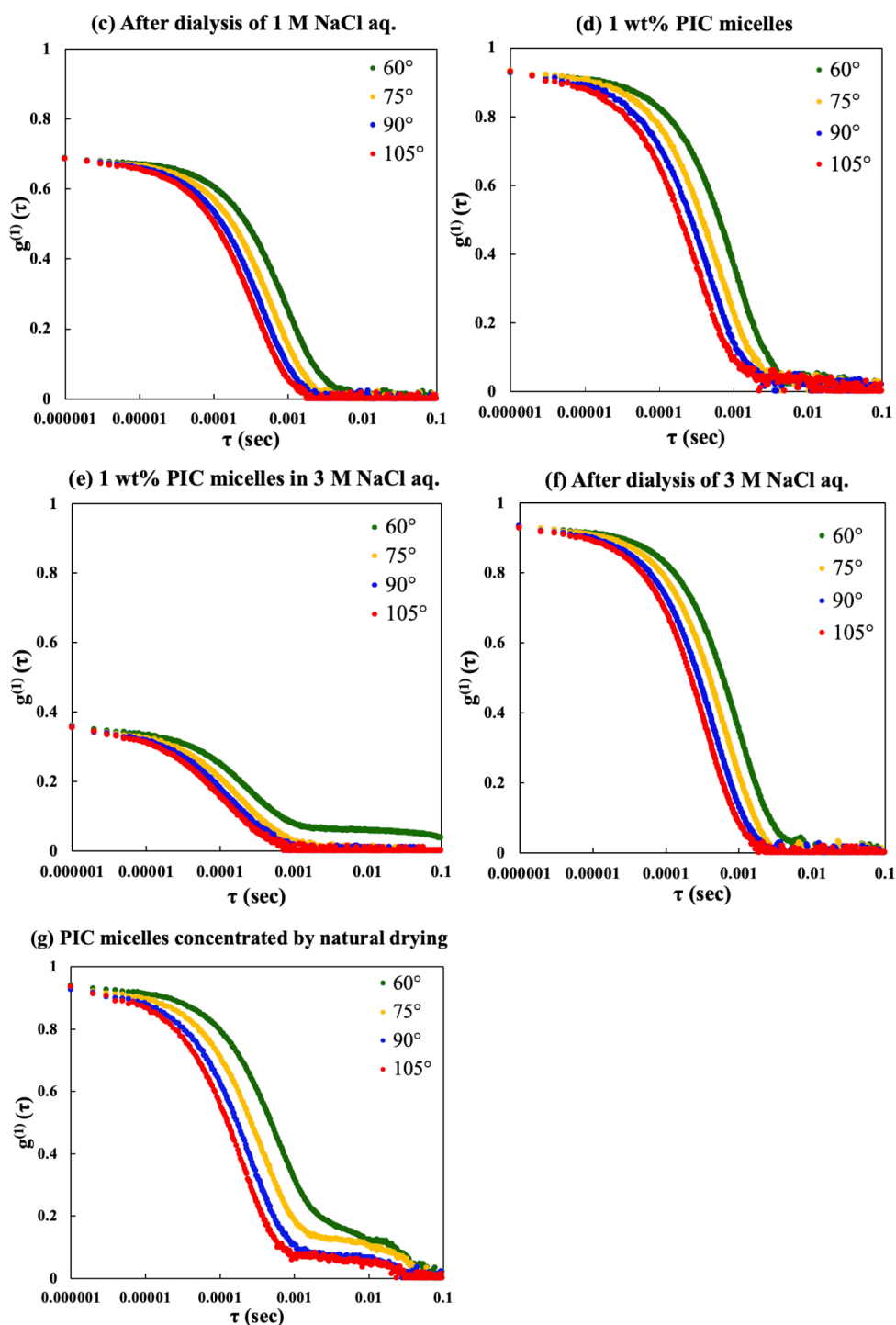
Figure 4-A6. DLS autocorrelation functions with shape change of PIC micelles obtained at four angles (60°, 75°, 90°, and 105°): 0.1 wt% PIC micelles prepared by SSNa$_{36}$-*b*-SPP$_{66}$ and MAPTAC$_{51}$-*b*-SPP$_{66}$ (a) in water, (b) in 1 M NaCl aq., (c) after dialysis of 1 M NaCl at 25 °C, and 1 wt% PIC micelles prepared by SSNa$_{37}$-*b*-SPP$_{68}$ and MAPTAC$_{51}$-*b*-SPP$_{68}$ (d) at 60 °C, (e) in 3 M NaCl aq. at 25 °C, (f) after dialysis of 3 M NaCl aq. at 25 °C,, (g) concentrated by natural drying at 60 °C.

4.6 Reference

[1] A. Laschewsky, *Polymers* **2014**, 6, 1544-1601.

[2] S. Yusa, K. Fukuda, T. Yamamoto, K. Ishihara, Y. Morishima, *Biomacromolecules* **2005**, 6, 663-670.

[3] J. Du, Y. Tang, A. L. Lewis, S. P. Armes, *J. Am. Chem. Soc.* **2005**, 127, 17982-17983.

[4] L. Mi, S. Jiang, *Angew. Chem. Int. Ed.* **2014**, 53, 1746-1754.

[5] H. Jiang, X. B. Wang, C. Y. Li, J. S. Li, F. J. Xu, C. Mao, W. T. Yang, J. Shen, *Langmuir.* **2011**, 27, 11575-11581.

[6] P. S. Liu. Q. Chen, S. S. Wu, J. Shen, S. C. Lin, *J. Membr. Sci.* **2010**, 350, 387-394.

[7] G. Cheng, G. Li, H. Xue, S. Chen, J. D. Bryers, S. Jiang, *Biomaterials* **2009**, 30, 5234-5240.

[8] D. Kim, H. Matsuoka, Y. Saruwatari, *Langmuir* **2019**, 35, 1590-1597.

[9] D. Kim, H. Matsuoka, Y. Saruwatari, *Langmuir* **2020**, 36, 10130-10137.

[10] V. Hildebrand, A. Laschewsky, E. Wischerhoff, *Polym. Chem.* **2016**, 7, 731-740.

[11] H. Willcock, A. Lu, C. F. Hansell, E. Chapman, I. R. Collins, R. K. O'Reilly, *Polym. Chem.* **2014**, 5, 1023-1030.

[12] J. T. Sun, Z. Q. Yu, C. Y. Hong, C. Y. Pan, *Macromol. Rapid Commun.* **2012**, 33, 811-818.

[13] B. Yameen, M. Ali, R. Neumann, W. Ensinger, W. Knoll, O. Azzaroni, *J. Am. Chem. Soc.* **2009**, 131, 2070-2071.

[14] D. B. Thomas, Y. A. Vasilieva, R. S. Armentrout, C. L. McCormick, *Macromolecules.* **2003**, 36, 9710-9715.

[15] M. J. Fevola, J. K. Bridges, M. G. Kellum, R. D. Hester, C. L. McCormick, *J. Appl. Polym. Sci.* **2004**, 94, 24-39.

[16] T. Wang, R. Kou, H. Liu, L. Liu, G. Zhang, G. Liu, *Langmuir* **2016**, 32, 2698-2707.

[17] K. Iso, T. Okada, *Langmuir* **2000**, 16, 9199-9204.

[18] E. O. Ningrum, Y. Ohfuka, T. Gotoh, S. Sakohara, *Polymer* **2015**, 59, 144-154.

[19] Y. Matsuda, M. Kobayashi, M. Annaka, K. Ishihara, A. Takahara, *Langmuir* **2008**, 24, 8772-8778.

[20] X. Peng, H. Liu, Q. Yin, J. Wu, P. Chen, G. Zhang, G. Liu, C. Wu, Y. Xie, *Nat. Commun.* **2016**, 7, 11782.

[21] J. Ning, G. Li, K. Haraguchi, *Macromolecules* **2013**, 46, 5317-5328.

[22] R. R. Maddikeri, S. Colak, S. P. Gido, G. N. Tew, *Biomacromolecules* **2011**, 12, 3412-3417.

[23] S. Liu, S. P. Armes, *Angew. Chem. Int. Ed.* **2002**, 41, 1413-1416.

[24] M. J. Rosen, *Langmuir* **1991**, 7, 885-888.

[25] K. W. Herrmann, *J. Colloid Interface Sci.* **1966**, 22, 352-359.

[26] S. Mura, J. Nicolas, P. Couvreur, *Nat. Mater.* **2013**, 12, 991-1003.

[27] N. Rapoport, *Prog. Polym. Sci.* **2007**, 32, 962-990.

[28] Q. Zhang, N. R. Ko, J. K. Oh, *Chem. Commun.* **2012**, 48, 7542-7552.

[29] F. Checot, S. Lecommandoux, Y. Gnanou, H. A. Klok, *Angew. Chem. Int. Ed.* **2012**, 41, 1339-1343.

[30] F. Checot, A. Brulet, J. Oberdisse, Y. Gnanou, O. M. Monval, S. Lecommandoux, *Langmuir* **2005**, 21, 4308-4315.

[31] M. Oishi, S. Sasaki, Y. Nagasaki, K. Kataoka, *Biomacromolecules* **2003**, 4, 1426-1432.

[32] Q. Jin, T. Cai, Y. Wang, H. Wang, J. Ji, *ACS Macro Lett.* **2014**, 3, 679-683.

[33] Y. Anraku, A. Kishimura, M. Oba, Y. Yamasaki, K. Kataoka, *J. Am. Chem. Soc.* **2010**, 132, 1631-1636.

[34] S. Chuanoi, Y. Anraku, M. Hori, A. Kishimura, K. Kataoka, *Biomacromolecules* **2014**, 15, 2389-2397.

[35] M. Antonietti, S. Forster, *Adv. Mater.* **2003**, 15, 1323-1333.

[36] Z. Li, E. Kesselman, Y. Talmon, M. A. Hillmyer, T. P. Lodge, *Science* **2004**, 306, 98-101.

[37] H. Cui, Z. Chen, S. Zhong, K. L. Wooley, D. J. Pochan, *Science* **2007**, 317, 647-650.

[38] A. Makino, E. Hara, I. Hara, E. Ozeki, S. Kimura, *Langmuir* **2014**, 30, 669-674.

[39] O. Zumbuehl, H. G. Weder, *BBA. Biomembranes* **1981**, 640, 252-262.

[40] G. Hattori, M. Takenaka, M. Sawamoto, T. Terashima, *J. Am. Chem. Soc.* **2018**, 140, 8376-8379.

[41] H. Wei, X. Z. Zhang, Y. Zhou, S. X. Cheng, R. X. Zhuo, *Biomaterials* **2006**, 27, 2028-2034.

[42] Y. kametani, M. Sawamoto, M. Ouchi, *Angew. Chem. Int. Ed.* **2018**, 57, 10905-10909.

[43] M. V. Smoluchowski, Phys. Z. **1916**, 17, 557-585.

[44] A. Einstein, *Ann. der Physik* **1905**, 322, 549-560.

[45] W. Sutherland, *Phil. Mag.* **1905**, 9, 781-785.

[46] F. Hofmeister, *Arch. Exp. Pathol. Pharmacol.* **1888**, 24, 247-260.

[47] Y. Zhang, P. S. Cremer, *Curr. Opin. Chem. Biol.* **2006**, 10, 658-663.

[48] T. Ye, Y. Song, Q. Zheng, *Colloid Polym. Sci.* **2016**, 294, 389-397.

[49] P. Koberle, A. Laschewsky, *Macromolecules* **1994**, 27, 2165-2173.

Part 2

Chapter 5

The Behavior of Micelle Formation and Functional Expression in Sulfobetaine-Containing Entirely Ionic Block Copolymer / Ionic Homopolymer System

The author investigated the behavior of micelle formation in the sulfobetaine-containing entirely ionic block copolymer/ionic homopolymer system and its functional expression. Poly(sulfopropyl dimethylammonium propylacrylamide) (PSPP) was used as the sulfobetaine, poly[3-(methacrylamido)propyl trimethylammonium chloride] (PMAPTAC) was used as the cationic polymer, and poly(sodium styrenesulfonate) (PSSNa) was used as the anionic polymer. The changes in transition temperature with the concentration and the behavior of micelle formation in the block-/cationic homopolymer and block-/anionic homopolymer system were compared and examined by transmittance, DLS, AFM, and ^{1}H NMR. Only block-/cationic homopolymer systems with a core-shell (polyion complex-sulfobetaine) structure showed temperature responsivity of upper critical solution temperature (UCST) type, and the responsiveness was dependent on the concentration. On the other hand, the block-/anionic homopolymer system had a core-shell structure at a concentration of 0.05 wt%, but temperature responsiveness was not observed at this concentration. At higher concentrations, electrostatic attraction caused the anionic homopolymer and block copolymer to interact as a whole, resulting in loss of responsiveness. When the ionic homopolymer had a higher degree of polymerization (DP) than the sulfobetaine, it could not form a core-shell structure by interacting with the sulfobetaine and ionic polymer moieties of the block copolymer; thus, resulting in the loss of responsiveness. The block-/ionic homopolymer system prepared by the reforming method through dialysis formed uniform and small micelles, but lost responsiveness

due to morphological stability and electrostatic interaction between the block copolymer and ionic homopolymer.

5.1 Introduction

Zwitterionic betaine polymers having both anions and cations in one repeating unit have high moisturizing properties due to their structural specificity and have been used in cosmetics and the like for a long time.[1-5] Recently, these polymers have been found to have high biocompatibility because they have a structure similar to that of the lipids that make up the cells,[3,6,7] and are applied to biomedical materials[8,9] and biosensors.[10,11] Furthermore, research is being conducted on energy materials to stabilize the interface.[12-14]

Betaine polymers are neutral in an aqueous solution, and the solubility changes depending on the concentration of salt and the ionic species of the added salt.[2,3,6] The typical ionic polymer of anionic and cationic polymers shrinks with the addition of salts,[15,16] whereas the zwitterionic betaine chains exhibit the exact opposite behavior of stretching.[17]

Betaine polymers are divided into carboxybetaine (CB), phosphobetaine (PB), and sulfobetaine (SB) according to functional groups.[3,6] Among them, only sulfobetaine shows upper critical solution temperature (UCST) behavior in which the solubility increases rapidly when a certain temperature is exceeded.[2,3,6] The expression mechanism predicts that anions and cations form an intra- or intermolecular pair below the transition temperature, and that the intra- or intermolecular pair is relaxed and dissolved by an increase in the kinetic energy of the molecular chain above the transition temperature.[2,3,6] The carboxybetaine is pH-responsive depending on the functional group.[3,6,18] Phosphobetaine has high biocompatibility and solubility due to its structural properties.[19,20] These have been studied in various fields such as

brushes,[17,21,22] micelles,[23,24] organic-inorganic hybrid solar cells,[12-14] surfactants,[25-27] and gels.[26,28,29]

Zwitterionic polyion complex (PIC) micelles form a novel self-assembling complex with a polyion complex of polyanions and polycations as the core and zwitterionic polybetaines as the corona (shell).[23,24] In ordinary amphiphilic block copolymers, the core is formed by the association of hydrophobic chains to form polymeric micelles,[30,31] but in PIC micelles, the driving force is the electrostatic attraction between polyanions and polycations and the increased entropy according to counterions released by the association.[32] Therefore, the stability as micelles and the response to added salt is significantly different. In most cases, the shell of normal PIC micelles is water-soluble and nonionic polyethylene glycol (PEG).[32-34] Recently, research on PIC micelles of the diblock/diblock system whose shell is betaine is in progress.[23,24]

In this study, the author investigated the behavior of micelle formation and functional expression of PIC micelles in the sulfobetaine-containing diblock copolymer/ionic homopolymer system. The transmittance revealed a change in responsiveness in the block-/ionic homopolymer system according to the charge (anion or cation). Changes in transition temperature and shape of aggregate due to changes in concentration of polymer aqueous solution and interaction between block copolymers and ionic homopolymers were confirmed by DLS, AFM, ^{1}H NMR, and transmittance. The effect of the degree of polymerization of the ionic homopolymers on the block-/ionic homopolymer system was investigated. Furthermore, the temperature responsivity and the behavior of micelle formation of PIC micelles prepared by simple mixing and PIC micelles reformed by dialysis were compared.

5.2 Experimental

5.2.1 Materials

p-Styrenesulfonic acid sodium salt (SSNa), 4,4′-azobis(4-cyanovaleric acid) (ACVA, 98%), sodium nitrate (NaNO$_3$), and disodium hydrogenphosphate (Na$_2$HPO$_4$), were purchased from Wako (Osaka, Japan). Sulfobetaine (SPP) and 3-(methacrylamido)propyl trimethylammonium chloride (MAPTAC) monomers were kindly donated by Osaka Organic Chemical Industry Ltd. (Osaka, Japan). Acetic acid (CH$_3$COOH) was purchased from Nacalai Tesque (Kyoto, Japan). Sodium sulfate (Na$_2$SO$_4$) and acetonitrile (CH$_3$CN, 99.5%) were purchased from FUJIFILM Wako Pure Chemical Corporation (Osaka, Japan). 4-Cyanopentanoic acid dithiobenzoate was used as a chain transfer agent (CTA), which was synthesized as reported by Mitsukami et al.[35] Deuterium oxide (D$_2$O, 99.9%) was a product of Cambridge Isotope Laboratory (CIL) (U.K.). The ultrapure water used for synthesis, solution preparation, and dialysis was obtained using the Milli-Q system (18.2 MΩcm). Homopolymers (PSPP, PMAPTAC and PSSNa) and PMAPTAC-*b*-PSPP, PSSNa-*b*-PSPP diblock copolymers were purified using a dialysis tube from Orange Scientific (MWCO: 3500 and 12000~16000).

5.2.2 Synthesis of Homopolymers and Diblock Copolymers.

The homopolymers (PSPP, PMAPTAC, and PSSNa) were synthesized by the reversible addition-fragmentation chain transfer (RAFT) polymerization. The synthesis was carried out by mixing each monomer, CTA and initiator (ACVA) in various molar ratios as reported previously.[23] The degree of polymerization (DP) and dispersity (Đ) of the obtained solid homopolymers (PSPP, PMAPTAC, and PSSNa) were evaluated by GPC. Homopolymers thus obtained were confirmed by ^{1}H NMR.

The PSPP homopolymer was used as macro-CTA, and diblock copolymers were

synthesized by adding MAPTAC (or SSNa) monomer and ACVA at 1: 50: 1 (PSPP-macro CTA: ionic monomer: initiator). The solid PMAPTAC-*b*-PSPP and PSSNa-*b*-PSPP were obtained in the same way. The block ratio and *Đ* were determined by analyzing the ^{1}H NMR spectrum and GPC, respectively.

5.2.3 ^{1}H Nuclear Magnetic Resonance (NMR)

^{1}H NMR spectra for homopolymers (PSPP, PMAPTAC, and PSSNa), diblock copolymers composed of PSPP and PSSNa (or PMAPTAC), and the PIC micelles in the block-/ionic homopolymer system were obtained with a JEOL JNM-AL 400 spectrometer using as a solvent D_2O (CIL, 99.99%). The concentration of polymer solution was 0.05~1 wt%.

5.2.4 Gel Permeation Chromatography (GPC)

The degree of polymerization (DP) and its dispersity (*Đ*) were determined by a JASCO GPC system (Tokyo, Japan) composed of a 830-RI RI detector, UV-2075 Plus UV detector, CO-2065 Plus column oven, PU-2080 Plus HPLC pump, DG-2080-53 3-line degasser and Shodex SB-804 HQ column. The pH 3 buffer solution (0.3 M Na_2SO_4, 0.5 M CH_3COOH) was used as the cationic eluent and the mixed solution (20 wt% CH_3CN aq, 0.05 M $NaNO_3$, 0.01 M Na_2HPO_4) as the anionic eluent. Poly(2-vinylpyridine) (P2VP) (Scientific Polymer Product, Inc.) and poly(*p*-styrenesulfonic acid sodium salt) (PSSNa) (Sigma-Aldrich) samples were used as cationic and anionic standards, respectively.

5.2.5 Turbidity

The temperature responsivity and cloud point of the block-/ionic homopolymer system PIC micelles were determined with a UV-vis spectrometer U-3310 (Hitachi) for various concentrations of solution (0.05~2 wt%). The author designated the cloud point as the

temperature at which the turbidity suddenly changed at a wavelength of 400 nm.

5.2.6 Atomic Force Microscopy (AFM)

Images of the PIC micelles in the block-/ionic homopolymer system at various concentrations and images of shape change by a method of forming the PIC micelles were confirmed by using Seiko SPI3800 probe station and a SPA300 unit system of the SPI3900 series scanning probe microscopy (Tokyo, Japan). The microcantilever with OMCL-AC240TS-C3 (Olympus Corp.) (Tokyo, Japan) and a spring constant of 1.7 N/m, and the resonant frequency of 70 kHz was used. Samples for AFM were prepared by placing 1~2 drops of the polymer aqueous solution onto a 1.0 mm microscope slide glass. The samples were dried for 2~3 days at room temperature.

5.2.7 Dynamic Light Scattering (DLS)

The hydrodynamic radius (R_h) of block-/ionic homopolymer system PIC micelles was estimated using a Photal SLS-7000DL (Otsuka Electronics Co., LTD, Osaka, Japan) equipped with a GC-1000 photon correlator and a 15-mW He-Ne laser (wavelength 632.8 nm). DLS measurements were carried out at various concentrations and temperatures. The time correlation function of the scattered field was measured at four scattering angles (60°, 75°, 90°, and 105°) with an accumulation time of 10~30 min. The hydrodynamic radius (R_h) was calculated using the well-known Stokes-Einstein equation.[36]

Table 5-1. Characteristics of Homopolymers (PSPP, PSSNa, and PMAPTAC) and Diblock Copolymers (PSSNa-*b*-PSPP and PMAPTAC-*b*-PSPP).

Polymer[a]	Yield (%)	M_n (g/mol)[b]	Đ (M_w/M_n)[b]	Degree of polymerization	
				m^c	n^c
SPP$_n$-1	88	19100	1.06	-	68
SSNa$_n$-1	73	11000	1.19	-	52
SSNa$_n$-2	54	15600	1.13	-	74
MAPTAC$_n$-1	25	13200	1.17	-	59
MAPTAC$_n$-2	54	19000	1.11	-	85
SSNa$_m$-*b*-SPP$_n$-1	81	26700	1.12	37	68
MAPTAC$_m$-*b*-SPP$_n$-1	79	30300	1.17	51	68

[a]SPP, sulfobetaine; SSNa, p-styrene sulfonic acid sodium salt; and MAPTAC, 3-(methacryl-amido)propyl trimethylammonium chloride. [b]Determined by GPC with an anionic eluent (PSSNa standard) or a cationic eluent (P2VP standard). PSSNa, PSPP and PSSNa-*b*-PSPP were determined by an anionic eluent (20 wt% CH_3CN(aq), 0.05 M $NaNO_3$, 0.01 M Na_2HPO_4), and PMAPTAC and PMAPTAC-*b*-PSPP were used as a cationic eluent (0.5 M CH_3COOH, 0.3 M Na_2SO_4). [c]m, n: Degree of polymerization of ionic and sulfobetaine blocks, respectively. (*m* was determined by 1H NMR).

5.3 Results and Discussion

5.3.1 Characterization of Homopolymers and Block Copolymers

PSPP, PMAPTAC, and PSSNa homopolymers with various degrees of polymerization (DP) could be synthesized. The DP and narrow dispersity (1.19 or less) confirmed by GPC are listed in Table 5-1. Detailed information is shown in Figure 5-A1. Using the obtained SPP_{68} as the macro-CTA, $MAPTAC_{51}$-b-SPP_{68} and $SSNa_{37}$-b-SPP_{68} were synthesized. The Đ was 1.12 and 1.17, respectively. The chemical structures of the ionic homopolymers and the block copolymers are shown in Figure 5-1.
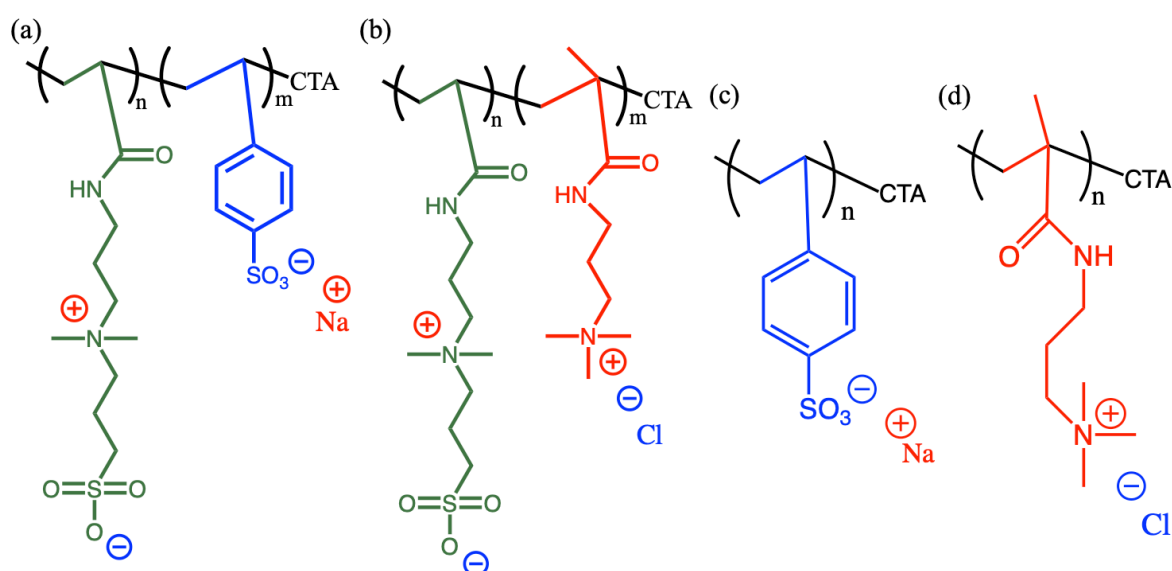
Figure 5-1. Chemical structures of (a) PSSNa-b-PSPP, (b) PMAPTAC-b-PSPP, (c) PSSNa, and (d) PMAPTAC.

5.3.2 Preparation and Confirmation of PIC micelles

Polyion complex (PIC) micelles were prepared using block copolymers ($MAPTAC_{51}$-b-SPP_{68} and $SSNa_{37}$-b-SPP_{68}) and ionic homopolymers with various DP ($MAPTAC_{59}$, $MAPTAC_{85}$, $SSNa_{52}$, and $SSNa_{74}$). PIC micelles are prepared by mixing the block copolymer aqueous solution and an aqueous solution of ionic homopolymer that is charged opposite to the

PSSNa or PMAPTAC portion of the block copolymers so that the anion and cation are equal in charge.[23]

As previously reported,[23] the author confirmed the formation of PIC micelles from the disappearance of the peaks of the ionic chains to become a core and the size of the PIC micelles by ^{1}H NMR and DLS, respectively. Then, the presence of aggregate and the temperature responsivity of the PIC micelles were confirmed by the turbidity. The morphology was observed by AFM.
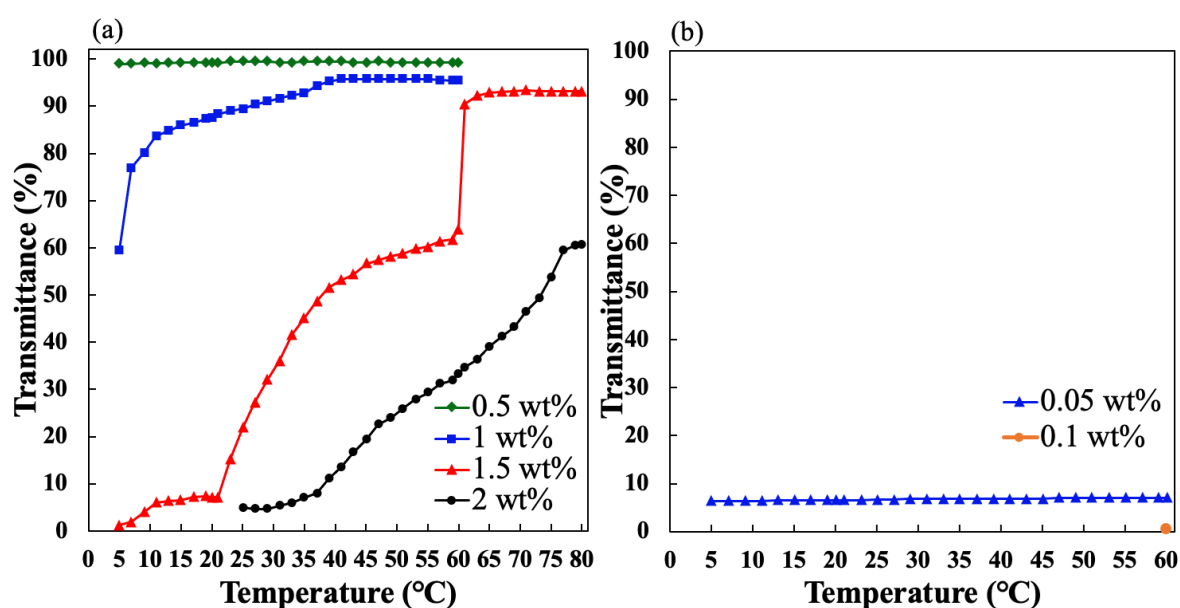
Figure 5-2. Effects of concentration on temperature responsivity of PIC micelles: (a) block copolymer/MAPTAC$_{59}$ and (b) block copolymer/SSNa$_{52}$.

5.3.3 Effects of Concentration on Temperature Responsivity of PIC Micelles

Block-/ionic homopolymer system PIC micelles were prepared using SSNa$_{37}$-b-SPP$_{68}$ and MAPTAC$_{51}$-b-SPP$_{68}$ as the block copolymer, MAPTAC$_{59}$ as a cationic homopolymer, and SSNa$_{52}$ as an anionic homopolymer. Sulfobetaine exhibits temperature responsivity of upper critical solution temperature (UCST) type. However, two block copolymers did not have temperature responsivity due to the influence of the block ratio.[37] The temperature

responsiveness of the PIC micelles in the block-/cationic homopolymer system was investigated by the transmittance. Different concentrations (0.5~2 wt%) of PIC micelles were prepared using $SSNa_{37}$-b-SPP_{68} and $MAPTAC_{59}$. As shown in Figure 5-2a, the PIC micelle aqueous solution did not show temperature responsivity at a concentration of 0.5 wt%. However, the temperature response began to appear from the concentration of 1 wt%, and the transition temperature shifted to the higher temperature side as the concentration increased (from 5 to 59 °C). This tendency resembled that of the system consisting of sulfobetaine-containing entirely ionic diblock copolymers, due to the increased sulfobetaine content at increasing concentrations.[23] Increasing the content of sulfobetaine not only facilitates the formation of intra- or intermolecular salts of sulfobetaine chain but also increases the overall hydrophobicity of polymer solution and shifts the transition temperature to the higher temperature side.[38,39] At 2 wt%, precipitation occurred at room temperature, but stable PIC micelles were formed in the high-temperature region. The higher the concentration, the larger the aggregate is formed in the region below the transition temperature, and the stability of the PIC micelles diminishes. The hysteresis (cooling-heating cycles) of the temperature response of PIC micelles in the block-/cationic homopolymer system due to changes in concentration and the images of 2 wt% samples at different temperatures are shown in Figure 5-A2.

At a concentration of 0.05~0.5 wt%, the PIC micelles in the block-/anionic homopolymer system ($MAPTAC_{51}$-b-SPP_{68}/$SSNa_{52}$) observed by the transmittance, did not show temperature responsivity (Figure 5-2b). At concentration of 0.05 and 0.1 wt% the micelles appeared opaque without precipitating, and at 60 °C, the transmittance was 7 and 0.5 %, respectively. However, at 0.3 and 0.5 wt%, the micelles precipitated immediately even at 90 °C. The details are shown in Figure 5-A3.
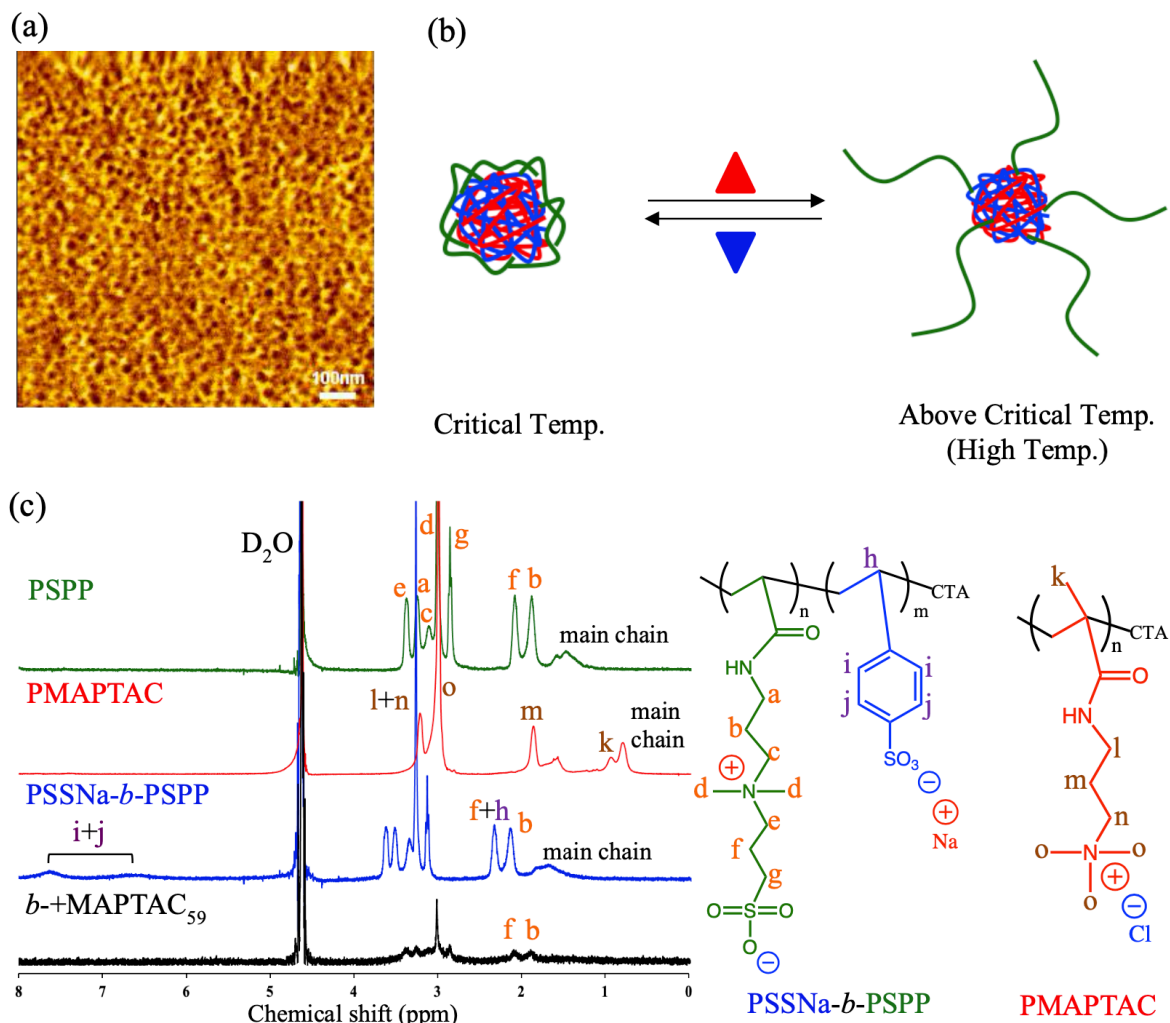
Figure 5-3. PIC micelles in the block-/MAPTAC$_{59}$ system: (a) the height AFM image of the PIC micelles with scale bar 100 nm and (b) schematic illustration of PIC micelles response to temperature changes. (c) Confirmation of formation of PIC micelles by ^{1}H NMR spectra.

5.3.4 Interaction between the Block Copolymer and Ionic Homopolymer Depending on the Concentration

Block-/cationic homopolymer system (SSNa$_{37}$-b-SPP$_{68}$/MAPTAC$_{59}$) micelles at a concentration of 0.5~2 wt% had almost the same size (44~49 nm) at 77~78 °C. Since the extended chain lengths of the block copolymers and the cationic homopolymer were 26.67 nm and 14.99 nm, respectively, they had formed micelles. Then, spherical micelles were formed

as shown in the AFM image (Figure 5-3a). The corona (shell) expended and contracted in response to the change of temperature (Figure 5-3b). Furthermore, as shown in Figure 5-3c, it was confirmed from ^{1}H NMR that the PSSNa peaks (h, i, and j) of the block copolymer and PMAPTAC peaks (k, l, m, n, and o) disappeared by forming PIC micelles. This result suggests the formation of micelles with PSSNa and PMAPTAC as the core and PSPP as the shell. The block copolymer, which did not show temperature responsivity due to the introduction of the ionic chain, forms a polyion complex (PIC) by interacting with the cationic homopolymer, and the influence of the ionic chain on sulfobetaine was weakened and responsiveness could be expressed.[23,37]

The micelles in the 0.05 and 0.1 wt% block-/anionic homopolymer system (MAPTAC$_{51}$-b-SPP$_{68}$ /SSNa$_{52}$) had a hydrodynamic radius (R_h) of 122 nm and 145 nm respectively, at room temperature. The extended chain length of the block copolymer and that of the anionic homopolymer were 30.23 nm and 13.21 nm, respectively. The aggregate was slightly larger than the micelles. For this system, the shape of the aggregates changed with the increase in the concentration of the micelles. As shown in Figure 5-4a, the rod-like aggregate at a concentration of 0.05 wt% became a spherical aggregate when the concentration was 0.1 wt%. In the 0.05 wt% block-/SSNa$_{52}$ system, the PMAPTAC peaks (k, l, m, n, and o) of the block copolymer and the peaks of PSSNa (i and j) disappeared, indicating that PMAPTAC and PSSNa formed the core and PSPP became the shell (Figure 5-4b). PIC micelles having a sulfobetaine as the shell could be formed, but the concentration was too low to express temperature responsivity.[23] On the other hand, at 0.1 wt%, the PMAPTAC peaks (k, l, m, n, and o) of the block copolymer disappeared, but the peaks of the PSSNa homopolymer (h, i, and j) and a broadened the PSPP peak (d) could be confirmed at the same time (Figure 5-4b). This result suggests that the PSSNa homopolymer interacts not only with the PMAPTAC but also with the PSPP. Therefore, the aggregate changed from rod-shaped to spherical due to the

change in concentration. At higher concentrations, the PSSNa homopolymer and block copolymer interacted more strongly to form large aggregates, resulting in precipitation.

It was revealed that only the block-/cationic homopolymer system forms temperature-responsive micelles. The interaction behavior between the ionic homopolymer and the block copolymer was the key point of functional expression.
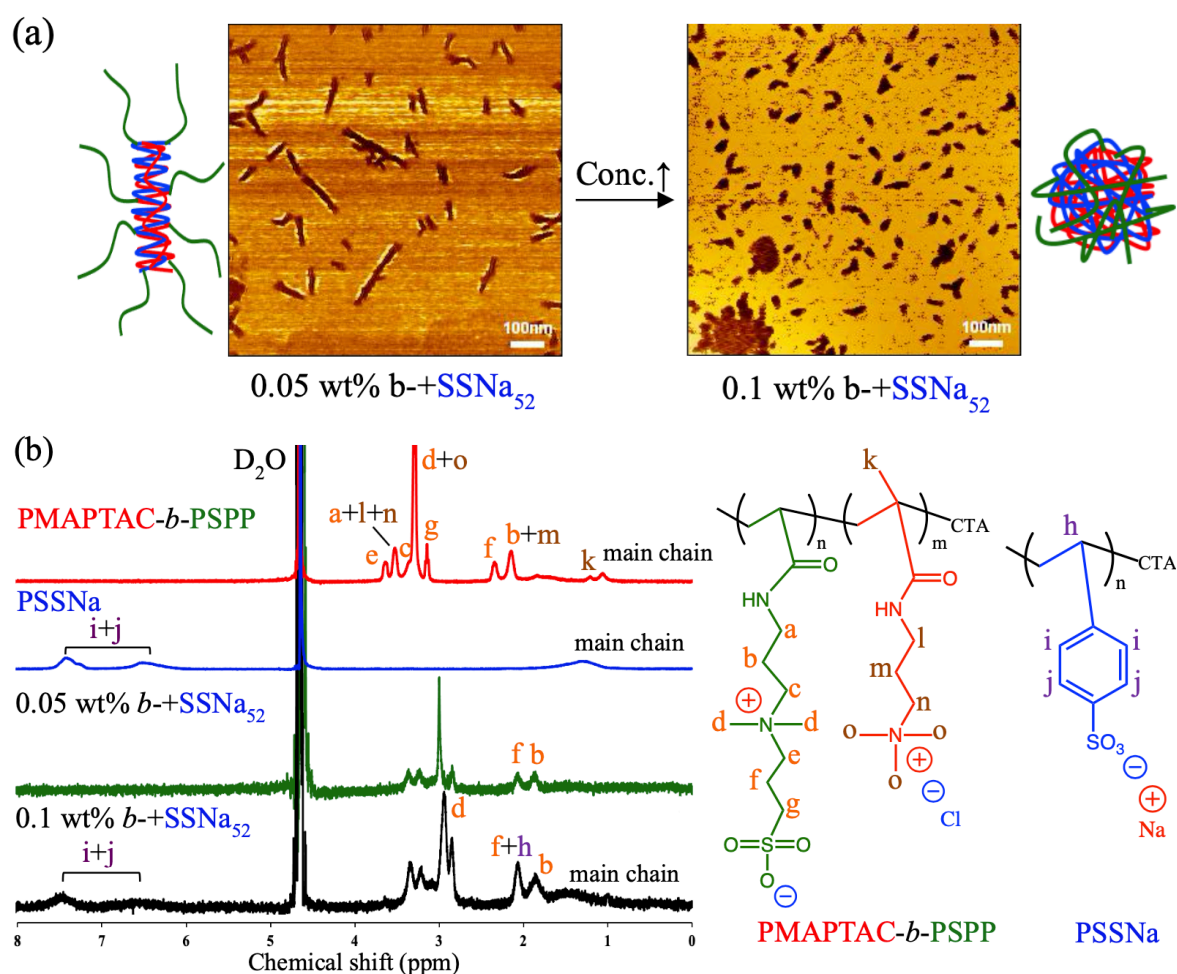
Figure 5-4. PIC micelles in the block-/SSNa$_{52}$ system: (a) the height AFM images of changes in the shape of PIC micelles according to change of concentration with scale bar 100 nm. (b) confirmation of formation of PIC micelles by ^{1}H NMR spectra.

5.3.5 The Effect of DP of Ionic Homopolymers on Formation Behavior and Temperature Responsiveness of PIC Micelles.

The effect of the degree of polymerization (DP) of ionic homopolymers (PMAPTAC or PSSNa) in the block-/ionic homopolymer system was investigated. Unlike the block-/MAPTAC$_{59}$ system, which formed PIC micelles with temperature responsivity in the 1 to 2 wt% concentration range, as shown in Figure 5-5a, the temperature responsiveness disappeared in all concentration ranges when the DP was changed by MAPTAC$_{85}$. This may be because MAPTAC$_{85}$ could not form a core-shell (PIC-sulfobetaine) structure by electrostatically interacting with both PSSNa and PSPP moieties of the block copolymer (SSNa$_{37}$-b-SPP$_{68}$).
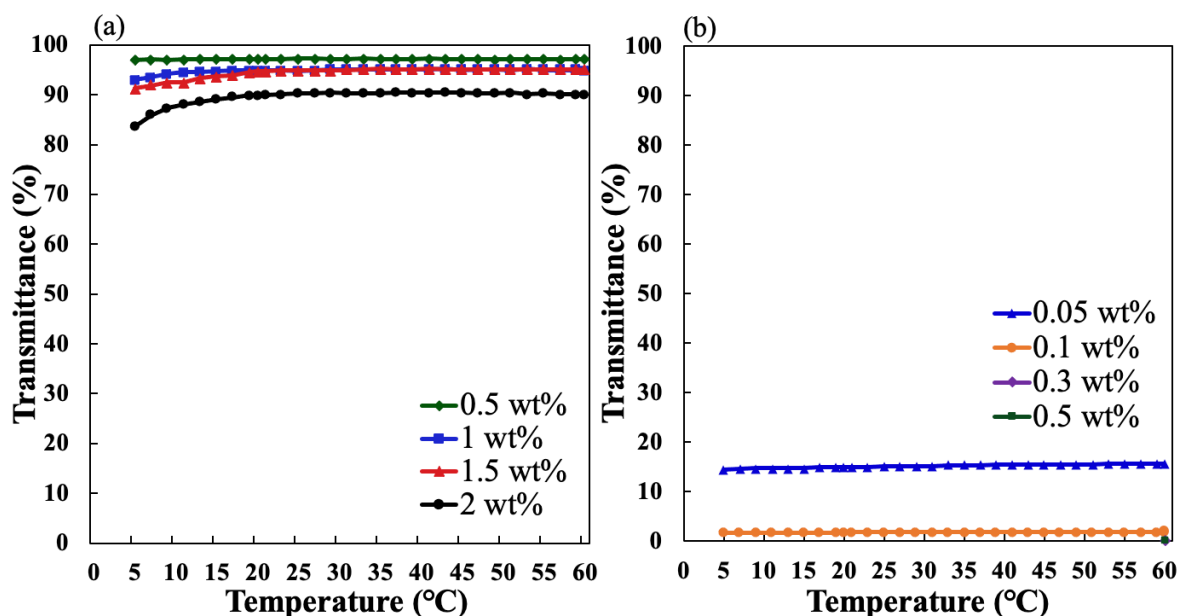
Figure 5-5. The effect of the degree of polymerization of the ionic homopolymers on the temperature responsiveness on the block-/ionic homopolymer system: (a) block-/MAPTAC$_{85}$ and (b) block-/SSNa$_{74}$.

Figure 5-5b shows that the micelles in the block-/anionic homopolymer system prepared by changing the DP of PSSNa homopolymer from SSNa$_{52}$ to SSNa$_{74}$, showed no responsiveness in the concentration range of 0.05~0.5 wt%. This seems to be due to the

interaction between $SSNa_{74}$ and the block copolymer. The micelles in the block-/$SSNa_{74}$ system did not precipitate at a concentration of 0.3 and 0.5 wt% over extended periods of time; with the transmittance being of 0.2 and 0.1 % at 60 °C, respectively. Then, at a concentration of 0.05 wt%, the transmittance was about 15 %, which was higher than that of the micelles in the block-/$SSNa_{52}$ system. The PSSNa homopolymer interacts with PSPP after interacting with the PMAPTAC of the block copolymer ($MAPTAC_{51}$-b-SPP_{68}). The PSSNa homopolymer with a low DP can enter easily and interact with the quaternary ammonium cation in the middle of the sulfobetaine chain.[37] Therefore, $SSNa_{74}$ had a weaker interaction strength and higher transmittance than $SSNa_{52}$, and did not precipitate at a higher concentration.

Figures 5-6a to 5-6d compare the shapes of micelles according to the degree of polymerization of PMAPTAC from AFM. The samples were prepared by naturally drying at a concentration of 1 wt%. A uniform and small spherical aggregate was formed with $MAPTAC_{59}$, but when the DP was increased $MAPTAC_{85}$, a non-uniform and large aggregate was formed. The R_h of the block-/$MAPTAC_{59}$ and block-/$MAPTAC_{85}$ at 77 °C was 49 nm and 110 nm, respectively. As shown in Figure 5-6e, the particle size in block-/$MAPTAC_{59}$ was small and uniform, while the block-/$MAPTAC_{85}$ showed a large particle size consisting of multiple sizes. Here, the significant decrease in the value of the autocorrelation function that is due to the electrostatic interaction was screened by the increase in counterions due to increased DP of PMAPTAC.[40] Furthermore, the interaction between the block copolymer and the cationic homopolymer due to the change in DP from ^{1}H NMR was compared (Figure 5-6f). Unlike the block-/$MAPTAC_{59}$ system, which formed PIC micelles with a core-shell structure, peaks of PMAPTAC (k, l, m, n, and o) were observed in the block-/$MAPTAC_{85}$ system. Consistent with the peaks of PMAPTAC-b-PSPP, $MAPTAC_{85}$ was suggested to interact with both the PSSNa and PSPP moieties of the block copolymer. This was the cause of the loss of temperature responsivity at the higher DP. Then, $MAPTAC_{85}$ interacted with the negative charge (SO_3^-)

outside the sulfobetaine chain to form a large aggregate. From these results, in order to prepare a block-/cationic homopolymer system with PIC micelles having temperature responsiveness, it is necessary to use a cationic homopolymer having a DP lower than that of the sulfobetaine chain which becomes the shell.
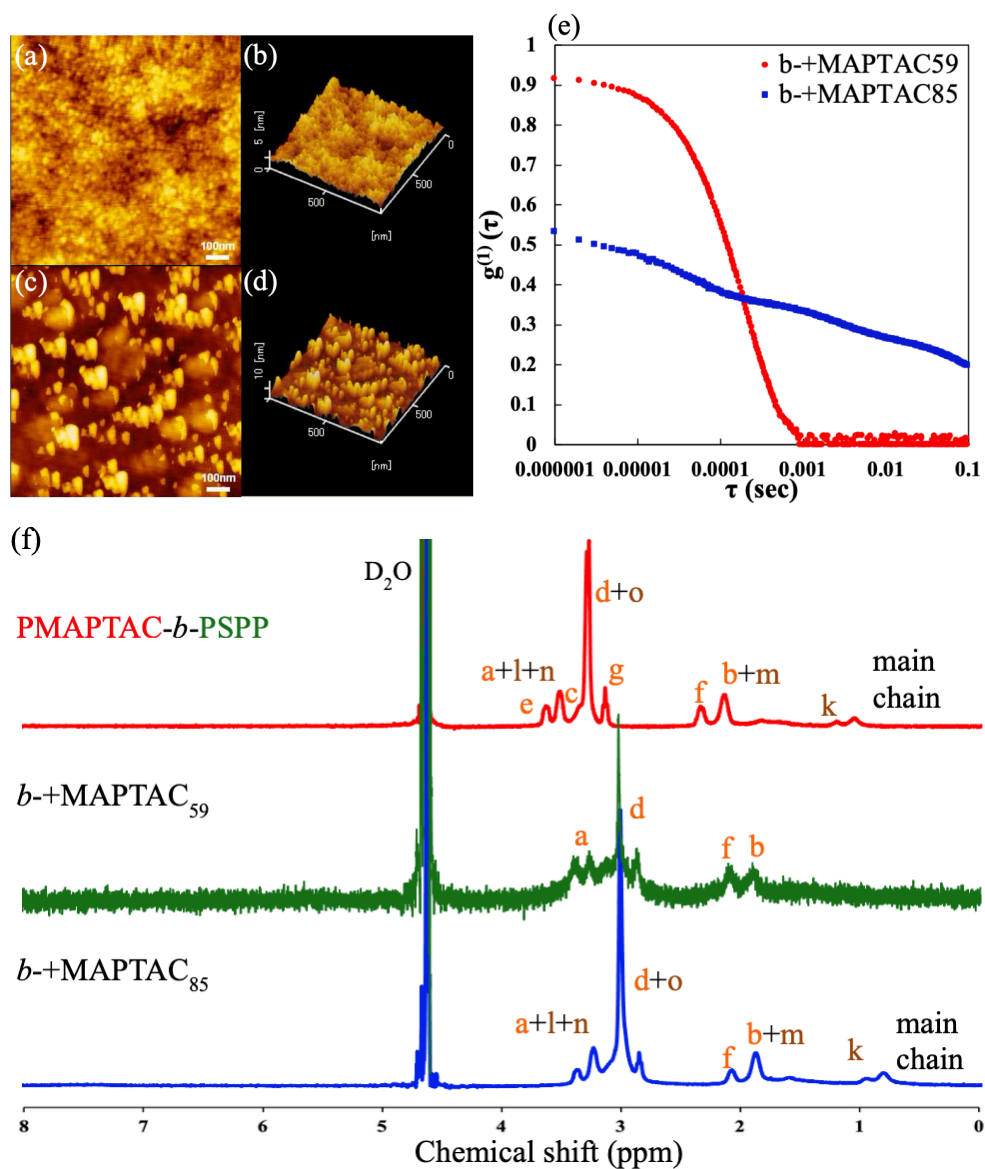

Figure 5-6. Effect of DP on the block-/cationic homopolymer system: the (a) phase and (b) bird's eye view AFM images of block-/MAPTAC59, and the (c) phase and (d) bird's eye view AFM images of block-/MAPTAC85 with scale bar 100 nm. Comparison of (e) results of DLS at 90 °C and (f) 1H NMR spectra.
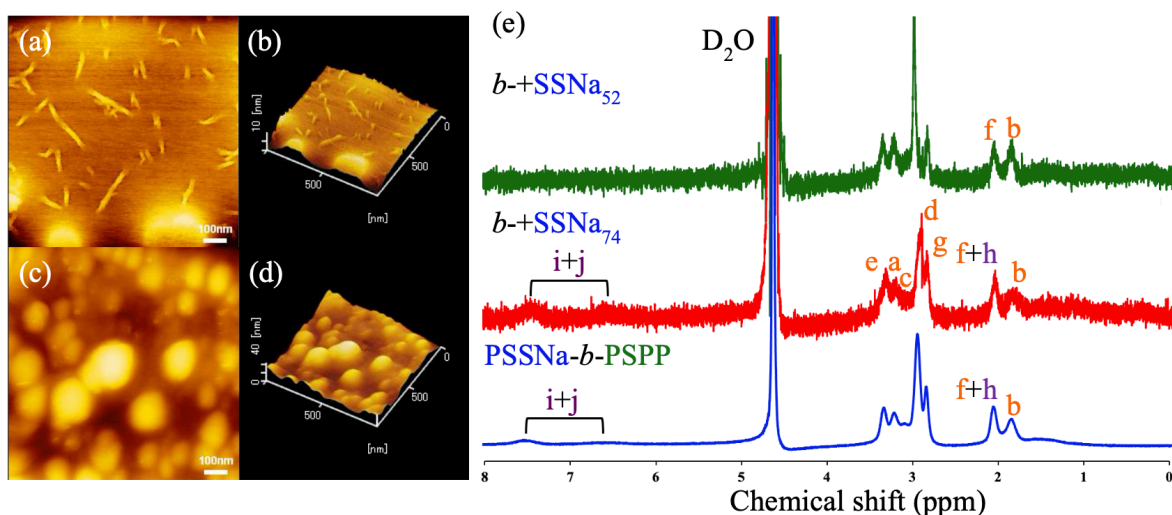
Figure 5-7. Effect of DP on the block-/anionic homopolymer system: the (a) phase and (b) bird's eye view AFM images of block-/SSNa$_{52}$, and the (c) phase and (d) bird's eye view AFM images of block-/SSNa$_{74}$ with scale bar 100 nm. (e) Comparison of 1H NMR spectra.

Figures 5-7a to 5-7d compare the shapes of micelles according to the DP of PSSNa from AFM. The samples were prepared by naturally drying at a concentration of 0.05 wt%. In contrast to the block-/SSNa$_{52}$ system, which has a core-shell (PIC-Sulfobetaine) structure and rod-like shape, the block-/SSNa$_{74}$ system was spherical. The cause was considered to be the interaction between SSNa$_{74}$ and block copolymer, and ^{1}H NMR measurement was performed. As shown in Figure 5-7e, the PMAPTAC peaks disappeared in the block-/SSNa$_{74}$ system, but the PSSNa peaks (h, i, and j) and broadened PSPP peaks (a, c, d, e, and g) were observed. It was the same as the peaks of PSSNa-*b*-PSPP. This suggested that SSNa$_{74}$ interacted with both the PMAPTAC and PSPP moieties of the block copolymer. From these results, it was clarified that in the block-/ionic homopolymer system, temperature-responsive PIC micelles could not be formed by using the anionic homopolymer.
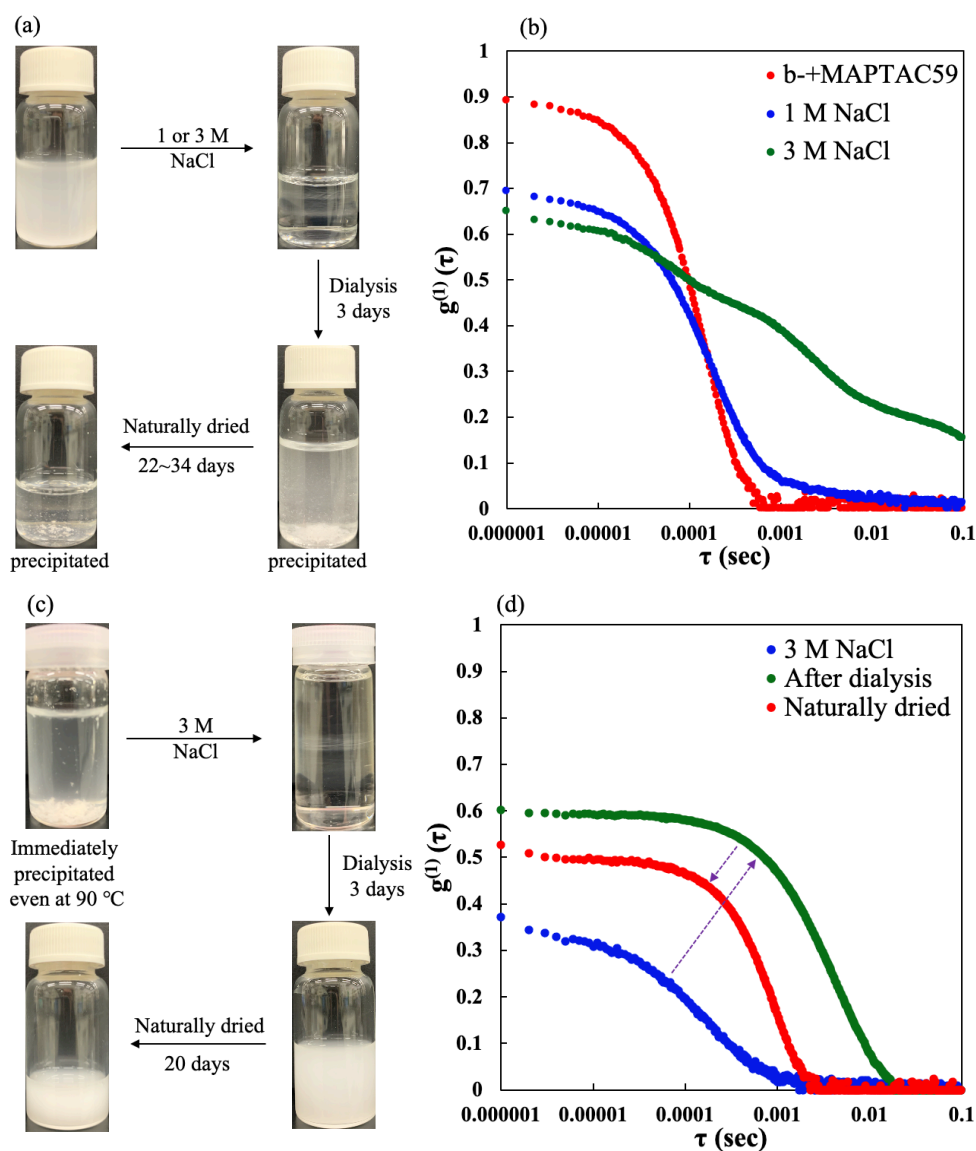
Figure 5-8. The behavior of micelle formation in block-/ionic homopolymer system when prepared by reforming method by dialysis: (a) Images of changes according to the reformation process (collapse of PIC micelles by salt addition→ reformation by dialysis→ concentration by natural drying), and (b) DLS results of collapse due to the concentration of added salt in 1.5 wt% block-/MAPTAC$_{59}$. (c) Images of changes and (d) results of DLS according to the reformation process in 0.5 wt% block-/SSNa$_{52}$.

5.3.6 Formation Behavior by the Method of Preparing PIC Micelles

The formation behavior of PIC micelles prepared by the simple mixing method and that of the PIC micelles prepared by the reformation method by dialysis were compared. In the reformation method, the micelles collapse with the addition of salt to PIC micelles prepared by the simple mixing method. Then, the micelles are reformed in an equilibrium state by dialysis for 3 days. Figure 5-8a is an image of the process of the reformation of block-/MAPTAC$_{59}$ system micelles by dialysis. The opaque 1.5 wt% sample prepared by simple mixing became transparent due to the collapse of PIC micelles by salt addition. The addition of 3M NaCl collapsed micelles but formed aggregates with multiple size distributions (Figure 5-8b). This is considered to be due to the re-entrant effect.[41] On the other hand, when 1 M NaCl was added, the PIC micelles collapsed into small particles with a single size distribution. Here, the significant diminish in the value of the autocorrelation function that is due to the electrostatic interaction was screened by the concentration of added salt increased.[40] When the salt-collapsed samples were dialyzed for 3 days, precipitation occurred during the dialysis. This was the same behavior as that of the temperature-responsive micelles or vesicles whose morphological stability decreased over time, forming larger aggregates and precipitated. When it was concentrated by natural drying to the initial concentration, the aggregate precipitated and gave an almost transparent solution. The precipitate did not dissolve even at 95 °C. From these results, it was clarified that only PIC micelles prepared by a simple mixing method form stable micelles having temperature responsiveness.

Aggregates collapsed when 3 M NaCl was added to the block-/SSNa$_{52}$ system micelles that precipitated immediately after preparation at a concentration of 0.5 wt% (Figure 5-8c). Dialysis of the transparent sample for 3 days made it opaque by reformation of aggregates. However, after subsequent natural drying to obtain the initial concentration, unlike the micelles prepared by the simple mixing method, the micelles prepared by the reforming method by

dialysis did not precipitate even when left for a long time. The hydrodynamic radius (R_h) of the block-/SSNa$_{52}$ system collapsed by salt addition was 15 nm, and the R_h was 353 nm after reformation by dialysis. Then, the R_h changed at 102 nm due to natural drying. Figure 5-8d shows that dialysis increases the R_h of the aggregate and natural drying reduces it. This is because the higher the concentration, the closer the distance between the aggregates and the stronger the interaction, and the greater the influence of the PSSNa homopolymer.[37] Here, the significant decrease in the value of the autocorrelation function that is due to the electrostatic interaction was screened by the change in sample concentration and concentration of added salt.[40] The micelles reformed by dialysis and the micelles concentrated by natural drying were spherical. However, micelles concentrated by natural drying were more uniform and smaller. Detailed AFM information is shown in Figure 5-A4. As a result of observing the concentrated sample from ^{1}H NMR, it was confirmed that SSNa$_{52}$ interacted with both PMAPTAC and PSPP moieties of the block copolymer. This is the cause of the loss of temperature responsiveness. Detailed information of ^{1}H NMR spectra is shown in Figure 5-A5. From these results, it was clarified that the block-/anionic homopolymer system smaller micelles were prepared by the reforming method.

5.4 Conclusions

In summary, the author demonstrated that in the block-/ionic homopolymer system only the block-/cationic homopolymer system forms temperature-responsive PIC micelles. The temperature responsiveness was obtained only when the DP of the cationic homopolymer was lower than the sulfobetaine chain which became the shell.

The transition temperature of micelles in the block- (SSNa$_{37}$-*b*-SPP$_{68}$) /MAPTAC$_{59}$ system shifted to the higher temperature side (from 5 to 59 °C) as the concentration increased (from 1 to 2 wt%). The shape of the micelle was spherical, and it was confirmed by ^{1}H NMR

that it had a core-shell (polyion complex-sulfobetaine) structure. On the other hand, in the block-/MAPTAC$_{85}$ system, MAPTAC$_{85}$ interacted with both PSSNa and PSPP moieties of the block copolymer, resulting in loss of responsiveness.

The block- (MAPTAC$_{51}$-b-SPP$_{68}$) / SSNa$_{52}$ system had a core-shell structure at a concentration of 0.05 wt%, but the concentration was too low to express temperature responsivity. However, both PMAPTAC and PSPP moieties of the block copolymer began to interact with SSNa$_{52}$ with the increase in concentration to 0.1 wt%, and resulted in precipitation at a higher concentration (0.3 wt% or more). On the other hand, the block-/SSNa$_{74}$ system was unable to form a core-shell structure due to electrostatic interaction between the block copolymer and SSNa$_{74}$ even at a concentration of 0.05 wt%.

In the block-/ionic homopolymer system, the micelles prepared by the reforming method through dialysis, formed small and uniform micelles, but temperature responsiveness was not expressed due to morphological stability and electrostatic interaction between block copolymer and ionic homopolymers.

5.5 Appendix

5.5.1 Estimation of the Đ (M_w/M_n) of homopolymers (PSPP, PSSNa and PMAPTAC) and block copolymers (PSSNa-*b*-PSPP and PMAPTAC-*b*-PSPP)

The author conducted GPC measurements using two kinds of eluents. An anionic eluent (20 wt% CH_3CH aq, 0.05 M $NaNO_3$, 0.01 M Na_2HPO_4) was used for PSPP, PSSNa homopolymers and PSSNa-*b*-PSPP block copolymer. PSSNa was used as the standard sample. A cationic eluent (0.5 M CH_3COOH, 0.3 Na_2SO_4) was used for PMAPTAC homopolymers and PMAPTAC-*b*-PSPP block copolymer. P2VP was used as the standard sample. The results of PSPP-containing polymers are shown in Figure 5-A1a, and the results of ionic homopolymers (PSSNa and PMAPTAC) are shown in Figure 5-A1b.
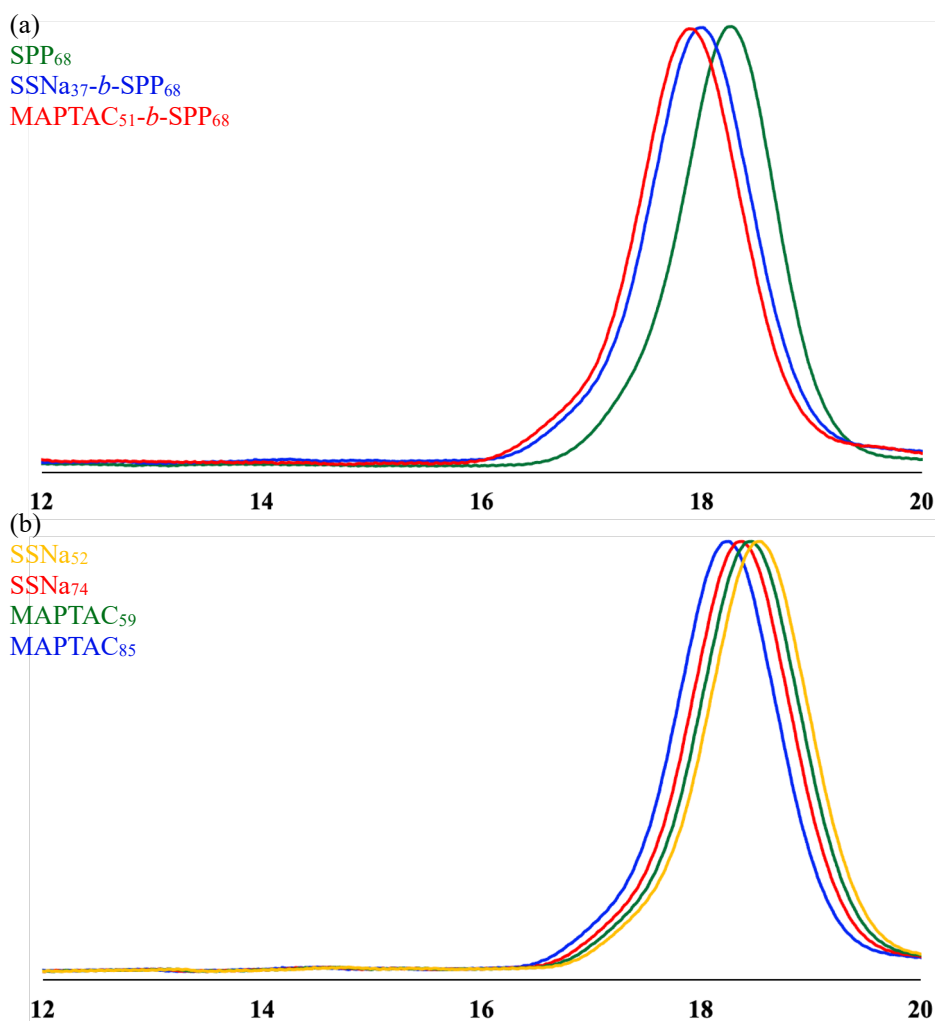
Figure 5-A1. GPC charts for (a) PSPP-containing polymers and (b) ionic homopolymers.

SPP$_{68}$: M_n=19100 and M_w/M_n=1.06

SSNa$_{37}$-*b*-SPP$_{68}$: M_n=27100 and M_w/M_n=1.12

MAPTAC$_{51}$-*b*-SPP$_{68}$: M_n=30200 and M_w/M_n=1.17

SSNa$_{52}$: M_n=11000 and M_w/M_n=1.19

SSNa$_{74}$: M_n=15600 and M_w/M_n=1.13

MAPTAC$_{59}$: M_n=13200 and M_w/M_n=1.17

MAPTAC$_{85}$: M_n=19000 and M_w/M_n=1.11
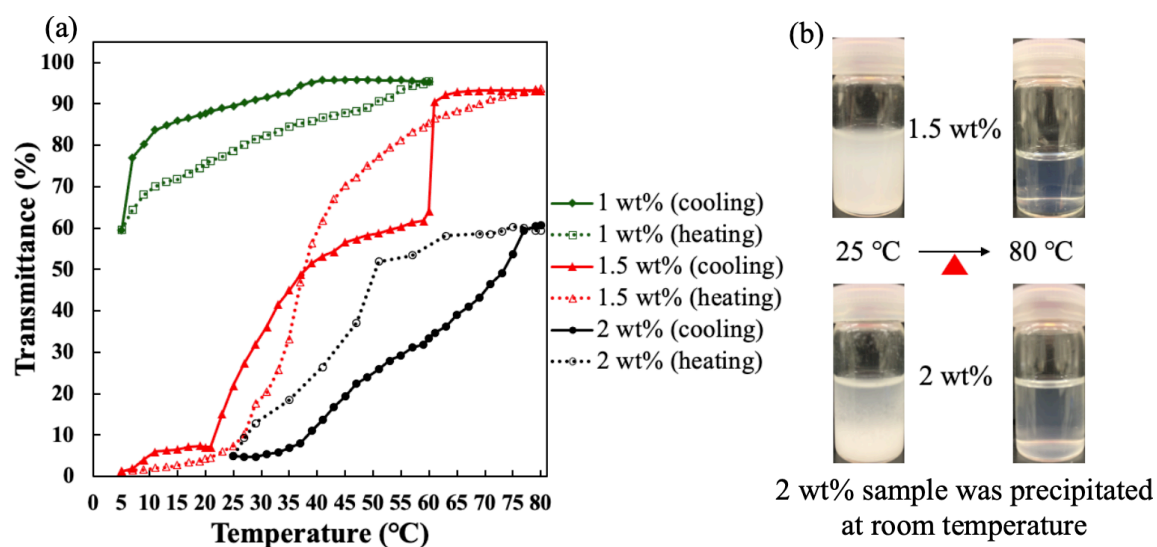
Figure 5-A2. Temperature responsivity of the block-/MAPTAC$_{59}$ system with different concentration of micelles: (a) hysteresis of temperature responsiveness and (b) images of changes in transmittance according to temperature changes.
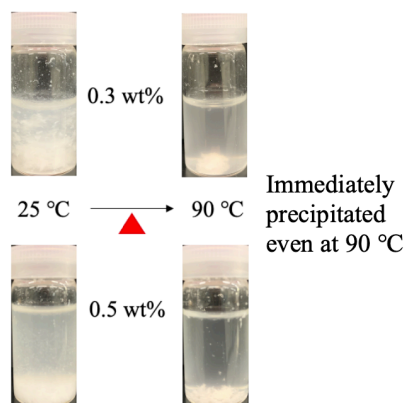
Figure 5-A3. The block-/SSNa$_{52}$ systems were prepared at micelle concentration of 0.3 and 0.5 wt%.

(a) 0.5 wt% block-/SSNa$_{52}$: after dialysis

Height Phase Bird's eye view

(b) 0.5 wt% block-/SSNa$_{52}$: after concentration
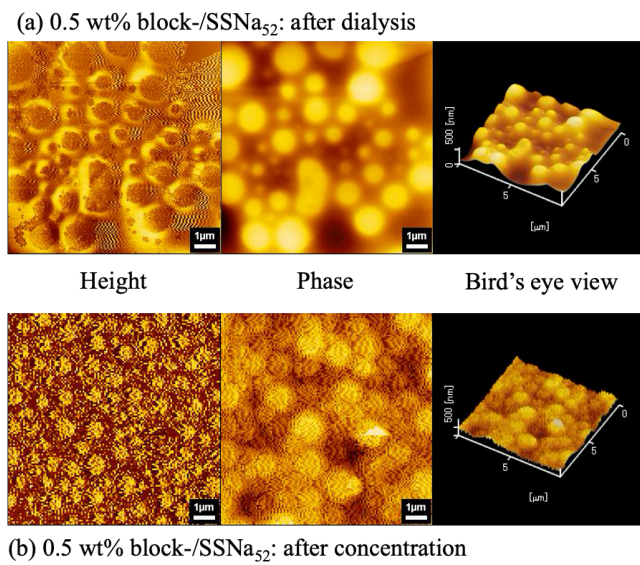
Figure 5-A4. Images of AFM (a) after dialysis and (b) after concentration in the 0.5 wt% block-/SSNa$_{52}$ system. Scale bar: 1μm.
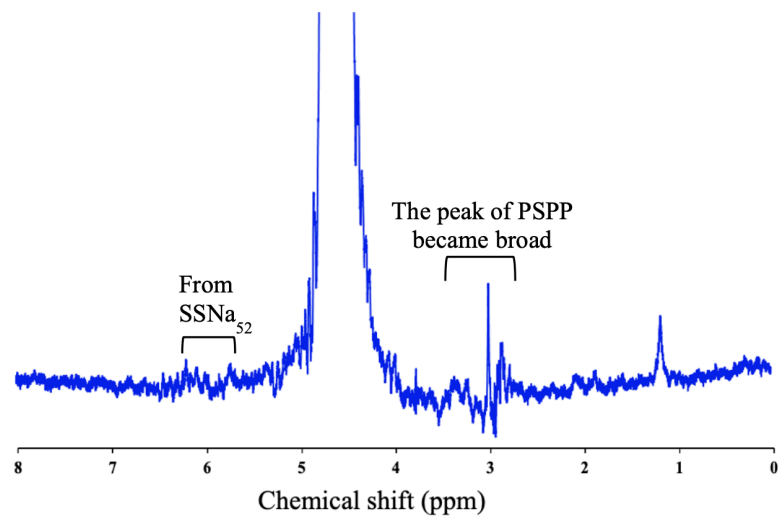
**Figure 5-A5.** ^{1}H NMR spectra of concentrated 0.5 wt% block-/SSNa$_{52}$ system.
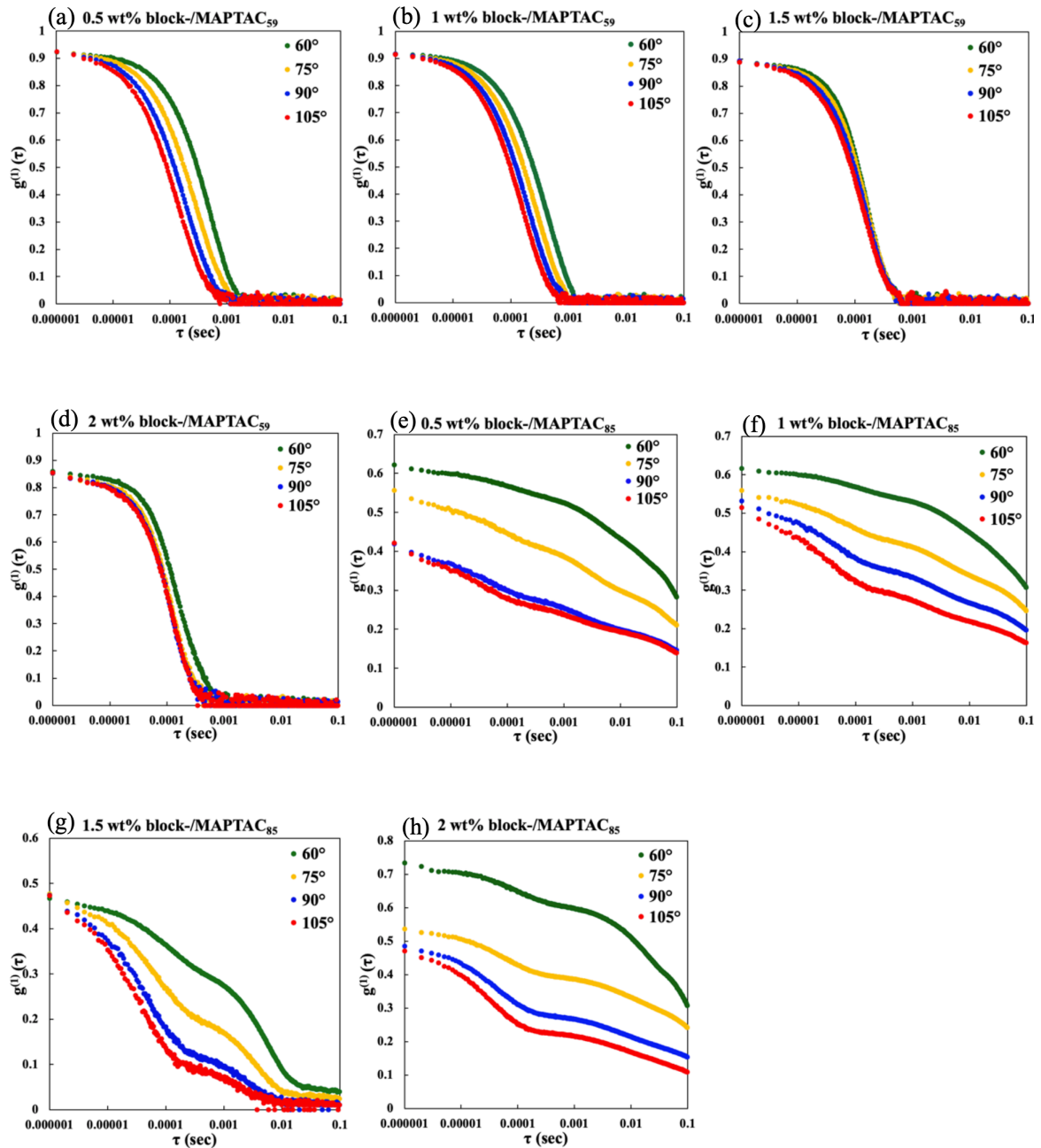
Figure 5-A6. The results of DLS according to concentration in block-/cationic homopolymer system: (a) 0.5, (b) 1, (c) 1.5, (d) 2 wt% of block-/MAPTAC$_{59}$ and (e) 0.5, (f) 1, (g) 1.5, (h) 2 wt% of block-/MAPTAC$_{85}$ at 77~78 °C.
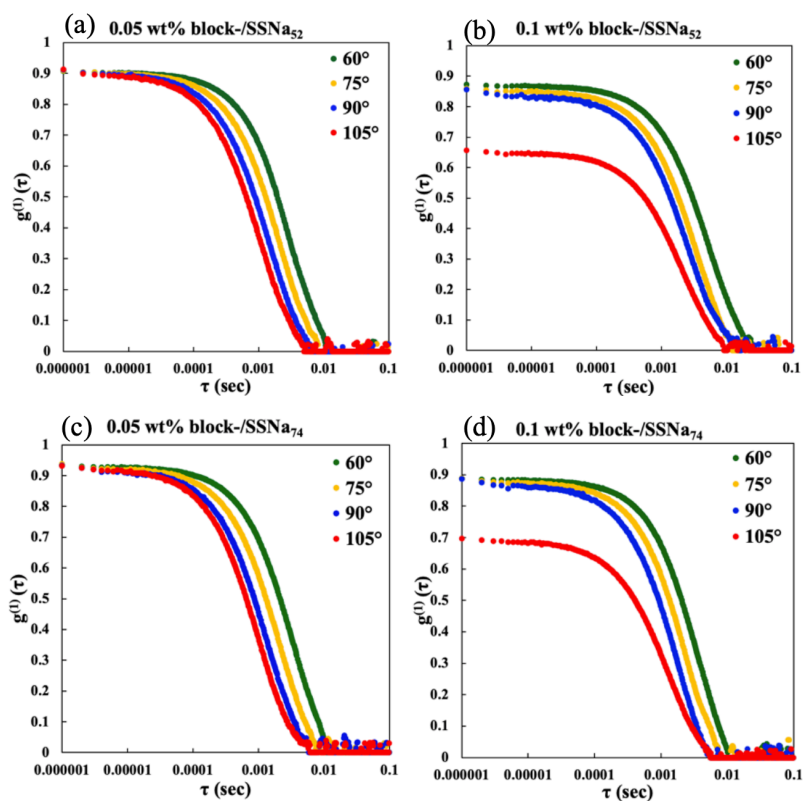
Figure 5-A7. The results of DLS according to concentration in block-/anionic homopolymer system: (a) 0.05, (b) 0.1 wt% block-/SSNa$_{52}$ and (c) 0.05, (d) 0.1 wt% of block-/SSNa$_{74}$ at 25 °C.
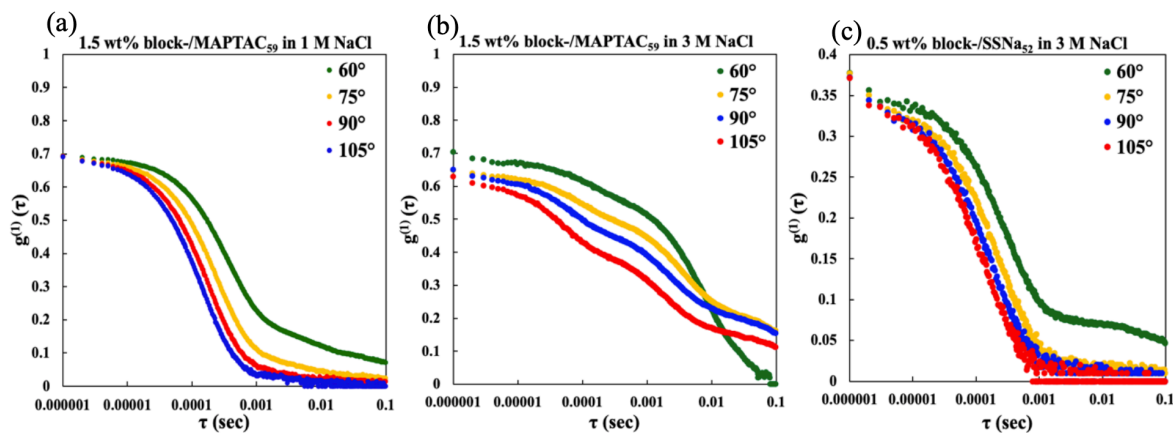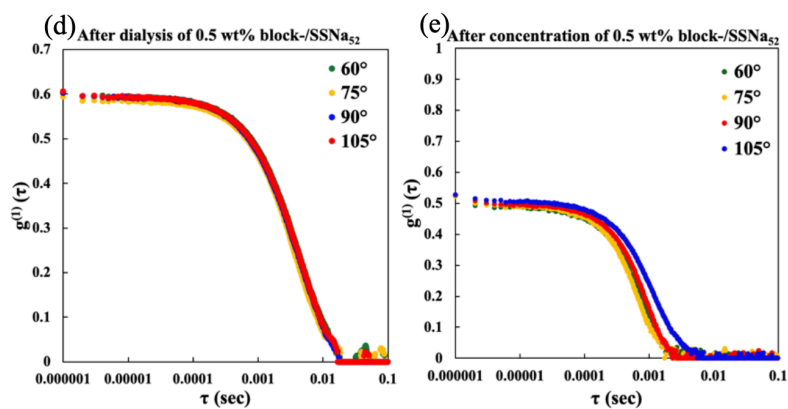
Figure 5-A8. Changes in Rh during the process of reformation method: the block-/MAPTAC$_{59}$ in (a) 1 M, (b) 3 M NaCl. The block-/SSNa$_{52}$ in (c) 3 M NaCl. (d) after dialysis and (e) after concentration of block-/SSNa$_{52}$.

5.6 Reference

[1] R. Hart, D. Timmerman, *J. Polym. Sci.* **1958**, 28, 638-640.

[2] A. B. Lowe, C. L. McCormick, *Chem. Rev.* **2002**, 102, 4177-4189.

[3] A. Laschewsky, *Polymers* **2014**, 6, 1544-1601.

[4] R. Graf, S. Anzali, J. Buenger, F. Pfluecker, H. Driller, *Clin. Dermatol.* **2008**, 26, 326-333

[5] R. Y. Lochhead, *Cosmetic Nanotechnology Chapeter1*, 3-56. ACS **2007**.

[6] S. Kudaibergenov, W. Jaeger, A. Laschewsky, *Adv. Polym. Sci.* **2006**, 201, 157-224.

[7] A. G. Kohli, C. L. Walsh, F. C. Szoka, *Chem. Phys. Lipids* **2012**, 165, 252-259.

[8] S. Jiang, Z. Cao, *Adv. Mater.* **2010**, 22, 920-932.

[9] J. T. Sun, Z. Q. Yu, C. Y. Hong, C. Y. Pan, *Macromol. Rapid Commun.* **2012**, 33, 811-818.

[10] Y. S. Wang, S. Yau, L. K. Chau, A. Mohamed, C. J. Huang, *Langmuir* **2019**, 35, 1652-1661.

[11] D. S. Han, M. S. Gong, *Macromol. Res.* **2010**, 18, 260-165.

[12] Q. Wang, X. Zheng, Y. Deng, J. Zhao, Z. Chen, J. Huang, *Joule* **2017**, 1, 371-382.

[13] V. H. Tran, S. K. Kim, S. H. Lee, *ACS Omega* **2019**, 4, 19225-19237.

[14] H. Kim, H. H. Nicholas, J. H. Kang, P. Bisnoff, S. Sundararajan, T. Thompson, M. Barnes, R. C. Hayward, T. Emrick, *Angew. Chem. Int. Ed.* **2020**, 59, 10802-10806.

[15] H. Matsuoka, Y. Kido, M. Hachisuka, *Chem. Lett.* **2015**, 44, 1622-1624.

[16] S. Alharthi, N. Grishkewich, R. M. Berry, K. C. Tam, *Carbohydr. Polym.* **2020**, 246, 11651-11659.

[17] S. Xiao, Y. Zhang, M. Shen, F. Chen, P. Fan, M. Zhong, B. Ren, J. Yang, J. Zheng, *Langmuir* **2018**, 34, 97-105.

[18] D. B. Thomas, Y. A. Vasilieva, R. S. Armentrout, C. L. McCormick, *Macromolecules.* **2003**, 36, 9710-9715.

[19] S. L. West, J. P. Salvage, E. J. Lobb, S. P. Armes, N. C. Billinghan, A. L. Lewis, G. W.

Hanlon, A. W. Lloyd, *Biomaterials* **2004**, 25, 1195-1204.

[20] B. Yu, A. B. Lowe, K. Ishihara, *Biomacromolecules* **2009**, 10, 950-958.

[21] M. Kobayashi, Y. Terayama, M. Kikuchi, A. Takahara, *Soft Matter* **2013**, 9, 5138-5148.

[22] Y. Higaki, Y. Inutsuka, T. Sakamaki, Y. Terayama, A. Takenaka, K. Higaki, N. L. Yamada, T. Moriwaki, Y. Ikemoto, A. Takahawa, *Langmuir* **2017**, 33, 8404-8412.

[23] D. Kim, H. Matsuoka, Y. Saruwatari, *Langmuir* **2020**, 36, 10130-10137.

[24] K. Nakai, M. Nishiuchi, M. Inoue, K. Ishihara, Y. Sanada, K. Sakurai, S. Yusa, *Langmuir.* **2013**, 29, 9651-9661.

[25] D. Kim, H. Sakamoto, H. Matsuoka, Y. Saruwatari, *Langmuir* **2020**, 36, 12990-13000.

[26] R. Kumar, G. C. Kalur, L. Ziserman, D. Danino, S. R. Raghavan, *Langmuir* **2007**, 23, 12849-12856.

[27] L. Qi, Y. Fang, Z. Wang, N. Ma, L. Jiang, Y. Wang, *J. Surfact. Deterg.* **2008**, 11, 55-59.

[28] J. Ning, G. Li, K. Haraguchi, *Macromolecules* **2013**, 46, 5317-5328.

[29] M. Das, N. Sanson, E. Kumacheva, *Chem. Mater.* **2008**, 20, 7157-7163.

[30] K. Letchford, H. Burt, *Eur. J. Pharm. Biopharm.* **2007**, 65, 259-269.

[31] M. L. Adams, A. Lavasanifar, G. S. Kwon, *J. Pharm. Sci.* **2003**, 92, 1343-1355.

[32] A. Harada, K. Kataoka, *Macromolecules* **1995**, 28, 5294-5299.

[33] A. Harada, K. Kataoka, *Science* **1999**, 283, 65-67.

[34] Y. Anraku, A. Kishimura, M. Oba, Y. Yamasaki, K. Kataoka, *J. Am. Chem. Soc.* **2010**, 132, 1631-1636.

[35] Y. Mitsukami, M. S. Donovan, A. B. Lower, C. L. McCormick, *Macromolecules* **2001**, 34, 2248-2256.

[36] A. Einstein, *Ann. der Physik* **1905**, 322, 549-560.

[37] D. Kim, H. Matsuoka, Y. Saruwatari, *Langmuir* **2019**, 35, 1590-1597.

[38] D. N. Schulz, D. G. Peiffer, P. K. Agarwal, J. Larabee, J. J. Kaladas, L. Soni, B.

Handwerker, R. T. Garner, *Polymer* **1986**, 27, 1734-1742.

[39] V. Hildebrand, A. Laschewsky, E. Wischerhoff, *Polym. Chem.* **2016**, 7, 731-740.

[40] M. Drifford, J. P. Dalbiez, *Biopolymers* **1985**, 24, 1501-1514.

[41] G. Liu, D. Parsons, V. S. J. Craig, *J. Colloid Interface Sci.* **2020**, 579, 369-378.

Chapter 6

Complex Formation of Sulfobetaine Surfactant and Ionic Polymers and Their Stimuli Responsivity

The author investigated the kinds of complexes sulfobetaine surfactant and ionic polymer formed using lauramidopropyl hydroxysultane (LAPHS) as a sulfobetaine surfactant, poly (sodium styrenesulfonate) (PSSNa) as the anionic polymer and poly[3-(methacrylamido)propyl trimethylammonium chloride] (PMAPTAC) as the cationic polymer. The fundamental properties of LAPHS at various salt concentrations were estimated by various measurements, and it was confirmed that the LAPHS micelles alone did not show temperature responsiveness. The presence of large aggregates in addition to LAPHS micelles was confirmed in the aggregates prepared by adding PSSNa to LAPHS at a charge ratio of 1:0.5, 1:1, and 1:2. However, the aggregates could not be formed when the salt concentration was high or when a monomer was added instead of the polymer. This revealed that the cation part of sulfobetaine, which is the shell of LAPHS micelles, and the anion part of PSSNa electrostatically interacted with each other to form a large aggregate. On the other hand, unlike the case of LAPHS micelles alone and the aggregate consisting of LAPHS micelles and PSSNa, the aggregate of LAPHS micelles and PMAPTAC showed an unprecedented phenomenon of "clear→ opaque→ clear" with increasing concentration in the concentration range above CMC. The change in the transition temperature due to the change of concentration was a factor. Additionally, the author confirmed that the transition temperature was lowered when the concentration was higher than CMC or the salt concentration was increased, and the transition temperature was increased when the PMAPTAC with a high degree of polymerization was added. These results suggested that the LAPHS micelles and the ionic polymer form an aggregate, and the temperature

responsivity can be expressed by the interaction with the cationic polymer.

6.1 Introduction

Betaine polymer, which is a kind of zwitterionic polymer, has an equal number of negatively charged functional group and positively charged functional group.[1-3] Due to its structural characteristics, it has high biocompatibility with less protein adsorption[4-6] and less adherence to blood cells,[6-8] and is therefore being applied to new medical materials.[9,10] The effect of the added salt on the conformation of the polymer chain in the aqueous solution is exactly opposite of that of the common ionic chain polymer: the ionic chain polymer is contracted by the added salt,[11,12] while the betaine chain polymer is extended.[13,14] A betaine polymer has temperature responsivity of upper critical solution temperature (UCST) type[15-17] and pH-responsiveness[18-20] that vary greatly depending on the functional group of the ionic part, and has a high solubility in water[2,3,18] and is dependent on the added salt concentration,[2,18,22] regardless of the type of functional group. Utilizing its properties, it has been widely studied for gels,[23,24] micelles,[20,25] brushes,[13,26] vesicles,[19,22] surfactant,[27,28] monolayer,[5,14] etc.

There are various types of polymeric micelles and vesicles, prepared by using diblock[11,29] or triblock copolymers[25,30] consisting of hydrophilic and hydrophobic chains, or prepared by mixing two diblock copolymers composed of a non-ionic polymer or zwitterionic polymer chain and an ionic polymer chains (anionic or cationic).[19,31-33] By controlling the design of the polymer structures and the combination of polymer chains to be mixed, it is possible to have responsiveness to stimuli such as temperature responsivity (LCST (lower critical solution temperature)[34-36] or UCST type[33,36,37]), pH-responsivity,[19,32] photoresponsivity,[38,39] and enzyme responsivity.[40,41]

A surfactant is a type of amphiphilic molecule possessing both a hydrophilic group and

a lipophilic group in one molecule. It is adsorbed on the interface between polar and non-polar substances to form micelles, vesicles, and lamellar structures, which reduce the surface tension and mix evenly.[42-44] Among them, betaine surfactants are mainly used in cosmetics, detergents, disinfectants, anti-static agent, foaming agent, hydrophilic thickeners and the like.[27,42-44] Betaine surfactant micelles having a sulfobetaine structure, unlike sulfobetaine polymers, are difficult to exhibit temperature responsiveness by themselves. It is considered that this is due to the difference between high molecular weight (polymer) and low molecular weight.

In this study, the author aim to exhibit temperature responsiveness by forming aggregates of sulfobetaine surfactant micelles and ionic polymers by polyionic interaction. The author investigated the kind of aggregate formed using LAPHS micelles, which are sulfobetaine surfactant, and ionic polymers, and their stimuli responsivity. The fundamental properties and stimuli responsivity of the LAPHS micelles were confirmed by surface tension, fluorescence, dynamic light scattering (DLS), transmittance, and electrophoretic light scattering (ELS). The author investigated the effect of charge ratio and degree of polymerization (DP) of anionic polymers added to LAPHS micelles on the complex formation behavior and their stimuli responsivity. Then, the effects of the charge ratio and DP of the cationic polymer added to the LAPHS micelles on the complex formation behavior and stimulus response were investigated. Furthermore, the effects of DP and the concentration of added salt on the temperature responsiveness of LAPHS micelles alone and LAPHS micelles + PSSNa and LAPHS micelles + PMAPTAC were compared and examined.

6.2 Experimental

6.2.1 Materials

3-(Methacrylamido)propyl trimethylammonium chloride (MAPTAC) and lauramidopropyl hydroxysultaine (LAPHS) were kindly donated by Osaka Organic Chemical Industry

Ltd. (Osaka, Japan). 4,4′-Azobis(4-cyanovaleric acid) (ACVA, 98%), *p*-styrenesulfonic acid sodium salt (SSNa), sodium chloride (NaCl), pyrene, cetylpyridinium chloride (CPC), acetone, were purchased from Wako (Osaka, Japan). 4-Cyanopentanoic acid dithiobenzoate was used as a chain transfer agent (CTA), which was synthesized as reported by Mitsukami et al.[45] Deuterium oxide (D$_2$O, 99.9 %) was a product of Cambridge Isotope Laboratory (CIL) (U.K.). Ultrapure water obtained by Milli-Q system (18.2 MΩcm) was used for solution preparation and dialysis. Dialysis for ionic homopolymers was carried out with a dialysis tube from Orange Scientific (MWCO: 3500).

6.2.2 Synthesis of Homopolymers

The PSSNa and PMAPTAC homopolymers were synthesized by the reversible addition-fragmentation chain transfer (RAFT) polymerization. The synthesis was carried out by mixing ionic monomer (SSNa or MAPTAC), CTA and initiator (ACVA) at various molar ratios as reported previously. [15]

6.2.3 ^{1}H Nuclear Magnetic Resonance (NMR)

^{1}H NMR spectra for confirmation of PSSNa and PMAPTAC homopolymers were obtained with a JEOL JNM-EX 400 spectrometer using D$_2$O (CIL, 99.99%) as a solvent. The concentration of the polymer solution was 10 mg/mL.

6.2.4 Gel Permeation Chromatography (GPC)

The degree of polymerization (DP) of ionic homopolymers (PSSNa or PMAPTAC) and their polydispersity index were determined by a JASCO GPC system (Tokyo, Japan) composed of an 830-RI detector, UV-2075 Plus UV detector, CO-2065 Plus column oven, PU-2080 Plus HPLC pump, DG-2080-53 3-line degasser and Shodex SB-804 HQ column.

6.2.5 Transmittance

The temperature responsiveness of LAPHS micelles, the complex formed by LAPHS micelles and ionic polymers (PSSNa or PMAPTAC), and the effect of added salt concentration were determined using UV-vis spectrometer U-3310 (Hitachi). Observations were made at various salt concentrations and polymer aqueous solutions. The author designated the transition temperature as the temperature at which the sample characteristics (turbidity) suddenly changed at a wavelength of 400 nm and various temperature ranges.

6.2.6 Dynamic Light Scattering (DLS)

The change in hydrodynamic radius (R_h) according to the salt concentration and charge ratio of LAPHS to ionic polymers (PSSNa or PMAPTAC) when forming complex was estimated using a Photal SLS-7000DL (Otsuka Electronics Co., LTD) (Osaka, Japan) equipped with a 15 mW He-Ne laser (wavelength 632.8 nm) and GC-1000 photon correlator. The concentration of each sample was 10 mg/mL and DLS was observed at room temperature. The time correlation function of the scattered field was measured at four scattering angles (60°, 75°, 90°, and 105°) with an accumulation time of 30 min. The hydrodynamic radius (R_h) was calculated using the Stokes-Einstein equation[46,47] as follows

$$R_h = \frac{k_B T}{6\pi \eta D} \qquad (1)$$

where η, k_B, and T are the solvent viscosity, Boltzmann constant, and absolute temperature, respectively.

6.2.7 Static Light Scattering (SLS)

The changes in critical micelle concentration (CMC) according to the salt concentration and charge ratio of LAPHS to ionic polymers (PSSNa or PMAPTAC) when

forming complex were estimated using a Photal SLS-7000DL, which is the same equipment as used for measuring DLS. The samples were diluted with a saline solution, and the concentration was adjusted and measured at 25 °C. When the obtained scattering intensity was a log-log plotted against the polymer concentration, the slope of the scattering intensity changes with an increase in concentration.[48] The intensity due to the concentration of LAPHS or mixture systems did not change up to a certain concentration, but beyond the CMC, it began to increase rapidly because of aggregation of LAPHS or mixture systems. The author designated this inflection point as CMC.

6.2.8 Surface Tension

The surface tension of various samples was measured by the wilhelmy plate method using a FACE CBVP-Z Surface Tensiometer (Kyowa Interface Science Co., Ltd., Tokyo, Japan) at 25 °C. The samples were prepared in a petri dish and allowed to stand in a dark place for about 24 hours to equilibrate, and then measured. The inflection point at which surface tension drastically changes with respect to concentration while diluted is determined as CMC.

6.2.9 Fluorescence Measurement

The CMC of each samples was determined using a F-2500 Fluorescence Spectrophotometer (Hitachi). To the sample was added 4 µL of a solution (0.6 mM) of pyrene dissolved in acetone, and the mixture was allowed to stand for about 24 hours, and the measurement was performed after the solution reached an equilibrium state. The obtained values of the ratio of the intensity of the first and third vibronic peaks (I_1/I_3) exist in the polarity around pyrene, and it is suggested that the higher value, the greater polarity. CMC can be found from the change in the value.

In addition, the aggregation number (N_{agg}) of LAPHS micelles and complex composed

of LAPHS micelles and ionic polymer was determined by fluorescence quenching method. As a quencher for the fluorescent probe pyrene, a solution (1.65 mM) of 2.8 mg cetylpyridinium chloride (CPC) in 5 mL acetone was used. To the sample was added 20 μL of solution in which pyrene was dissolved in acetone, and then a quencher was added in increments of 50 μL for measurement. The samples were measured at room temperature at a concentration of 2 mg/mL that is above the CMC. The aggregation number was determined from the slope of the natural logarithm plotted of the I_1/I_3 against the concentration of quencher using the equation[49] as follows

$$\ln\left(\frac{I_0}{I}\right) = \frac{[Q]N_{agg}}{[C_S]-[CMC]} \qquad (2)$$

where C_s and $[Q]$ are the concentrations of the LAPHS surfactant and quencher, respectively, and I and I_0 are the intensities of fluorescence with and without the quencher, respectively.

6.2.10 Electrophoretic Light Scattering (ELS)

The zeta potential of 10 mg/mL LAPHS and LAPHS micelles-ionic polymer complex in 0.043 M NaCl (aq) was measured at room temperature using an ELSZ-2000 (Otsuka Electronics Co., Ltd, Osaka, Japan). The charge ratio between LAPHS micelles and ionic polymers was 1:1. The average value of the values obtained by repeating three times was designated as the zeta potential. The zeta potential was calculated from the obtained electrophoretic mobility using the Smoluchowski's equation[50] as follows

$$\zeta = \frac{4\pi\eta U}{\varepsilon} \qquad (3)$$

where U, η, and ε are the electrophoretic mobility, the viscosity of solvent and the dielectric constant of the solvent, respectively.

6.3 Results and Discussion

6.3.1 Characterization of Ionic Homopolymers

PSSNa and PMAPTAC homopolymers with various degrees of polymerization (DP) could be synthesized. The DP and narrow polydispersity (1.11 or less) confirmed from GPC are listed in Table 6-1 (see the Appendix for details). The chemical structures of the ionic homopolymers are shown in Figure 6-1.

Table 6-1. Characteristics of Ionic Homopolymers (PSSNa and PMAPTAC).

Polymer[a]	Yield (%)	M_n (g/mol)[b]	PDI (M_W/M_n)[b]	DP (n)
PSSNa-1	55	6900	1.10	32
PSSNa-2	69	13700	1.06	65
PSSNa-3	38	19500	1.11	95
PMAPTAC-1	85	14400	1.06	65
PMAPTAC-2	54	19000	1.11	85

[a]SSNa, SSNa, *p*-styrene sulfonic acid sodium salt; and MAPTAC, 3-(methacrylamido)propyl trimethylammonium chloride. [b]PSSNa was determined with an anionic eluent (20 wt% CH_3CN (aq), 0.05 M $NaNO_3$, 0.01 M Na_2HPO_4, and PMAPTAC was used as a cationic eluent (0.5 M CH_3COOH, 0.3 M Na_2SO_4).
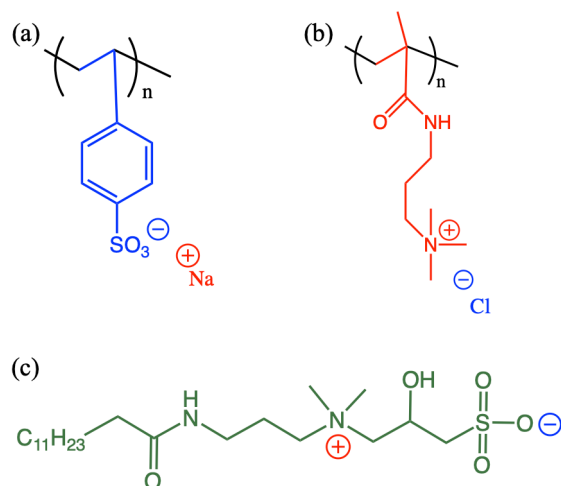
Figure 6-1. Chemical structure of (a) PSSNa, (b) PMAPTAC, and (c) LAPHS.

6.3.2 Effect of Added Salt Concentration on Characteristics and Stimuli-Response of LAPHS Micelles

Lauramidopropyl hydroxysultaine (LAPHS) was used as the sulfobetaine surfactant. LAPHS having the structure shown in Figure 1c is dissolved in 0.043 M NaCl aqueous solution, and the studies were conducted with diluted or adjusted salt concentration.

The critical micelle concentration (CMC) of LAPHS in 0.043 M NaCl aqueous solution was determined by surface tension and fluorescence measurements. As shown in Figure 6-2a, the inflection points according to surface tension coincided with the concentration showing micelle formation in pyrene fluorescence measurement; and, this concentration was designated as CMC (0.251 mg/mL). Furthermore, in order to investigate the change in CMC with the salt concentration, the same observation was made by changing the concentration of the aqueous solution from 0.023 M to 1.0 M NaCl (Figure 6-A2). As shown in Figure 6-2b, CMC changed from 0.549 to 0.191 mg/mL. Here, the presence of salts is impurities and they led to the minimum values of surface tension.[51] CMC decreased with the increase in salt concentration. Like an ionic surfactant, the decrease in the electrostatic repulsion between the

head group by the addition of salt is considered to have lowered CMC.[52] The changes in the CMC of LAPHS, anionic surfactants, and cationic surfactants due to changes in salt concentration were compared by the Corrin-Harkins equation.[53] As shown in Figure 6-A3, the effect of LAPHS on CMC by salts was insignificant as compared with anionic or cationic surfactants. The overall charge of betaine is neutral, unlike common ionic surfactant having only anions or cations, so electrostatic repulsion between the head group is weak, and the influence of salt on CMC was low.
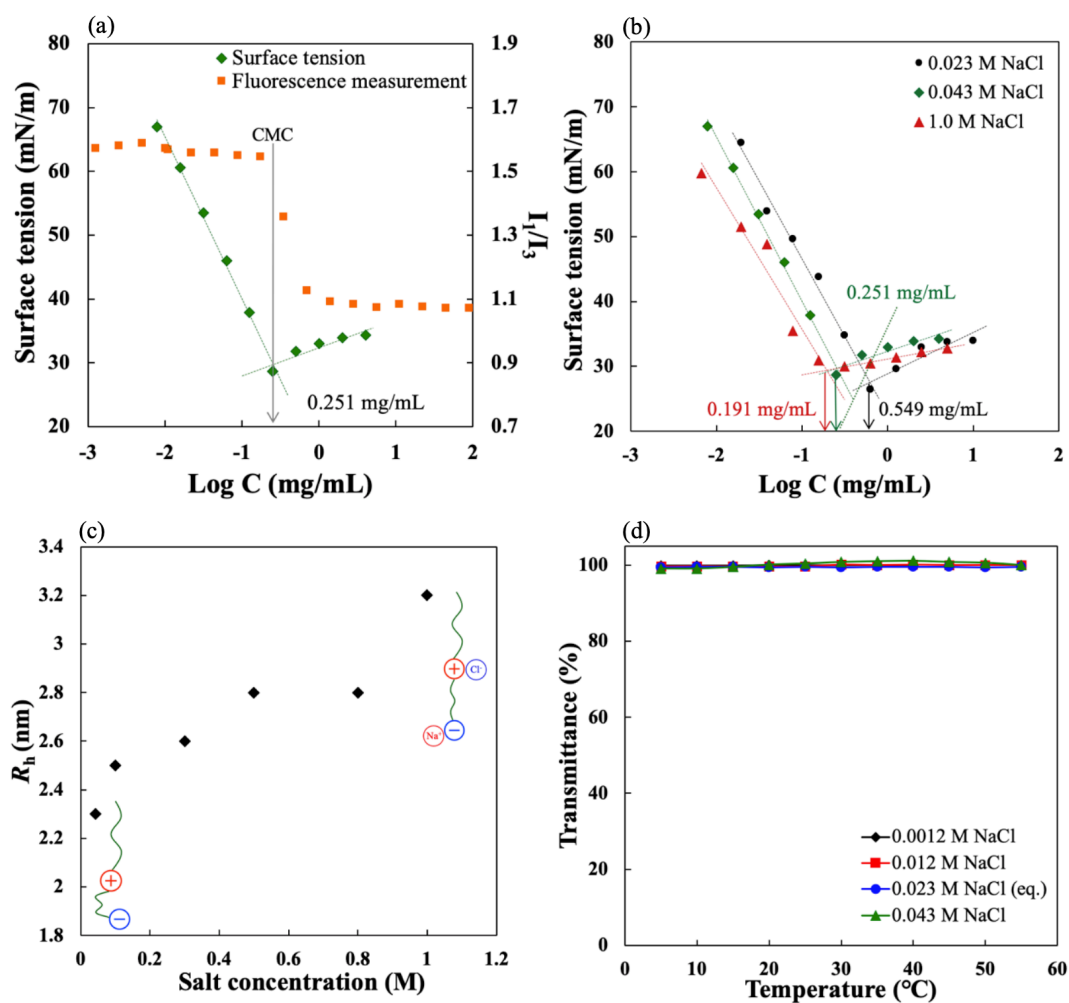
Figure 6-2. Estimate of CMC at LAPHS in 0.043 M NaCl (aq) by (a) surface tension and fluorescence measurements, and change in (b) CMC, (c) R_h, and (d) temperature responsivity depending on the concentration of added salt.

The change in the hydrodynamic radius (R_h) of the LAPHS micelles changed with salt concentration was observed. Each sample was prepared at 10 mg/mL, which is above the CMC where LAPHS micelles were formed, and it was measured at room temperature with salt concentration ranging from 0.1 M to 1.0 M. Figure 6-2c shows the R_h of LAPHS micelles increased with increasing salt concentration. It is because the hydrophilic part of LAPHS was contracted due to the interaction between the ions, but the intra- and intermolecular ion pairs were relaxed by the added salt, and the betaine chain was extended. Detailed information is shown in Figure 6-A4.

The temperature responsivity of 10 mg/mL LAPHS saline solutions with different salt concentrations (0.0012 M~0.043 M) was investigated by UV-vis spectrometry. As shown in Figure 6-2d, none of them showed a temperature response. Even, no temperature response was observed at 0.023 M NaCl, which is an equivalent to LAPHS, or at about 1/20 of the equivalent.

The effect of varying the concentration (0.043 M~0.5 M) of added salt on the aggregation number (N_{agg}) of LAPHS micelles was investigated by the fluorescence quenching method. The aggregation number in the 2 mg/mL LAPHS saline solution was almost the same 78 to 80, and the effect of the added salt concentration was not observed. Detailed information is shown in Figure 6-A5.

Furthermore, it was confirmed by electrophoretic light scattering (ELS) that the zeta potential was negatively charged (-19.97 mV) at 10 mg/mL LAPHS containing 0.043 M NaCl. It is considered that the quaternary ammonium cations of the sulfobetaine chain and the chlorine anions were bounded inside of the micelles, so they were negatively charged. Detailed information is shown in Figure 6-A6.
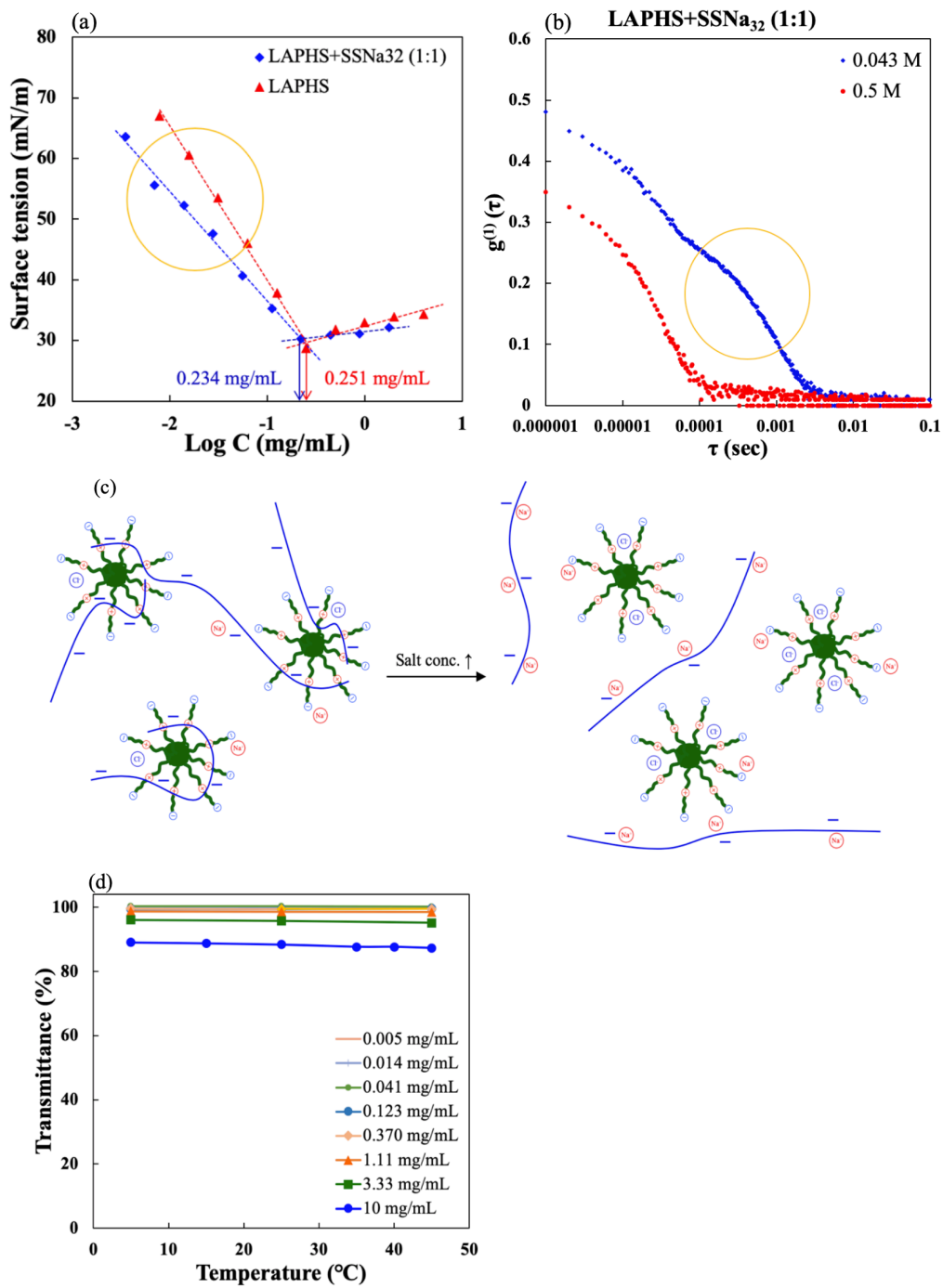
Figure 6-3. Comparison of surface tension slopes of (a) LAPHS alone and LAPHS+SSNa$_{32}$ (1:1), (b) results of DLS, (c) mechanism of aggregate formation behavior, and (d) temperature responsivity by added salt concentration.

6.3.3 Effects of Charge Ratio and Added Salt Concentration on the Complex of LAPHS Micelles and Anionic Polymer

The PSSNa as anionic polymer was mixed with LAPHS at a different charge ratio, and the change of CMC was investigated by surface tension and static light scattering (SLS) measurement. The salt concentrations of the samples were 0.043 M and 0.5 M, and the PSSNa used had a DP of 32. $SSNa_{32}$ was added to LAPHS in 0.043 M NaCl aqueous solution at a charge ratio of 1:0.5 and 1:1, and the CMC was 0.316 and 0.234 mg/mL, respectively, which was not significantly different from that the CMC (0.251 mg/mL) of LAPHS alone (Figure 6-A7a and Figure 6-3a). It was regarded as the effect of the addition of anionic polymer on micelle formation is insignificant. However, as shown in Figure 6-3a, the addition of $SSNa_{32}$ reduced the gradient of the surface tension in the concentration range below CMC, and reduced the surface excess amount. This suggested that LAPHS and PSSNa could interact. Even if the salt concentration of the samples was adjusted to 0.5 M, the change in CMC was slight. However, the slope of the surface tension in the concentration range below CMC, was larger than that when the salt concentration was 0.043 M, and was similar to that of LAPHS alone. It is considered that the interaction between LAPHS and PSSNa in aqueous solution was weakened at a high salt concentration. Furthermore, the change in CMC was slight even when SSNa, which is a monomer, was used instead of PSSNa. Detailed information is shown in Figure 6-A7.

The change in hydrodynamic radius (R_h) was investigated at a charge ratio of $SSNa_{32}$ to LAPHS of 1:0.5, 1:1, and 1:2 in 0.043 M NaCl aqueous solution, and the distributions of multiple sizes was confirmed (Figure 6-3b). In R_h (fast), the size was about the same as that of LAPHS alone, regardless of the proportion of PSSNa. The R_h (fast) for all conditions was 2.4 nm. The standard deviation (SD) was 0, 0.18, and 0 nm, respectively. Since sulfobetaine, which is the shell of LAPHS micelles, has a positive charge in the middle of the molecular chain, it is

considered that PSSNa penetrates into the micelle and strongly interacts with it.[15] By contrast, in R_h (slow), the presence of large aggregates of 54, 80, and 82 nm was observed depending on the ratio of SSNa$_{32}$ added (Figure 6-A8). Large aggregates were probably formed by bridging according to electrostatic interaction between positive charges of LAPHS micelles and negative charges of PSSNa. An increase in size was seen from a charge ratio of 1:0.5 to 1:1 and bridging was more advanced with the increasing amount of polymer. However, the size did not change at 1:2. Because the aggregate formed by bridging at a charge ratio of 1:1 became electrostatically stable, even if there was a larger amount of polymer, it did not lead to the growth of the aggregate, and the polymer existed as a simple substance. Larger aggregates formed by LAPHS micelles and PSSNa, which were confirmed at a low salt concentration (0.043 M), were not observed at a high salt concentration (0.5 M) (Figure 6-3b). Here, the significant decrease in the value of the autocorrelation function is due to the electrostatic interaction was screened by the concentration of added salt increased.[54] As described in Figure 6-3c, it is considered that electrostatic shielding when the salt concentration was high weakened the electrostatic interaction between LAPHS micelles and PSSNa, which made it difficult to form aggregates. Furthermore, the same way observation was performed using SSNa which is a monomer, and a large aggregate couldn't be confirmed. Detailed information is shown in Figure 6-A8. These results showed that only an aggregate of polymer and LAPHS micelles at a low salt concentration can form large aggregates.

The temperature responsiveness was investigated at various concentrations (0.005~10 mg/mL) where the charge ratio of LAPHS and SSNa$_{32}$ was 1:1, but none of the samples showed temperature responsivity. The salt concentration was fixed at 0.043 M. Previously the author found that the addition of PSSNa is very sensitive to the temperature response of sulfobetaine, and that the addition of even a small amount of PSSNa causes the temperature response to disappear.[15] The disappearance of temperature responsivity is due to the interaction between

PSS and the quaternary ammonium cation of sulfobetaine, which is the shell of LAPHS micelles. Moreover, the transmittance was 88 % at 10 mg/mL, compared to almost 100 % in other cases (Figure 6-3d), probably due to the presence of a large aggregate of LAPHS micelles and PSSNa that was confirmed by DLS.

The zeta potential of the complex consisting of LAPHS micelles and SSNa$_{32}$ became more negative than that of LAPHS micelles (changed from -19.97 to -39.02 mV). The positive charge of LAPHS may be shielded by the intrusion of PSSNa into the positive part of LAPHS, and the zeta potential changed significantly to a negative value. Detailed information is shown in Figure 6-A9.
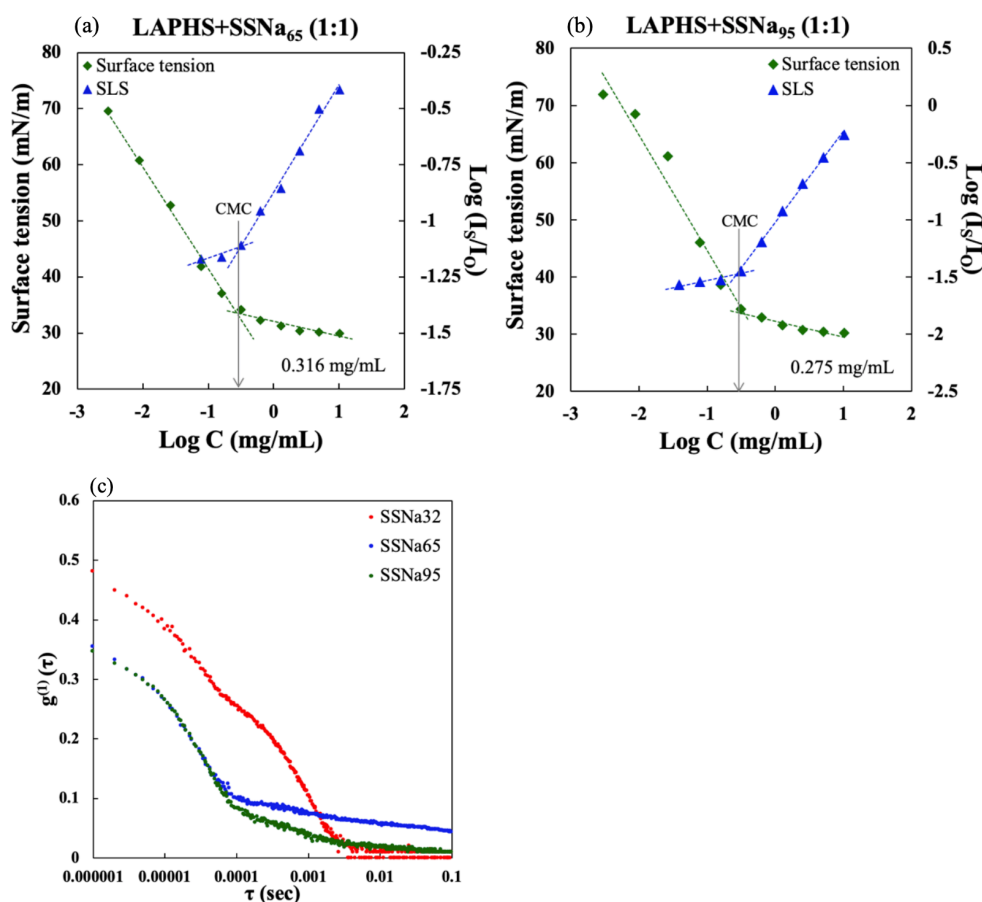
Figure 6-4. Change of CMC by the DP of PSSNa added to LAPHS and the confirmation of large aggregate: CMC at (a) SSNa$_{65}$, (b) SSNa$_{95}$, and (c) results of DLS.

6.3.4 Effect of DP on the Complex of LAHPS Micelles and Anionic Polymer

SSNa$_{65}$ and SSNa$_{95}$, which had different of degrees of polymerization (DP), were added to LAPHS in 0.043 M NaCl saline solution at the charge ratio of 1:1, and the change of CMC according to the DP was observed by surface tension and SLS. CMC for SSNa$_{65}$ and SSNa$_{95}$ was 0.316 and 0.275 mg/mL, respectively (Figure 6-4a, b). CMC was 0.234 mg/mL for SSNa$_{32}$, and a negligible change in CMC was observed depending on the DP of PSSNa.

The hydrodynamic radius of SSNa$_{65}$ and SSNa$_{95}$ showed multiple sizes was as the case for the mixture of LAPHS and SSNa$_{32}$ (Figure 6-4c). The results are summarized in Table 6-2. Here, the significant decrease in the value of the autocorrelation function is due to the electrostatic interaction was screened by the increasing the length of PSSNa.[54] In R_h (fast), the particle size (R_h=2.4~2.8 nm) did not change with the change of DP. On the other hand, in R_h (slow), the particle size (R_h= 80~107 nm) increased with the increase in DP of PSSNa. A larger aggregate was formed with a higher DP because the bridging length also became longer.

Table 2. Change of R_h Depending on the DP of PSSNa Added to LAPHS in 0.043 M NaCl (aq) (at a 1:1 Charge Ratio, the Concentration of the Samples was 10 mg/mL)

Sample	R_h (fast, nm)	R_h (slow, nm)
LAPHS+SSNa$_{32}$	2.4	80
LAPHS+SSNa$_{65}$	2.5	92
LAPHS+SSNa$_{95}$	2.8	107

Furthermore, the effects of the DP of the anionic polymer and the concentration of the aqueous solution on the temperature response were investigated. Studies were conducted in the concentration range of 0.006 to 10 mg/mL. As a result, similar to SSNa$_{32}$, none of the samples showed temperature responsivity, which indicated that DP and concentration had no effect (Figure 6-A10). However, the low transmittance for both DP (SSNa$_{65}$ and SSNa$_{95}$) at 10 mg/mL indicated the presence of large aggregates.

6.3.5 Effects of Charge Ratio and Added Salt Concentration on the Complex of LAPHS Micelles and Cationic Polymer

PMAPTAC as cationic polymer was mixed with LAPHS at charge ratios of 1:0.5, 1:1, and 1:2 and the change of CMC was investigated by surface tension, SLS, and fluorescence measurement. The salt concentrations were 0.043 M and 0.5 M, and the PMAPTAC used had a DP of 65. MAPTAC$_{65}$ was added to LAPHS in 0.043 M NaCl aqueous solution at a charge ratio of 1:0.5, 1:1, and 1:2; and, the CMC was 0.357, 0.313, and 0.355 mg/mL, respectively, which were not significantly different from that the CMC (0.251 mg/mL) of LAPHS alone. The addition of cationic polymer had no significant effect on micelle formation. There was little change in CMC, even when the salt concentration of the samples was adjusted to 0.5 M or the monomer was used instead of polymer (Figure 6-A11).

The change in R_h of the samples prepared by adding MAPTAC$_{65}$ to LAPHS in 0.043 M NaCl (aq) at a charge ratio of 1:0.5, 1:1, and 1:2 was investigated, and R_h was 3.6, 4.5, and 4.5 nm, respectively (Figure 6-5a). The SD was 0.16, 0.07, and 0.15 nm, respectively. Compared to the LAPHS micelles, the size doubled by the addition of MAPTAC$_{65}$. As shown in Figure 6-5b, the negative charges on the outside of the LAPHS micelles interacted with the positive charges of PMAPTAC and were adsorbed on the outside of the LAPHS micelles to form a complex. On the other hand, when the salt concentration was increased by 0.5 M, the

size of the aggregate consisting of LAPHS and PMAPTAC was similar to that of LAPHS micelles alone. This is because the electrostatic shielding when the concentration was high weakens the electrostatic interaction between LAPHS micelles and PMAPTAC. Furthermore, when MAPTAC which is a monomer was used, large aggregates were not observed. Detailed information is shown in Figure 6-A12. These results revealed that, as in the case of LAPHS micelles + PSSNa, only a mixture of polymer and LAPHS micelles at a low salt concentration can form aggregates.
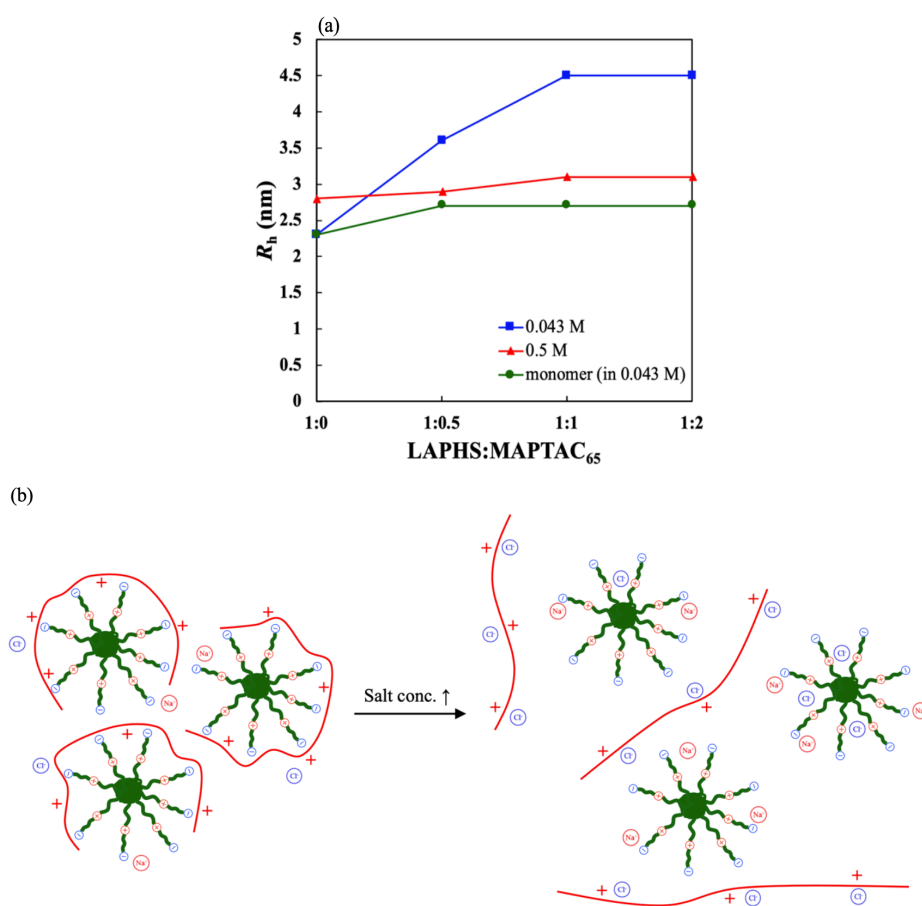
Figure 6-5. (a) Change of R_h and (b) mechanism of aggregate formation behavior depending on the concentration of added salt at LAPHS+MAPTAC$_{65}$ (1:1).

The zeta potentials of the LAPHS micelles alone and the aggregates prepared by adding MAPTAC$_{65}$ to the LAPHS micelles at a charge ratio of 1:0.5, 1:1, and 1:2 were compared. The zeta potentials of the aggregate consisting of LAPHS micelles and MAPTAC$_{65}$ were 4.20, 5.28, and 11.87 mV, respectively, in the order of charge ratio (Figure 6-A13). The zeta potential changed greatly to a positive value compared with the zeta potential (-19.97 mV) of the LAPHS micelles alone, the negative charge was considered to be shielded by the electrostatic interaction between the anion outside the LAPHS micelles and the cation of PMAPTAC, which was also suggested by the DLS. Moreover, the zeta potential changed to a positive value greatly in proportion to the amount of PMAPTAC added, which also indicated that PMAPTAC was adsorbed to the LAPHS micelles.

When MAPTAC$_{65}$ with a charge ratio of 1:1 was added to LAPHA micelles in 0.043 M NaCl (aq), the aggregation number (N_{agg}) was 81, which was not different from that of LAPHS alone (N_{agg}: 80) (Figure 6-A14). This result suggested that the addition of PMAPTAC had no effect such as the collapse of LAPHS micelles or the change in the N_{agg}.

The change in transmittance due to the change in concentration of the aggregate prepared using LAPHS micelles and MAPTAC$_{65}$ at a charge ratio of 1:1 was observed. The salt concentration was adjusted to 0.043 M in the concentration range of 0.014 to 20 mg/mL, and the results of transmittance at 25 °C were combined with the results of surface tension measurement (Figure 6-6a). Unlike the case of LAPHS micelles alone and the aggregate consisting of LAPHS micelles and PSSNa, an unprecedented phenomenon of "clear→ opaque→ clear" was observed with increasing concentration in the concentration range above CMC. This may be because LAPHS micelles and PMAPTAC form an aggregate, which allows the sulfobetaine moiety to form intra- or intermolecular pair. As the concentration of the aggregate increases, the content of cationic polymer increases, which makes the surface of the aggregate is the positive charge. It led to electrostatic repulsion between aggregates and

becomes a clear state. It is similar to the re-entrant behavior induced by salt concentration in the polyelectrolyte/electrolyte system.[55] The transition temperature increased as the concentration increased, and the transition temperature decreased at concentrations higher than CMC (Figure 6-6b). It was a typical UCST-type temperature responsive feature of the correlation between solution concentration and transition temperature.[56] This is considered to be the cause of the unprecedented phenomenon of "clear→ opaque→ clear" due to the change in concentration. In addition, as shown in Figure 6-6c, the hysteresis of the temperature response of the aggregate of LAPHS micelles and MAPTAC$_{65}$ was confirmed. Then, the concentration was 10 mg/mL. Furthermore, the same behavior was observed in the aggregates prepared with the charge ratios of 1:0.5 and 1:2, and the transition temperature decreased because the influence of PMAPTAC increased with the increase in the ratio of PMAPTAC (Figure 6-A15). The observation was performed using MAPTAC which is a monomer, the temperature responsivity couldn't be confirmed. These results indicated that only an aggregate of cationic polymer and LAPHS micelles showed the temperature responsiveness.

The effect of added salt concentration on the temperature responsiveness of the aggregate consisting of LAPHS micelles and MAPTAC$_{65}$ was investigated. Then, the concentration was 10 mg/mL. As a result, the transition temperature decreased with the increase in salt concentration, and the temperature responsiveness disappeared at 0.1 M. It is considered that the electrostatic shielding due to the addition of the salt weakened the electrostatic attraction between the LAPHS micelles and PMAPTAC, which made it difficult to form an aggregate (Figure 6-6d).
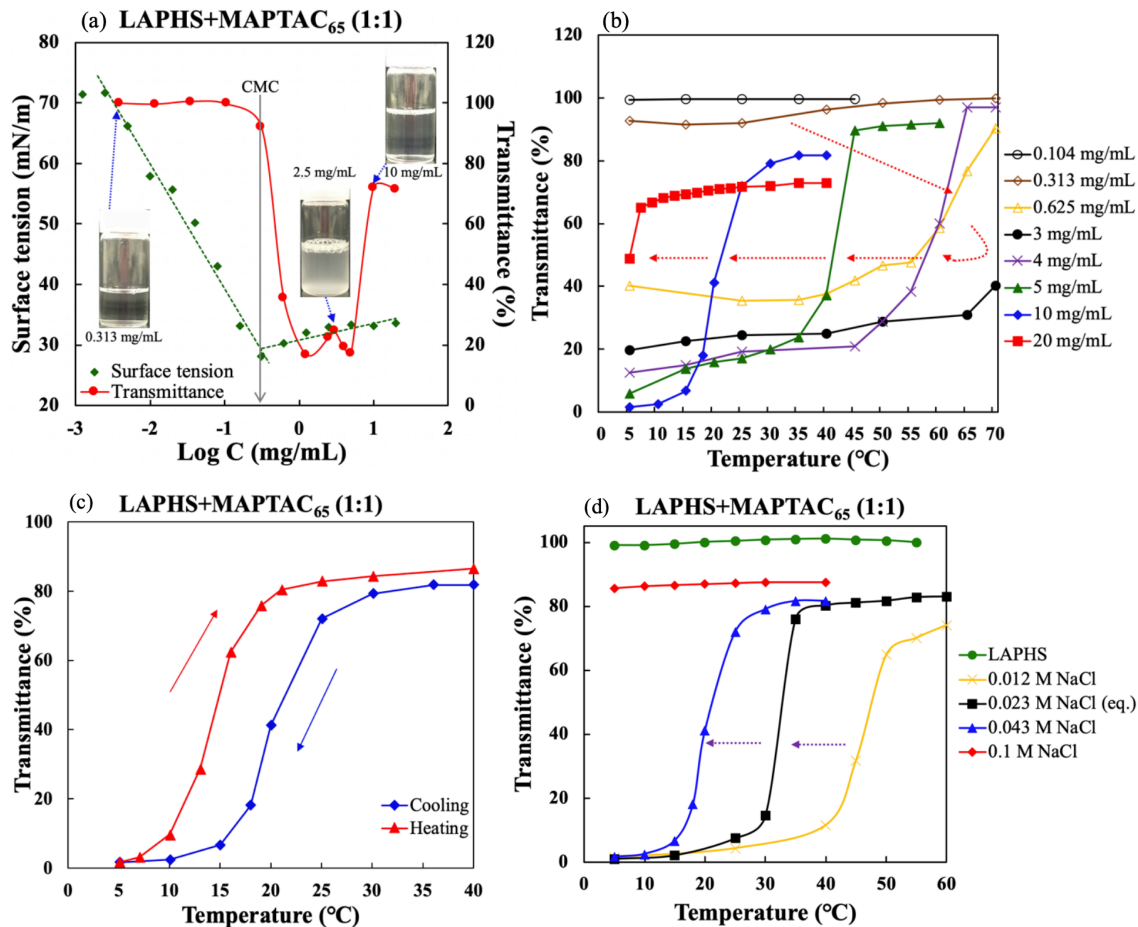
Figure 6-6. Change of (a) transmittance and (b) transition temperature depending on concentration of samples and (c) hysteresis of temperature responsivity of LAPHS + MAPTAC$_{65}$ (1:1) and (d) influence of added salt concentration.

6.3.6 Effect of DP on the Complex of LAHPS Micelles and Cationic Polymer

CMC of MAPTAC$_{85}$ added to LAPHS micelles in 0.043 M NaCl (aq) at charge ratios of 1:0.5 and 1:1, were 0.282 and 0.229 mg/mL, respectively, determined by surface tension, SLS, and fluorescence measurement. CMC changed slightly with the change in the charge ratio of the added MAPTAC$_{85}$. However, these values were lower than those obtained by addition of MAPTAC$_{65}$, 0.313 and 0.357 mg/mL, respectively. The charge of sulfobetaine part outside the LAPHS micelles became more shielded, and the micelles were considered to be formed more easily at a high DP (Figure 6-A16).

The R_h of the aggregate of the LAPHS micelles and MAPTAC$_{85}$ was 4.3 ± 0.11 and 4.6 ± 0.15 nm, respectively, depending on the charge ratio of the added MAPTAC$_{85}$. The values were 3.6 ± 0.16 and 4.5 ± 0.07 nm, respectively, when MAPTAC$_{65}$ was added at the same charge ratio. The aggregate became larger because PMAPTAC with a high DP was adsorbed on the LAPHS micelles (Figure 6-A16).
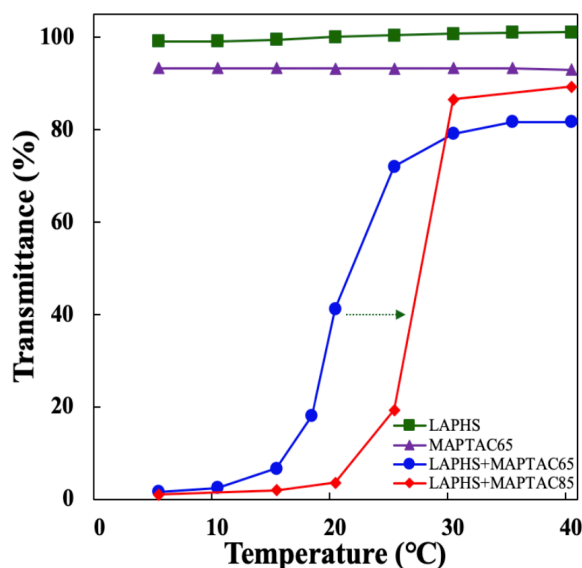
Figure 6-7. Effect of transition temperature on DP of the cationic polymer added to LAPHS.

Furthermore, the temperature responsivity of the aggregate consisting of LAPHS micelles and MAPTAC$_{85}$, showed the same tendency as that of MAPTAC$_{65}$ (Figure 6-A17). However, as shown in Figure 6-7, the transition temperature increased with the increase in the degree of polymerization (from 20 to 25 °C). The increase in the degree of polymerization of the cationic polymer is considered to shield the charge of the sulfobetaine chain on the outside of the LAPHS micelles and increase the overall hydrophobicity.[57]

6.4 Conclusions

When PSSNa was added to LAPHS at various charge ratios, formation of large aggregates in addition to LAPHS micelles was confirmed by DLS. This aggregate could not be confirmed when the high salt concentration or the monomer (SSNa). Then, addition of PSSNa to LAPHS changed the zeta potential significantly to a negative value (from -19.97 to -39.02 mV). These results showed that the quaternary ammonium cation of sulfobetaine, which is the shell of LAPHS micelles, interacted with the PSSNa acting as a bridge thus forming a large aggregate.

The sample with a concentration of 10 mg/mL prepared by adding PMAPTAC to LAPHS was opaque at room temperature, but it was transparent when the high salt concentration or the monomer (MAPTAC). Addition of PMAPTAC to LAPHS significantly changed the zeta potential to a positive value (from -19.97 to 5.28 mV), and the adsorption of PMAPTAC to LAPHS micelles was confirmed by DLS. The sulfur trioxide anion of sulfobetaine, which is the shell of LAPHS micelles, and the PMAPTAC interacted to form an aggregate. Unlike the case of LAPHS micelles alone and the aggregate consisting of LAPHS micelles and PSSNa, an unprecedented phenomenon of "clear→ opaque→ clear" was observed with increasing concentration in the concentration range above CMC. This was considered to be due to the change in transition temperature accompanying the change in concentration. As the concentration of the aggregate increases, the content of cationic polymer increases, which makes the surface of the aggregate is the positive charge. It led to electrostatic repulsion between aggregates and becomes a clear state. It is similar to the re-entrant behavior induced by salt concentration in the polyelectrolyte/electrolyte system. In this temperature responsivity, the transition temperature was lower when the concentration was higher than CMC or the salt concentration was increased, and the transition temperature increased with the addition of PMAPTAC with a high degree of polymerization.

These results revealed that 1) the LAPHS micelles and the ionic polymer form an aggregate, 2) the temperature responsiveness can be expressed by the interaction with the cationic polymer, and 3) the transition temperature can be controlled by adjusting the concentration of samples and degree of polymerization of PMAPTAC. The aggregates consisting of LAPHS micelles and PMAPTAC may be useful in the production of novel temperature materials.

6.5 Appendix

6.5.1 Confirmation and Estimation of Synthesis and Polydispersity Index (M_w/M_n) of PSSNa and PMAPTAC Homopolymers.

The synthesis could be confirmed by ^{1}H NMR spectra. The author conducted GPC measurements using two kinds of eluents. An anionic eluent (20 wt% CH_3CH aq, 0.05 M $NaNO_3$, 0.01 M Na_2HPO_4) was used for PSSNa homopolymers. PSSNa was used as the standard sample. The results are shown in Figure 6-A1a. A cationic eluent (0.5 M CH_3COOH, 0.3 Na_2SO_4) was used for PMAPTAC homopolymers. P2VP was used as the standard sample. The results are shown in Figure 6-A1b.
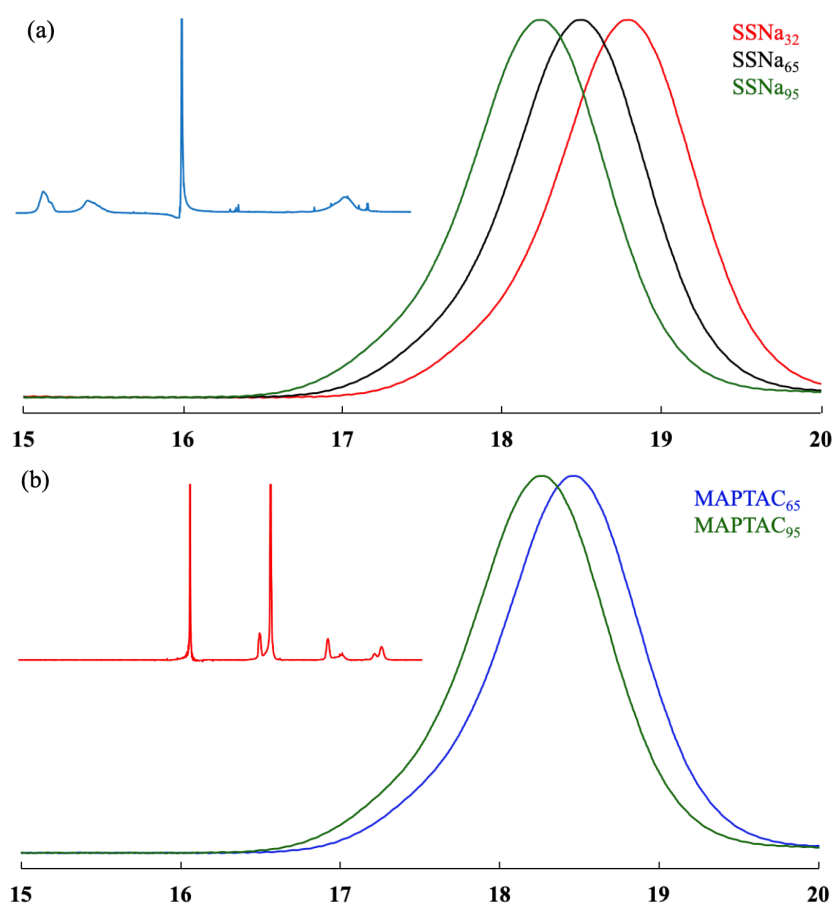
Figure 6-A1. 1H NMR spectra and GPC charts for (a) PSSNa and (b) PMAPTAC.

SSNa$_{32}$: M_n=6900 and M_w/M_n=1.10

SSNa$_{65}$: M_n=13700 and M_w/M_n=1.06

SSNa$_{95}$: M_n=19500 and M_w/M_n=1.11

MAPTAC$_{65}$: M_n=14400 and M_w/M_n=1.06

MAPTAC$_{95}$: M_n=19000 and M_w/M_n=1.11
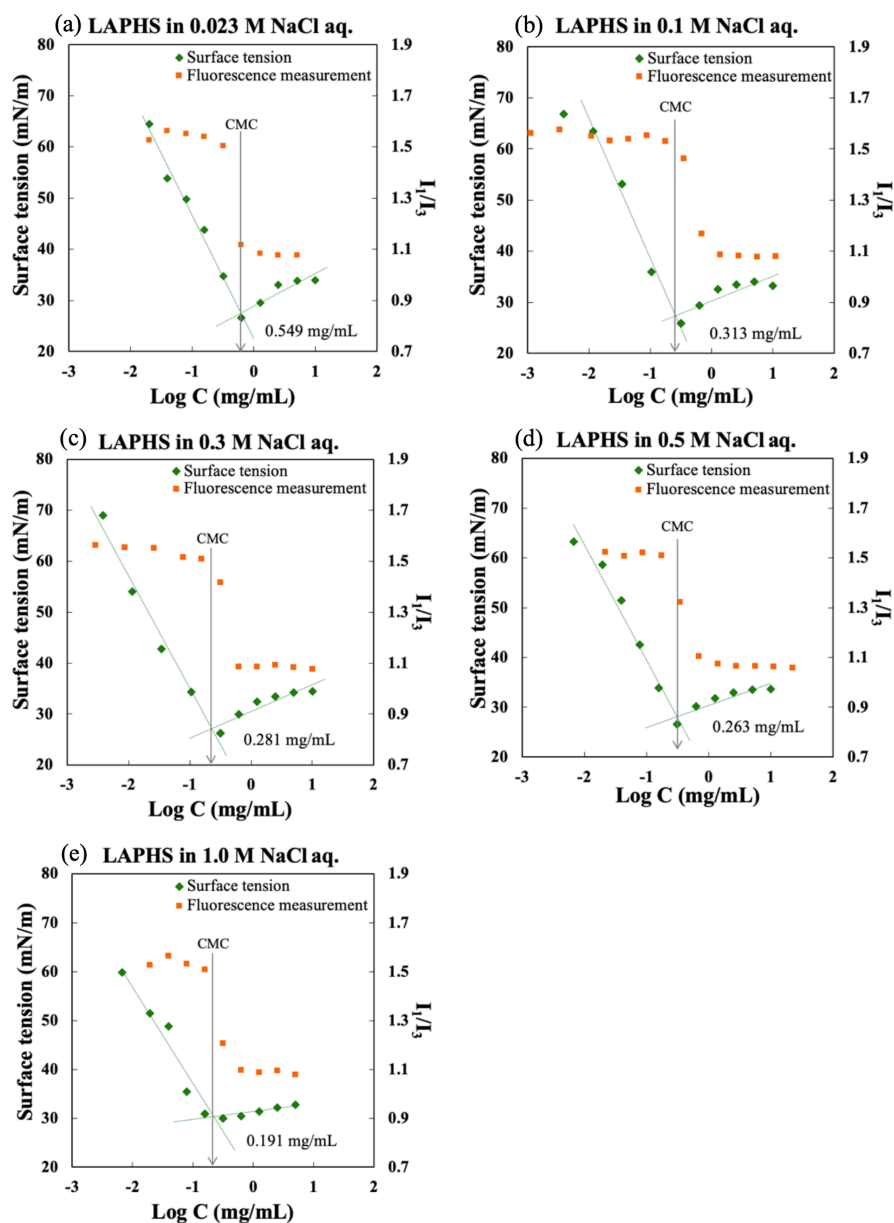
Figure 6-A2. The results of surface tension and fluorescence measurement of LAPHS in (a) 0.023, (b) 0.1, (c) 0.3, (d) 0.5, (e) 1 M NaCl.
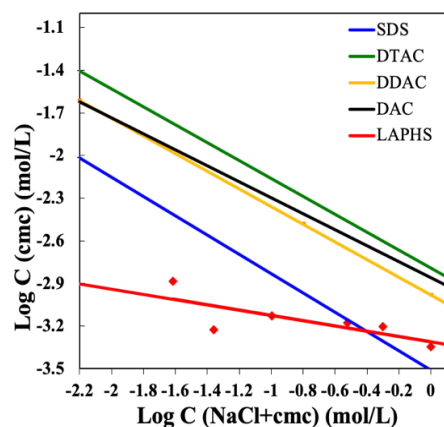
Figure 6-A3. Comparison of change in CMC with added salt concentration in LAPHS and ionic surfactant.
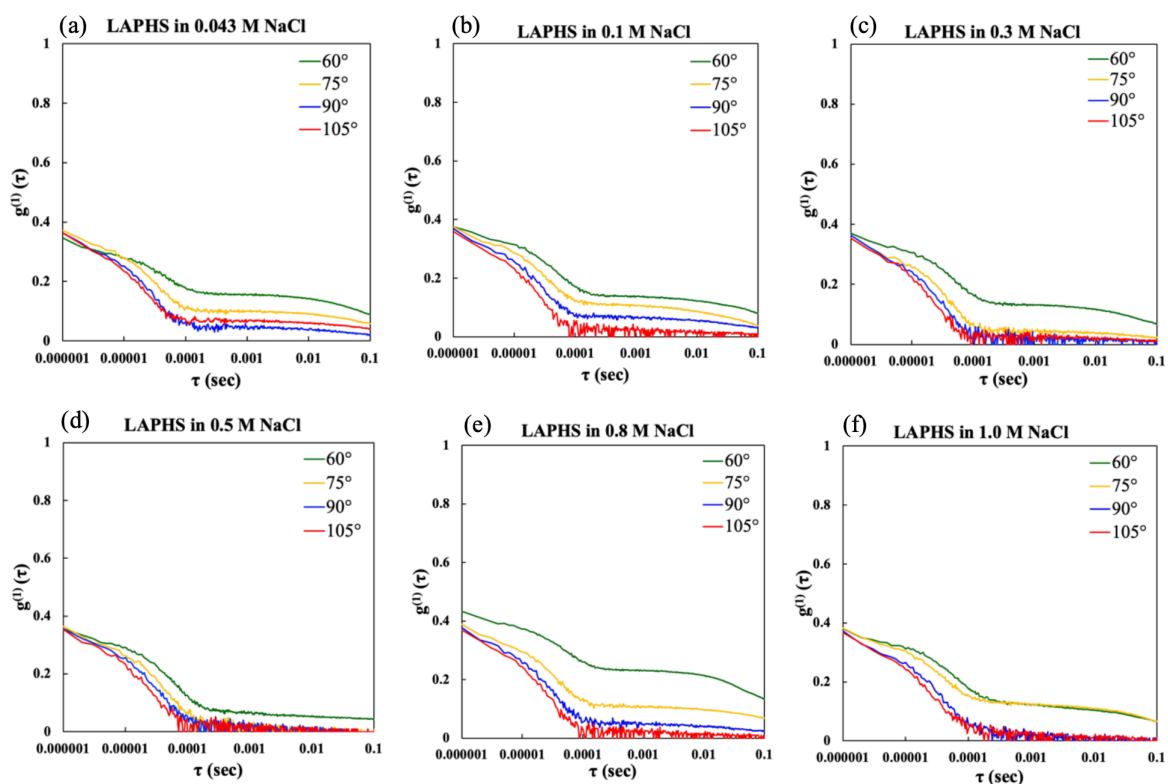
Figure 6-A4. Change in R_h of LAPHs with added salt concentration: (a) 0.043, (b) 0.1, (c) 0.3, (d) 0.5, (e) 0.8, (f) 1 M NaCl.
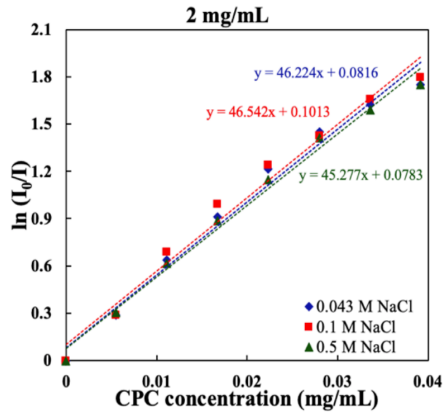
Figure 6-A5. Aggregation number of LAPHS depending on the concentration of added salt.
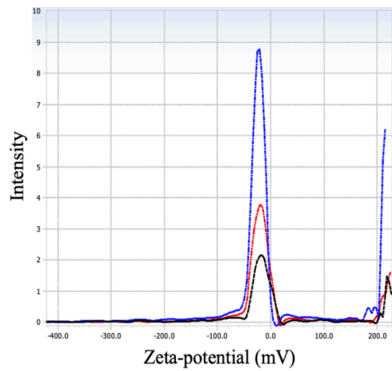
**Figure 6-A6.** Estimation of the zeta potential of LAPHS in 0.043 M NaCl by ELS.
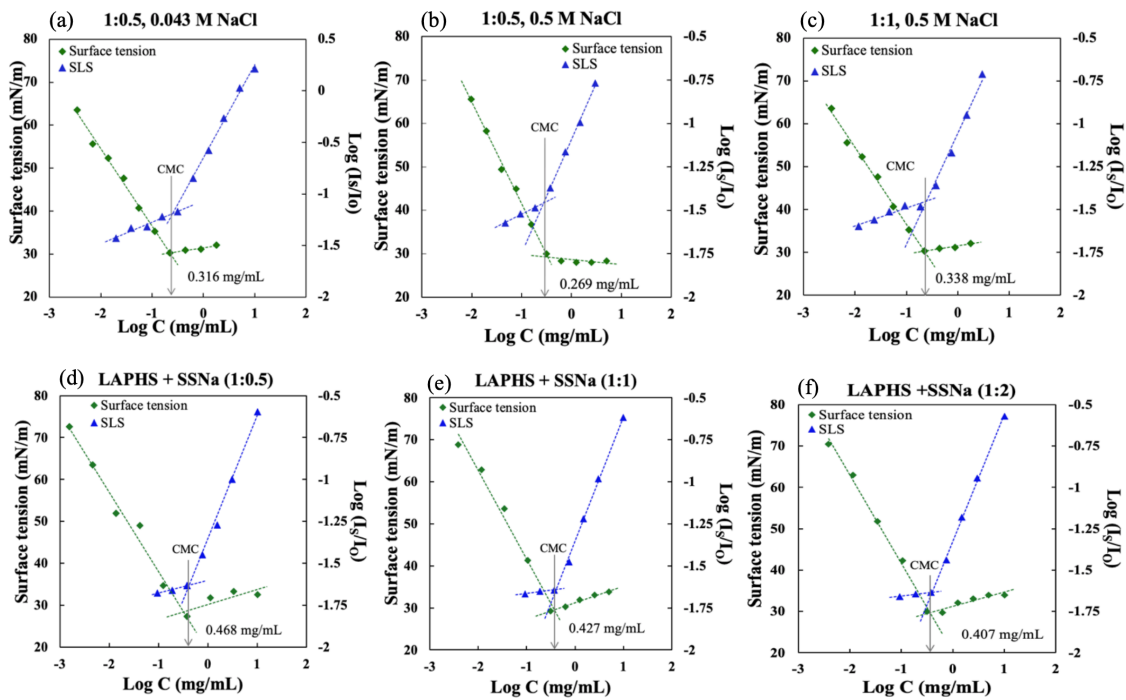
Figure 6-A7. Change of CMC with charge ratio, added salt concentration and monomer: (a) 1:0.5, 0.043 M, (b) 1:0.5, 0.5 M, (c) 1:1, 0.5 M of LAPHS+SSNa$_{32}$, and (d) 1:0.5, (e) 1:1, (f) 1:2 of LAPHS+SSNa in 0.043 M NaCl.
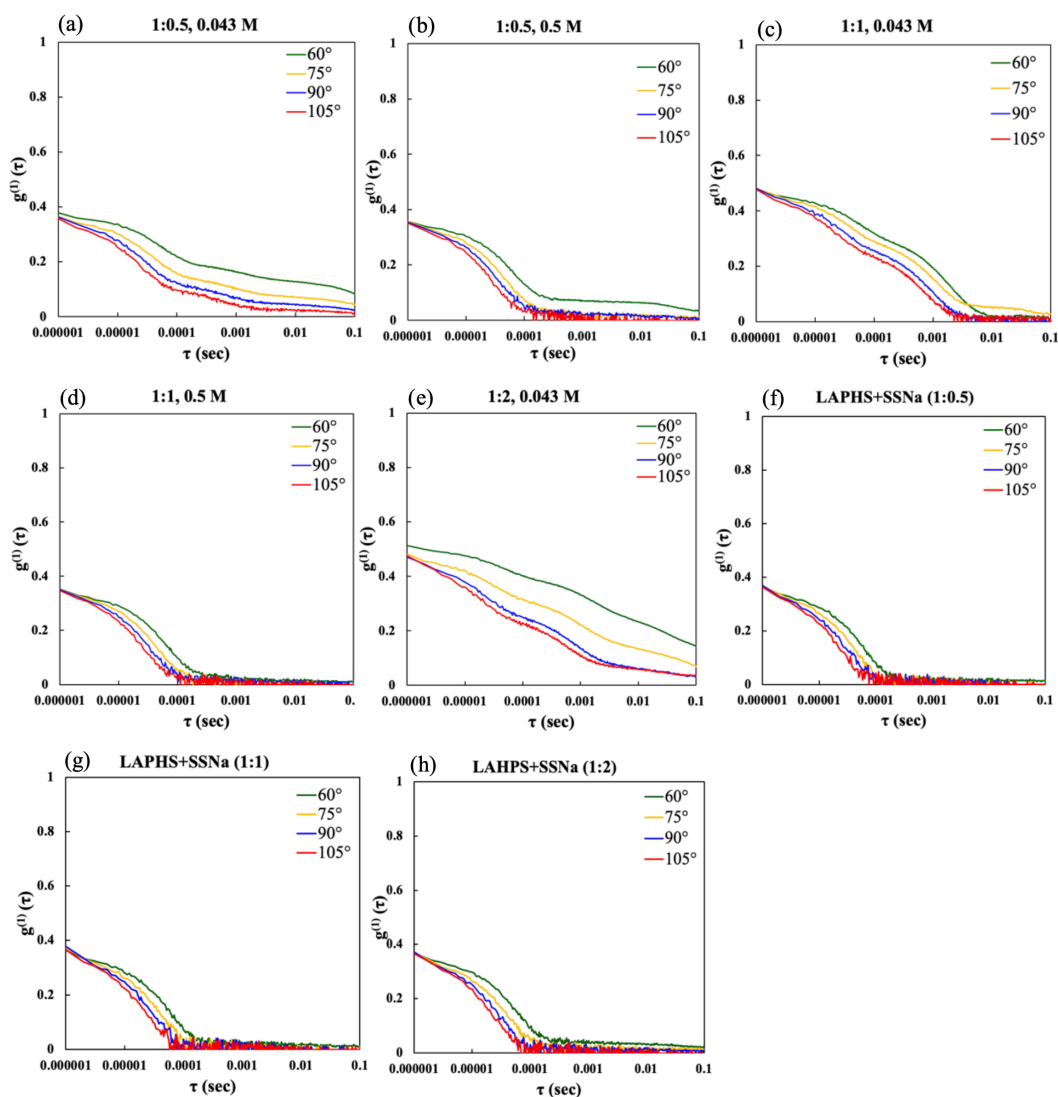

Figure 6-A8. Change in R_h due to charge ratio, added salt concentration and monomer: (a) 1:0.5, 0.043 M, (b) 1:0.5, 0.5 M, (c) 1:1, 0.043 M, (d) 1:1, 0.5 M, (e) 1:2, 0.043 in LAPHS+SSNa$_{32}$, and (f) 1:0.5, (g) 1:1, (h) 1:2 of LAPHS+SSNa in 0.043 M NaCl.

Run	Zeta-potential (mV)	Electrophoretic mobility (cm²/Vs)
1	-44.03	-3.433e-004
2	-38.99	-3.040e-004
3	-34.04	-2.654e-004
mean	-39.02	-3.043e-004
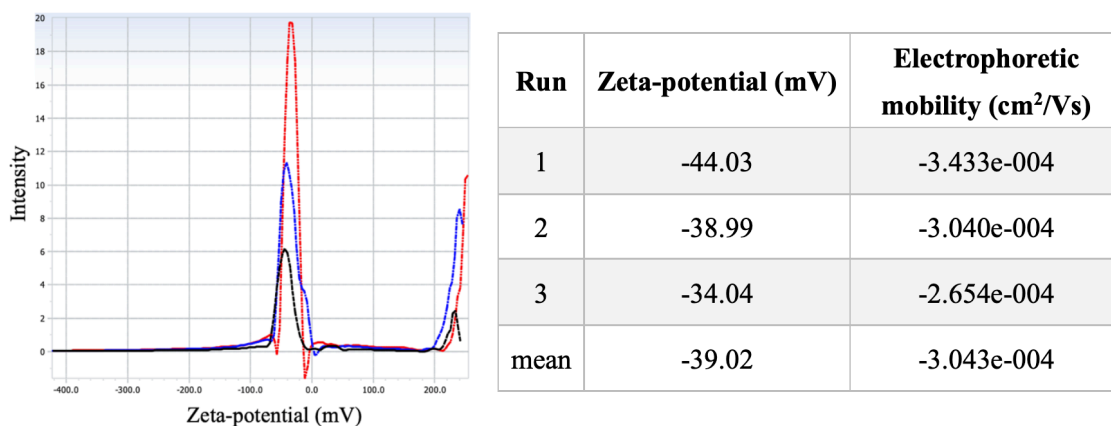
Figure 6-A9. Estimation of the zeta potential of LAPHS+SSNa$_{32}$ (1:1 of charge ratio) in 0.043 M NaCl by ELS.
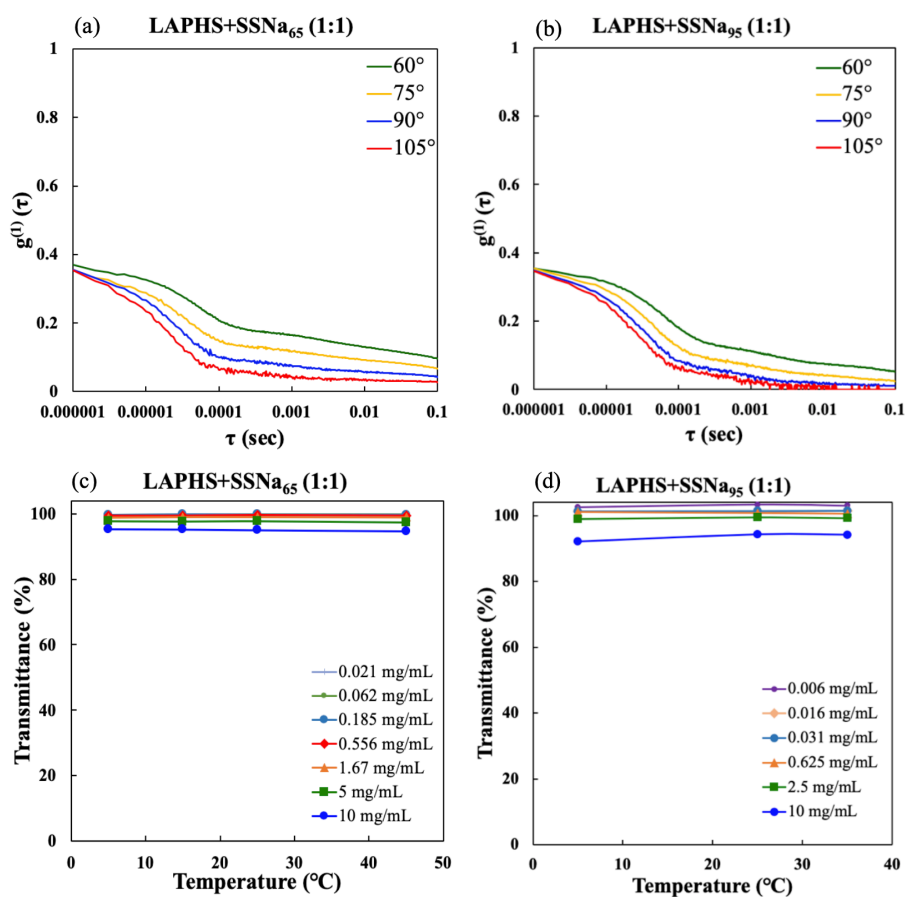
Figure 6-A10. Effect of DP of added anionic polymer: R_h of (a) SSNa$_{65}$, (b) SSNa$_{95}$, transmittance of (c) SSNa$_{65}$, (d) SSNa$_{95}$.
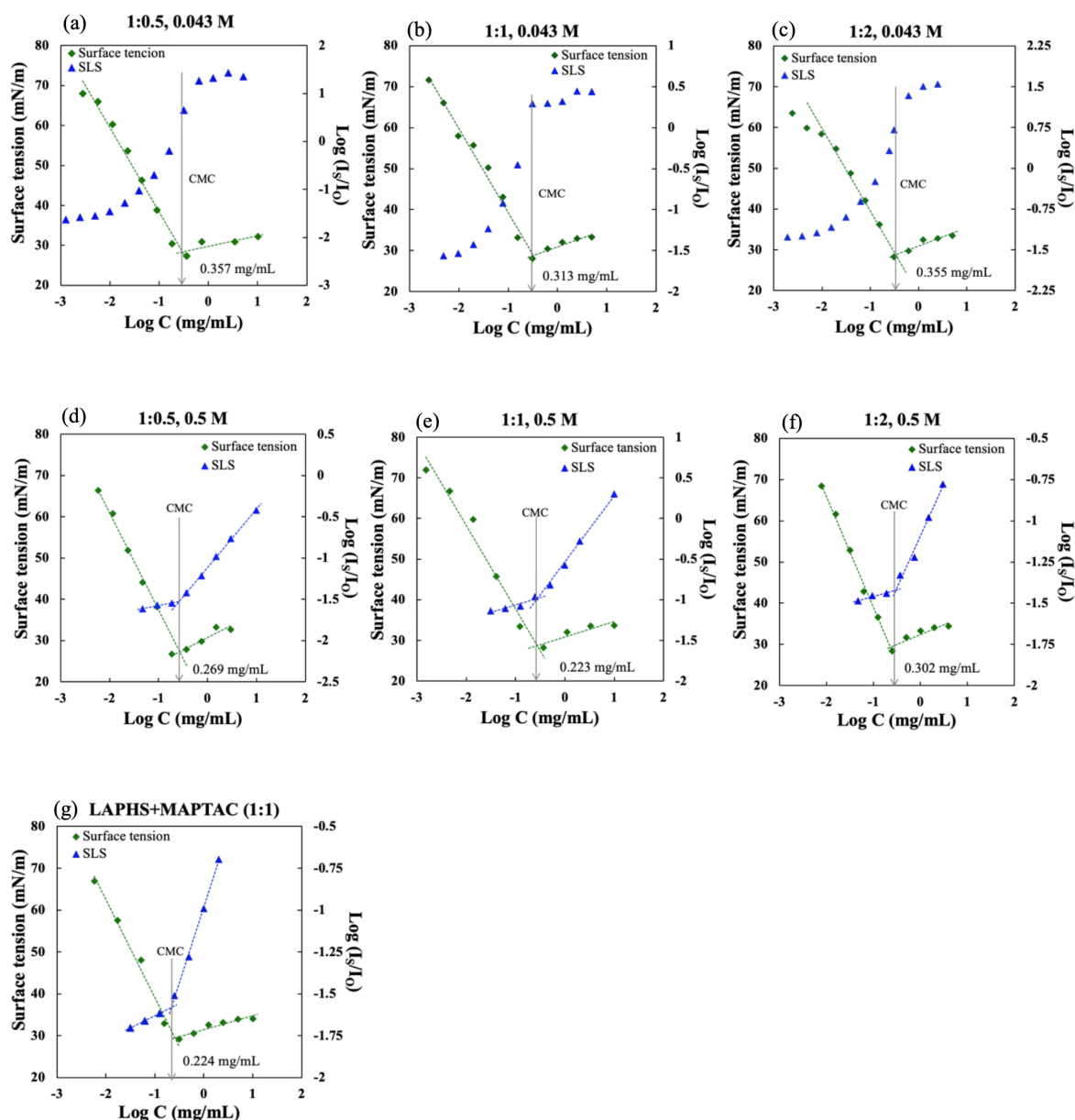
Figure 6-A11. Change of CMC with charge ratio, added salt concentration and monomer: (a) 1:0.5, (b) 1:1, (c) 1:2 in 0.043 M NaCl, (d) 1:0.5, (e) 1:1, (g) 1:2 in 0.5 M NaCl of LAPHS+MAPTAC$_{65}$, and (h) 1:1 of LAPHS+MAPTAC in 0.043 M NaCl.
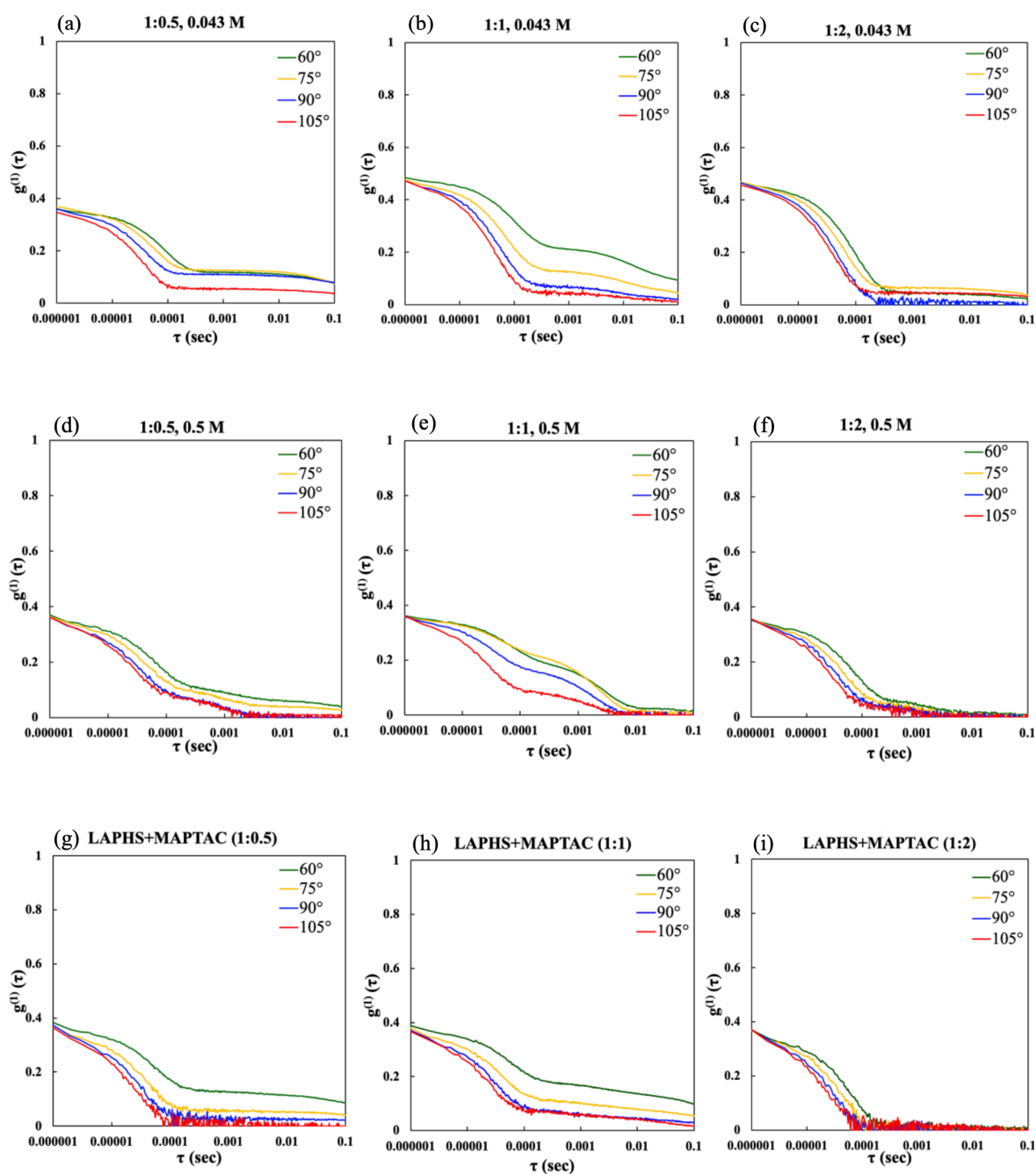
Figure 6-A12. Change in R_h due to charge ratio, added salt concentration and monomer: (a) 1:0.5, (b) 1:1, (c) 1:2 in 0.043 M NaCl and (d) 1:0.5, (e) 1:1, (f) 1:2 in 0.5 M NaCl in LAPHS+MAPTAC$_{65}$, and (f) 1:0.5, (g) 1:1, (h) 1:2 of LAPHS+MAPTAC in 0.043 M NaCl.

(a) LAPHS+MAPTAC$_{65}$ (1:0.5)
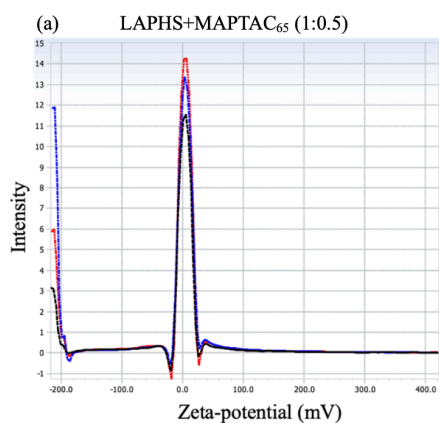
Run	Zeta-potential (mV)	Electrophoretic mobility (cm^2/Vs)
1	3.92	3.062e-005
2	4.34	3.381e-005
3	4.35	3.393e-005
mean	4.20	3.279e-005

(b) LAPHS+MAPTAC$_{65}$ (1:1)
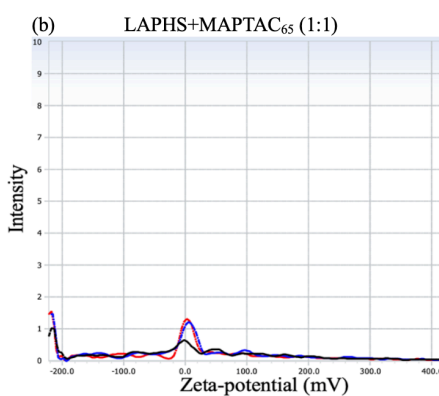
Run	Zeta-potential (mV)	Electrophoretic mobility (cm^2/Vs)
1	5.94	4.642e-005
2	5.67	4.421e-005
3	4.23	3.300e-005
mean	5.28	4.121e-005
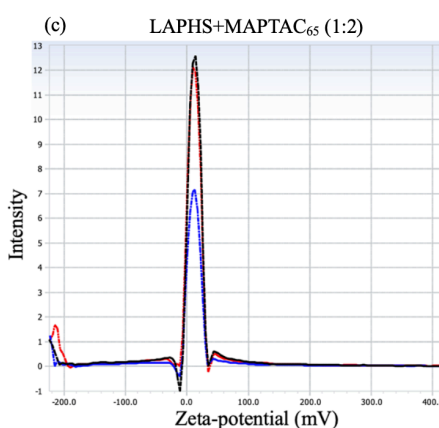
(c) LAPHS+MAPTAC$_{65}$ (1:2)

Run	Zeta-potential (mV)	Electrophoretic mobility (cm^2/Vs)
1	12.57	9.770e-005
2	11.49	8.980e-005
3	11.55	9.006e-005
mean	11.87	9.252e-005

Figure 6-A13. Estimation of the zeta potential of LAPHS+MAPTAC$_{65}$ in 0.043 M NaCl by ELS: charge ratio of (a) 1:0.5, (b) 1:1, and (c) 1:2.
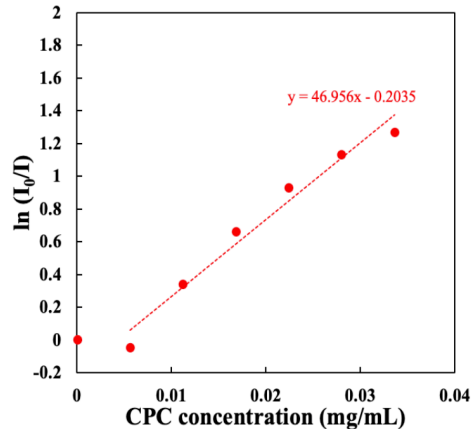
Figure 6-A14. Calculation of the aggregation number of LAPHS+MAPTAC$_{65}$ (1:1) in 0.043 M NaCl.
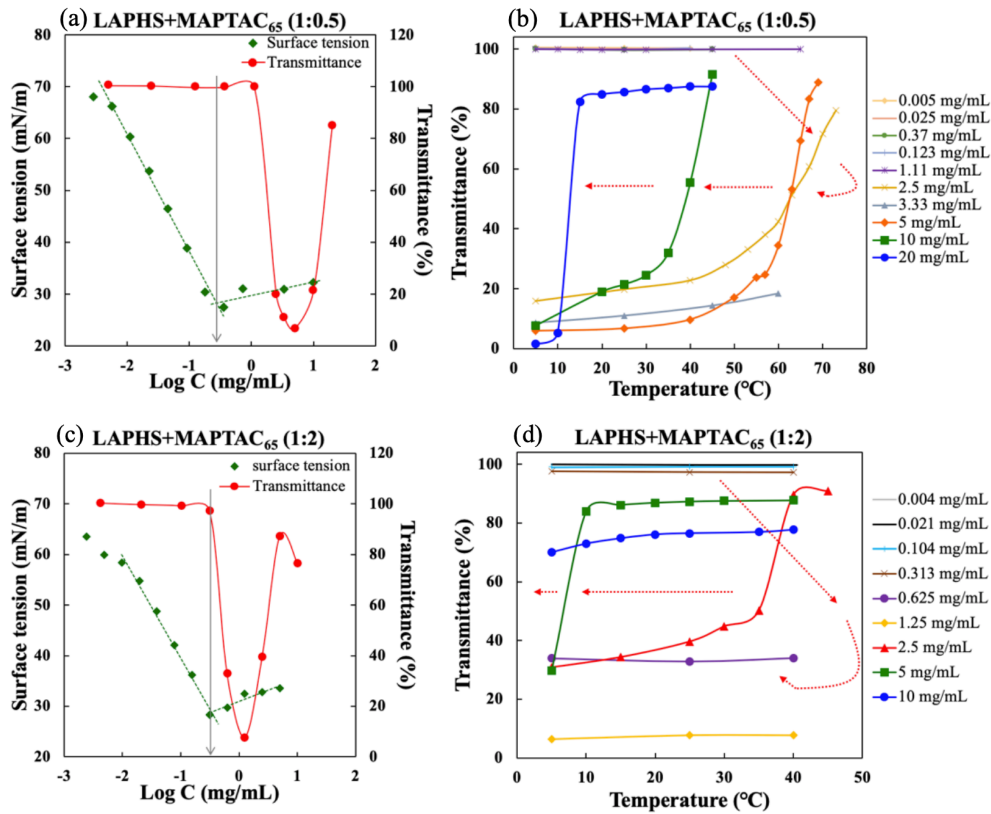
Figure 6-A15. Effect of charge ratio and concentration on temperature responsivity and of LAPHS+MAPTAC$_{65}$: change in transmittance (a) 1:0.5 and (c) 1:2 of charge ratio at room temperature in the concentration range above CMC, and change in transition temperature due to (b) 1:0.5 and (d) 1:2 of charge ratio.
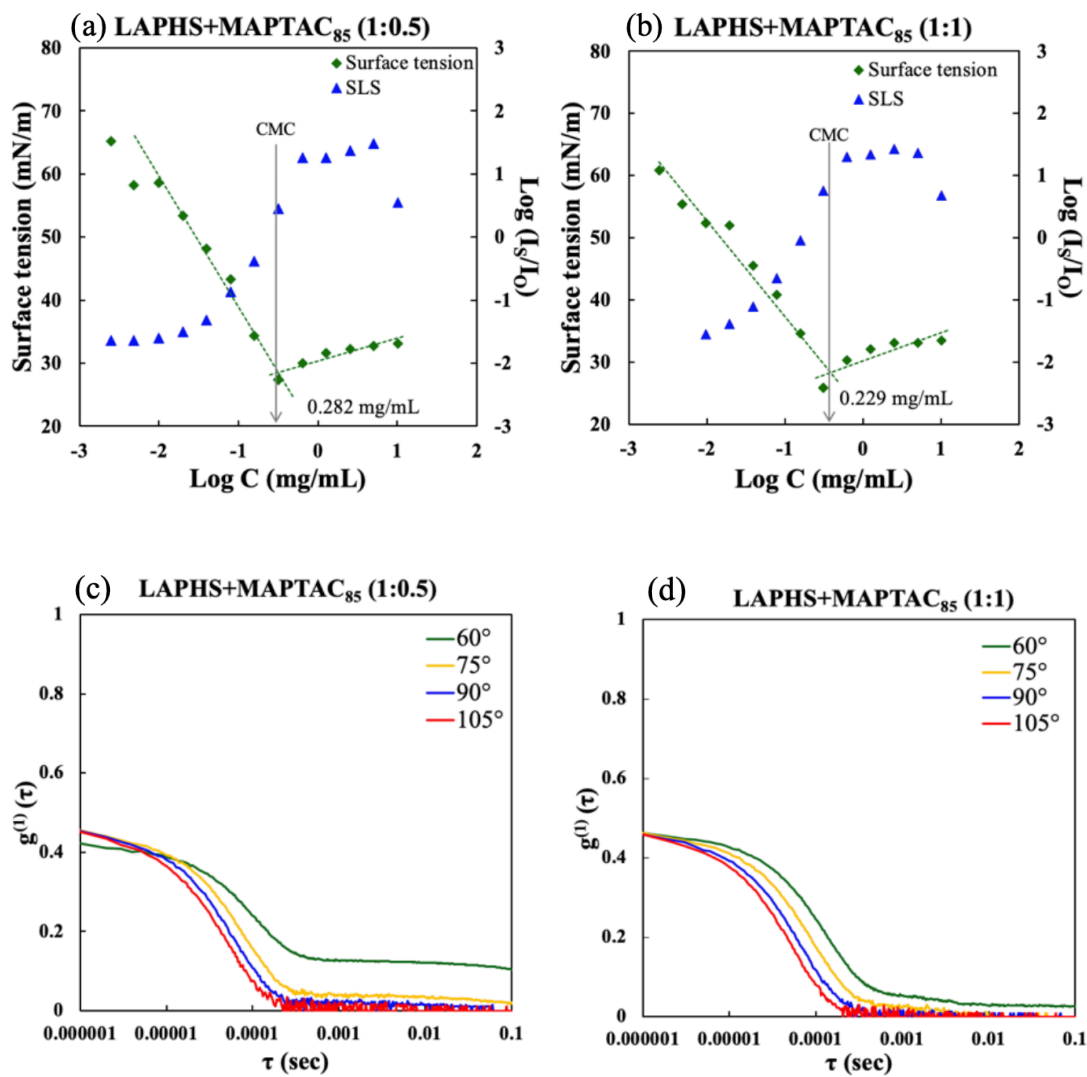
Figure 6-A16. Change of CMC and R_h due to charge ratio in LAPHS+MAPTAC$_{85}$: Change of CMC at (a) 1:0.5 and (b) 1:1, and change of R_h at (c) 1:0.5 and (d) 1:1.
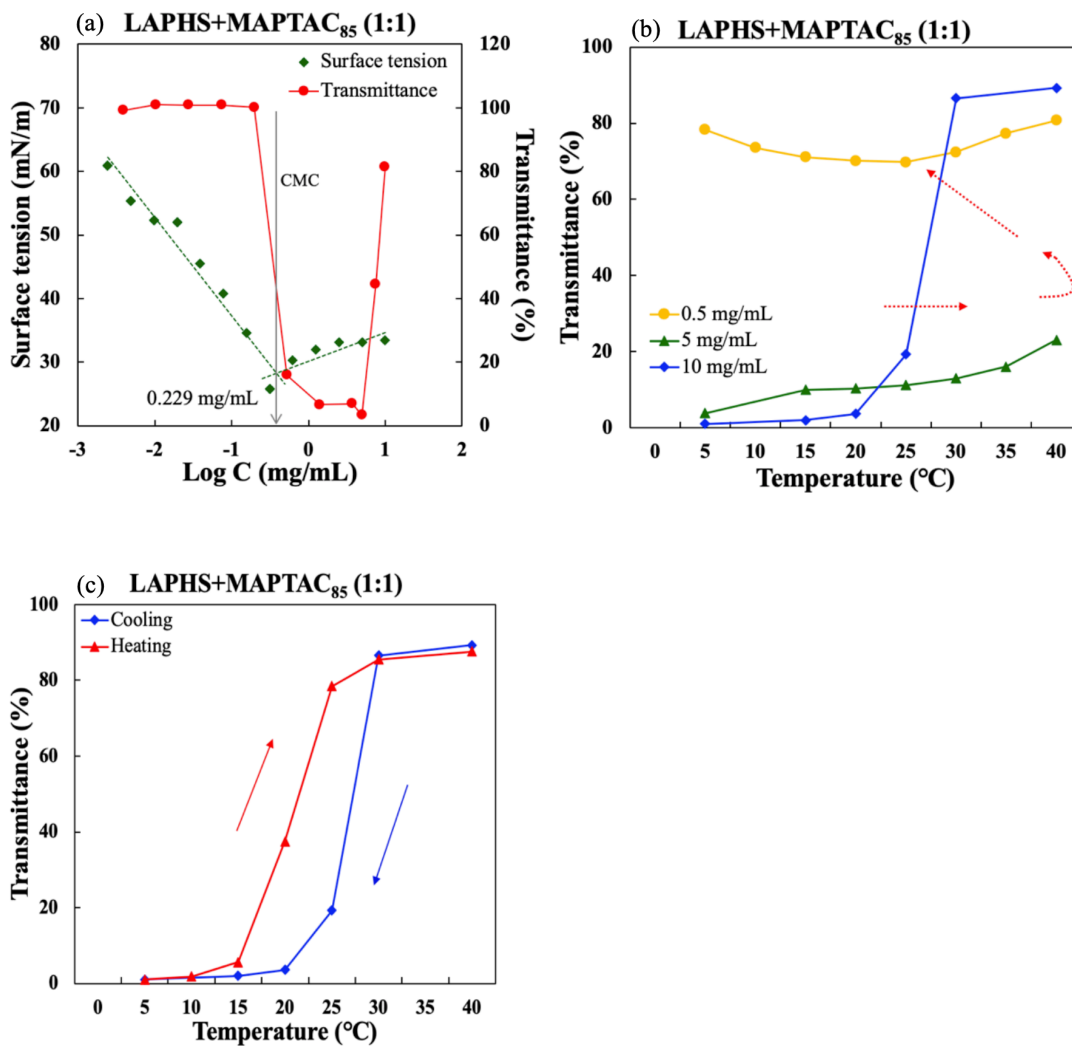
Figure 6-A17. Effect of concentration on temperature responsivity of LAPHS+MAPTAC$_{85}$ in 0.043 M NaCl: (a) change of transmittance of in the concentration range above CMC at room temperature, (b) change of transition temperature, (c) hysteresis of temperature responsivity.

6.6 Reference

[1] H. Ladenheim, H. Morawetz, *J. Polym. Sci.* **1957**, 26, 251-254.

[2] A. Laschewsky, *Polymers* **2014**, 6, 1544-1601.

[3] A. B. Lowe, C. L. McCormick, *Chem. Rev.* **2002**, 102, 4177-4189.

[4] J. Ladd, Z. Zhang, S. Chen, J. C. Hower, S. Jiang, *Biomacromolecules* **2008**, 9, 1357-1361.

[5] S. Chen, J. Zheng, L. Li, S. Jiang, *J. Am. Chem. Soc.* **2005**, 127, 14473-14478.

[6] P. S. Liu, Q. Chen, S. S. Wu, J. Shen, S. C. Lin, *J. Membr. Sci.* **2010**, 350, 387-394.

[7] Y. Chang, W. J. Chang, Y. J. Shih, T. C. Wei, G. H. Hsiue, *ACS Appl. Mater. Interfaces* **2011**, 3, 1228-1237.

[8] Y. J. Shih, Y. Chang, *Langmuir* **2010**, 26, 17286-17294.

[9] B. Cao, Q. Tang, L. Li, C. J. Lee, H. Wang, Y. Zhang, H. Castaneda, G. Cheng, *Chem. Sci.* **2015**, 6, 782-788.

[10] M. Bernards, Y. He, *J. Biomater. Sci. Polym. Ed.* **2014**, 25, 1479-1488.

[11] H. Matsuoka, Y. Kido, M. Hachisuka, *Chem. Lett.* **2015**, 44, 1622-1624.

[12] H. Matsuoka, S. Fujita, A. Ghosh, S. Nakayama, Y. Yamakawa, S. Yusa, Y. Saruwatari, *MATEC Web Conf.* **2013**, 4, 1-4.

[13] J. Yang, H. Chen, S. Xiao, M. Shen, F. Chen, P. Fan, M. Zhong, J. Zheng, *Langmuir* **2015**, 31, 9125-9133.

[14] L. Ni, J. Meng, G. M. Geise, Y. Zhang, J. Zhou, *J. Membr. Sci.* **2015**, 491, 73-81.

[15] D. Kim, H. Matsuoka, Y. Saruwatari, *Langmuir* **2019**, 35, 1590-1597.

[16] V. M. M. Soto, J. C. Galin, *Polymer* **1984**, 25, 254-262.

[17] J. C. Salamone, W. Volksen, A. P. Olson, S. C. Israel, *Polymer* **1978**, 19, 1157-1162.

[18] D. B. Thomas, Y. A. Vasilieva, R. S. Armentrout, C. L. McCormick, *Macromolecules.* **2003**, 36, 9710-9715.

[19] Y. Ohara, K. Nakai, S. Ahmed, K. Matsumura, K. Ishihara, S. Yusa, *Langmuir* **2019**, 35,

1249-1256.

[20] J. Ma, K. Kang, Q. Yi, Z. Zhang, Z. Gu, *RSC Adv.* **2016**, 6, 64778-64790.

[21] V. Hildebrand, A. Laschewsky, D. Zehm, *J. Biomater. Sci. Polym. Ed.* **2014**, 25, 1602-1618.

[22] E. K. Perttu, F. C. Szoka, *Chem. Commun.* **2011**, 47, 12613-12615.

[23] V. A. Vasantha, S. Jana, A. Parthiban, J. G. Vancso, *Chem. Commun.* **2014**, 50, 46-48.

[24] J. Ning, G. Li, K. Haraguchi, *Macromolecules* **2013**, 46, 5317-5328.

[25] Y. Cai, S. P. Armes, *Macromolecules* **2004**, 37, 7116-7122.

[26] A. T. Nguyen, J. Baggerman, J. M. J. Paulusse, C. J. M. Rijn, H. Zuilhof, *Langmuir* **2011**, 27, 2587-2594.

[27] A. Laschewsky, I. Zerbe, *Polymer* **1991**, 32, 2070-2080.

[28] P. Meneghetti, S. Qutubuddin, *Langmuir* **2004**, 20, 3424-3430.

[29] J. F. Gohy, *Adv. Polym. Sci.* **2005**, 190, 65-136.

[30] T. H. Kim, C. W. Mount, W. R. Gombotz, S. H. Pun, *Biomaterials* **2010**, 31, 7386-7397.

[31] Y. Anraku, A. Kishimura, M. Oba, Y. Yamasaki, K. Kataoka, *J. Am. Chem. Soc.* **2010**, 132, 1631-1636.

[32] M. Oishi, S. Sasaki, Y. Nagasaki, K. Kataoka, *Biomacromolecules* **2003**, 4, 1426-1432.

[33] D. Kim, H. Matsuoka, Y. Saruwatari, *Langmuir* **2020**, 36, 10130-10137.

[34] M. Cao, H. Nie, Y. Hou, G. Han, W. Zhang, *Polym. Chem.* **2019**, 10, 403-411.

[35] T. Thavanesan, C. Herbert, F. A. Plamper, *Langmuir* **2014**, 30, 5609-5619.

[36] T. Ougizawa, T. Inoue, *Polym. J.* **1986**, 18, 521-527.

[37] P. Woodfield, Y. Zhu, Y. Pei, P. J. Roth, *Macromolecules* **2014**, 47, 750-762.

[38] N. Marjanovic, Th. B. Singh, G. Dennler, S. Gunes, H. Neugebauer, N. S. Sariciftci, R. Schwodiauer, S. Bauer, *Org. Electron.* **2006**, 7, 188-194.

[39] W. Chen, X. Wei, A. C. Balazs, K. Matyjaszewski, T. P. Russell, *Macromolecules* **2011**,

44, 1125-1131.

[40] C. Wang, Q. Chen, Z. Wang, X. Zhang, *Angew. Chem. Int. Ed.* **2010**, 49, 8612-8615.

[41] Y. Li, G. Liu, X. Wang, J. Hu, S. Liu, *Angew. Chem. Int. Ed.* **2016**, 55, 1760-1764.

[42] M. J. Rosen, *Wiley: New York* **1989**.

[43] A. Laschewsky, I. Zerbe, *Polymer* **1991**, 32, 2081-2086.

[44] R. J. Farn, *Blackwell Publishing: Oxford* **2006**.

[45] Y. Mitsukami, M. S. Donovan, A. B. Lowe, C. L. McCormick, *Macromolecules* **2001**, 34, 2248-2256.

[46] A. Einstein, *Ann. der Physik* **1905**, 322, 549-560.

[47] W. Sutherland, *Phil. Mag.* **1905**, 9, 781-785.

[48] P. Debye, *J. Phys. Chem.* **1949**, 53, 1-8.

[49] N. J. Turro, M. Gratzel, A. M. Braun, *Angew. Chem. Int. Ed.* **1980**, 19, 675-696.

[50] M. V. Smoluchowski, *Phys. Z.* **1916**, 17, 557-585.

[51] J. W. Russo, M. M. Hoffmann, *J. Chem. Eng. Data* **2010**, 55, 5900-5905.

[52] A. Chatterjee, S. P. Moulik, S. K. Sanyal, B. K. Mishra, P. M. Puri, *J. Phys. Chem. B* **2001**, 105, 12823-12831.

[53] M. L. Corrin, W. D. Harkins, *J. Am. Chem. Soc.* **1947**, 69, 3, 683-688.

[54] M. Drifford, J. P. Dalbiez, *Biopolymers* **1985**, 24, 1501-1514.

[55] M. O. Cruz, L. Belloni, M. Delsanti, J. P. Dalbiez, O. Spalla, M. Drifford, *J. Chem. Phys.* **1995**, 103, 5781-5791.

[56] J. Niskanen, H. Tenhu, *Polym. Chem.* **2017**, 8, 220-232.

[57] V. Hildebrand, A. Laschewsky, M. Pach, P. M. Buschbaum, C. M. Papadakis, *Polym. Chem.* **2017**, 8, 310-322.

List of Publications

Chapter 2.

"Synthesis and Stimuli Responsivity of Diblock Copolymers

Composed of Sulfobetaine and Ionic Blocks: Influence of

the Block Ratio"

Dongwook Kim, Hideki Matsuoka, Yoshiyuki Saruwatari

Langmuir **2019**, 35, 1590-1597.

Chapter 3.

"Formation of Sulfobetaine-Containing Entirely Ionic

PIC (Polyion Complex) Micelles and

Their Temperature Responsivity"

Dongwook Kim, Hideki Matsuoka, Yoshiyuki Saruwatari

Langmuir **2020**, 36, 10130-10137.

Chapter 4.

"Collapse Behavior of Polyion Complex (PIC) Micelles

upon Salt Addition and Reforming Behavior by Dialysis

and Its Temperature Responsivity"

Dongwook Kim, Hideki Matsuoka, Shin-ichi Yusa, Yoshiyuki Saruwatari

Langmuir **2020**, 36, 15485-15492.

Chapter 5.

"The Behavior of Micelle Formation and Functional Expression

in Sulfobetaine-Containing Entirely Ionic Block Copolymer/

Ionic Homopolymer System"

Dongwook Kim, Hideki Matsuoka, Yoshiyuki Saruwatari

Submitted to *Langmuir*

Chapter 6.

"Complex Formation of Sulfobetaine Surfactant and Ionic Polymers

and Their Stimuli Responsivity"

Dongwook Kim, Hitomi Sakamoto, Hideki Matsuoka, Yoshiyuki Saruwatari

Langmuir **2020**, 36, 12990-13000.

Other Publication

"Morphology Transition of Polyion Complex (PIC) Micelles with Carboxybetaine

as a Shell Induced at Different Block Ratios and Their pH-Responsivity"

Dongwook Kim, Hiro Honda, Hideki Matsuoka, Shin-ichi Yusa, Yoshiyuki Saruwatari

Submitted to *Langmuir*

Acknowledgements

March 2021

Dongwook Kim